PHA biosynthesis, recovery, and application

A circular value chain for production of self-healing concrete from waste

Vermeer, C.M.

DOI
10.4233/uuid:3b180cf0-8ff7-4dba-a76a-09709271141a

Publication date
2022

Document Version
Final published version

Citation (APA)
Vermeer, C. M. (2022). *PHA biosynthesis, recovery, and application: A circular value chain for production of self-healing concrete from waste*. [Dissertation (TU Delft), Delft University of Technology]. https://doi.org/10.4233/uuid:3b180cf0-8ff7-4dba-a76a-09709271141a

Important note
To cite this publication, please use the final published version (if applicable).
Please check the document version above.

PHA biosynthesis, recovery, and application

A circular value chain for production of self-healing concrete from waste

PHA biosynthesis, recovery, and application

A circular value chain for production of self-healing concrete from waste

Proefschrift

ter verkrijging van de graad van doctor
aan de Technische Universiteit Delft,
op gezag van de Rector Magnificus, Prof.dr.ir. T.H.J.J. van der Hagen,
voorzitter van het College voor Promoties,
in het openbaar te verdedigen op,
vrijdag 25 november 2022 om 10:00 uur

door

Christian Maarten VERMEER

Master of Science in Life Science and Technology,
Technische Universiteit Delft, Nederland, geboren te Delft, Nederland.

Dit proefschrift is goedgekeurd door de promotoren.

Samenstelling promotiecommissie bestaat uit:

Rector Magnificus	voorzitter
Dr. ir. R. Kleerebezem	Technische Universiteit Delft, promotor
Prof. dr. H.M. Jonkers	Technische Universiteit Delft, promotor

Onafhankelijke leden:

Prof. dr. K. U. Loos	Rijksuniversiteit Groningen
Prof. dr. P. A. S. Daran-Lapujade	Technische Universiteit Delft
Prof. dr. ir A. B. de Haan	Technische Universiteit Delft
Dr. P. A. da Costa Lemos	Universidade Nova de Lisboa

Overige leden:

Dr. ir. J. Tamis	Technische Universiteit Delft

Printed by: Proefschriftmaken.nl

Cover design: Simone Golob

Een elektronische versie van deze dissertatie is beschikbaar op
http://respository.tudelft.nl/.

Examine everything carefully. Hold fast to that which is good.

1 Thessalonians 5:21

CONTENTS

SUMMARY

Polyhydroxyalkanoates (PHA) are a family of biopolymers produced intracellular by a range of different bacteria.PHA have attracted widespread attention as an environmental friendly replacement of fossil-based polymers, because they have thermoplastic and/or elastomeric properties, and are also biobased and biodegradable.Moreover, the properties of PHA can be adjusted by tuning the monomeric composition of the polymer.Currently, more than 150 different monomers have been discovered which can form the building blocks of the PHA polymer.

PHA production can be divided in three parts: biosynthesis, recovery, and application. The first part is the biotechnological production of bacteria with PHA inside their cell. First, an organic substrate can be anaerobically converted into volatile fatty acids (VFA). These VFA form the preferred substrate for PHA production by bacteria in the next steps. An approach to make PHA biosynthesis cost-effective is by using organic waste streams as substrate in combination with mixed microbial communities. This reduces the relatively large costs for raw materials and for sterilization of the equipment. Thus far, at least 19 pilot projects have been operated to produce PHA from municipal or industrial organic waste streams using this approach. In nearly all cases, the random copolymer poly(3-hydroxybutyrate-co-3-hydroxyvalerate) (PHBV) was produced, indicating that the biosynthesis of this specific polymer is reasonably well-established. Research on the production of other types of PHA from waste streams is still scarce **(Chapter 2 and 3)**.

The main obstacles that prevent the large-scale industrial implementation of waste-derived PHA are the recovery and the application step. First of all, the PHA recovery costs are responsible for a large fraction of the total production cost due to high energy and chemical demand. Another challenge of the PHA recovery step is to achieve a high and consistent quality product when waste is used as substrate. More research is required to predict the relationship between raw material input, process parameters, and final mechanical properties of the produced PHA accurately **(Chapter 4)**.

For the application of PHA, it appeared that introducing waste-derived PHA into the conventional plastic market is a lasting and complicated procedure. This is mainly caused by a lack of distribution channels, a lack of experience in bioplastic processing, and by the small scale at which PHA is currently produced compared to petrochemical plastics. Therefore, the market entry of waste-derived

PHA could have a higher chance of success if the initial aim is not to produce bioplastics. Instead, the focus should be on new applications where minor fractions of impurities, and small variations in polymer characteristics are not regarded as problematic. Such a niche application can stimulate the introduction of waste-derived PHA into the market, while avoiding the obstacles and the complexity of the conventional plastic industry. Moreover, these applications can potentially exploit the unique properties of PHA (e.g., biodegradability) more effectively **(Chapter 5)**.

The aim of this thesis was to optimize and balance waste-derived PHA biosynthesis with recovery, and to target for a niche application of PHA in self-healing concrete. To this end, research was conducted on all parts of the value chain from waste to self-healing concrete: PHA biosynthesis **(Chapter 2 and 3)**, PHA recovery **(Chapter 4)**, and the application of PHA **(Chapter 5)**.

Chapter 2 investigates isobutyrate as sole carbon source for a microbial enrichment culture in comparison to its structural isomer butyrate. Isobutyrate is a VFA appearing in multiple waste valorization routes, such as anaerobic fermentation, chain elongation, and microbial electrosynthesis, but has never been assessed individually on its PHA production potential. The results reveal that the enrichment of isobutyrate has a very distinct character regarding microbial community development, PHA productivity, and even PHA composition. Although butyrate is a superior substrate in almost every aspect, this research shows that isobutyrate-rich waste streams have a noteworthy PHA producing potential. The main finding is that the dominant microorganism, a *Comamonas sp.*, is linked to the production of a unique PHA family member, poly(3-hydroxyisobutyrate) (PHiB), up to 37% of the cell dry weight. This chapter is the first scientific report identifying microbial PHiB production, demonstrating that mixed microbial communities can be a powerful tool for discovery of new metabolic pathways and new types of polymers.

In **Chapter 3**, another uncommon VFA was examined for PHA production, octanoate. Several enrichment strategies were tested to select for a community with a high medium-chain-length PHA (mcl-PHA) storage capacity when feeding octanoate. Based on the analysis of the metabolic pathways, the hypothesis was formulated that mcl-PHA production is more favorable under oxygen limited conditions than short-chain-length PHA (scl-PHA). This hypothesis was confirmed by bioreactor experiments showing that oxygen limitation during the PHA accumulation resulted in a higher fraction of mcl-PHA over scl-PHA (i.e., a PHA content of 76 wt% with a mcl-fraction of 0.79 with oxygen limitation, compared to a PHA content of 72 wt% with a mcl-fraction of 0.62 without oxygen limitation). Physicochemical analysis revealed that the extracted PHA could be separated efficiently into a hydroxybutyrate-rich fraction and a hydroxyhexanoate/hydroxyoctanoate-rich fraction. The ratio between the two fractions could be adjusted by changing the environmental conditions. Almost all enrichments were dominated by

Sphaerotilus sp. This chapter is the first scientific report that links this genus to mcl-PHA production, demonstrating that microbial enrichments can be a powerful tool to explore mcl-PHA biodiversity and to discover novel industrially relevant strains. In solvent extraction of PHA, the choice of solvent has a profound influence on many aspects of the process design.

Chapter 4 provides a framework to perform a systematic solvent screening for PHBV extraction. First, a database was constructed of 35 solvents that were assessed according to six different selection criteria. Then, six solvents were chosen for further experimental analysis, including 1-butanol, 2-butanol, 2-ethyl hexanol (2-EH), dimethyl carbonate (DMC), methyl isobutyl ketone (MIBK), and acetone. The main findings are that the extractions with acetone and DMC obtained the highest yields (91-95%) with reasonably high purities (93-96%), where acetone had a key advantage of the possibility to use water as anti-solvent. Moreover, the results provided new insights in the mechanisms behind PHBV extraction by pointing out that at elevated temperatures the extraction efficiency is less determined by the solvent's solubility parameters and more determined by the solvent size. Although case-specific factors play a role in the final solvent choice, we believe that this chapter provides a general strategy for the solvent selection process.

In **Chapter 5**, a niche application for waste-derived PHA is proposed and tested, using it as bacterial substrate in self-healing concrete. Self-healing concrete is an established technology developed to overcome the inevitable problem of crack formation in concrete structures, by incorporating a so-called bacteria-based healing agent. Currently, this technology is hampered by the cost involved in the preparation of this healing agent. This chapter provides a proof-of-concept for the use of waste-derived PHA as bacterial substrate in healing agent. The results show that a PHA-based healing agent, produced from PHA unsuitable for thermoplastic applications, can induce crack healing in concrete specimens, thereby reducing the water permeability of the cracks significantly compared to specimens without a healing agent. For the first time these two emerging fields of engineering, waste-derived PHA and self-healing concrete, both driven by the need for environmental sustainability, are successfully linked. We foresee that this new application will facilitate the implementation of waste-derived PHA technology, while simultaneously supplying circular and potentially more affordable raw materials for self-healing concrete.

Chapter 6 will provide a general discussion where overarching topics were selected for a thorough analysis. Finally, recommendation for further research are proposed and an outlook for the field is given.

SAMENVATTING

Polyhydroxyalkanoaten (PHA) zijn een familie van biopolymeren die intracellulair worden geproduceerd door veel verschillende soorten bacteriën. PHA heeft veel aandacht getrokken als een milieuvriendelijke vervanging van fossiele polymeren, omdat ze thermoplastische of elastische eigenschappen hebben, maar ook biobased en biologisch afbreekbaar zijn. Bovendien kunnen de eigenschappen van PHA worden aangepast door de monomeer samenstelling van het polymeer af te stemmen. Momenteel zijn er meer dan 150 verschillende monomeren ontdekt die als bouwstenen van het PHA-polymeer kunnen dienen.

PHA-productie kan worden onderverdeeld in drie delen: biosynthese, zuivering en toepassing. Het eerste deel is de biotechnologische productie van bacteriën gevuld met PHA. Dit begint met het anaeroob omzetten van het organisch substraat in vluchtige vetzuren. Deze vluchtige vetzuren vormen het voorkeurssubstraat voor PHA-productie door bacteriën in de stappen erna. Een methode om PHA-biosynthese kosteneffectief te maken is door organische afvalstromen als substraat te gebruiken in combinatie met microbiële verrijkingsculturen. Dit reduceert de relatief hoge kosten voor grondstoffen en voor de sterilisatie van de apparatuur. Tot nu toe zijn er minstens 19 pilotprojecten uitgevoerd om PHA te produceren uit huishoudelijke of industriële organische afvalstromen met behulp van deze aanpak. In bijna alle gevallen werd het copolymeer poly(3-hydroxybutyraat-co-3-hydroxyvaleraat) (PHBV) geproduceerd, wat aangeeft dat de biosynthese van dit specifieke polymeer redelijk goed ontwikkeld is. Onderzoek naar de productie van andere soorten PHA uit afvalstromen staat nog aan het begin van de ontwikkeling **(Hoofdstuk 2 en 3)**.

De belangrijkste obstakels die de grootschalige industriële implementatie van PHA uit afval in de weg staan, zijn de zuivering en de toepassing. Allereerst zijn de PHA zuiveringskosten verantwoordelijk voor een groot deel van de totale productiekosten vanwege de hoge vraag naar energie en chemicaliën. Een andere uitdaging voor de PHA zuivering is om een product van hoge en consistente kwaliteit te bereiken wanneer afval als substraat wordt gebruikt. Er is meer onderzoek nodig om de relatie tussen input van grondstoffen, procesparameters en uiteindelijke mechanische eigenschappen van het geproduceerde PHA nauwkeurig te voorspellen **(Hoofdstuk 4)**.

Voor de toepassing van PHA bleek het introduceren van uit afval verkregen PHA in de conventionele kunststofindustrie een langdurige en gecompliceerde procedure. Dit wordt voornamelijk veroorzaakt door een gebrek aan distributiekana-

len, een gebrek aan ervaring in de verwerking van bioplastics en door de klein-schaligheid waarmee PHA momenteel wordt geproduceerd in vergelijking met petrochemische plastics. Daarom zou de markttoetreding van uit afval afgeleide PHA een grotere kans van slagen kunnen hebben als het aanvankelijke doel niet is om bioplastics te produceren. In plaats daarvan zou de nadruk moeten liggen op nieuwe toepassingen waar kleine fracties van onzuiverheden en kleine varia-ties in polymeereigenschappen niet als problematisch worden beschouwd. Een dergelijke nichetoepassing kan de markttoetreding van PHA stimuleren, terwijl de obstakels en de complexiteit van de conventionele kunststofindustrie worden vermeden. Bovendien kunnen deze toepassingen de unieke eigenschappen van PHA (bijv. biologische afbreekbaarheid) mogelijk effectiever benutten **(Hoofd-stuk 5)**.

Het doel van dit proefschrift was om PHA biosynthese te optimaliseren en uit te balanceren met de zuivering, en om te streven naar een nichetoepassing van PHA in zelfhelend beton. Hiervoor is onderzoek gedaan naar alle onderdelen van de waardeketen van afval tot zelfhelend beton: PHA-biosynthese **(Hoofdstuk 2 en 3)**, PHA zuivering **(Hoofdstuk 4)** en de toepassing van PHA **(Hoofdstuk 5)**.

Hoofdstuk 2 onderzoekt isobutyraat als koolstofbron voor een microbiële ver-rijkingscultuur in vergelijking met zijn isomeer butyraat. Isobutyraat is een vluch-tig vetzuur die voorkomt in meerdere afvalvalorisatieroutes, zoals anaerobe fer-mentatie, ketenverlenging en microbiële elektrosynthese, maar is nooit individu-eel beoordeeld op zijn PHA-productiepotentieel. De resultaten laten zien dat de verrijkingscultuur op isobutyraat een heel duidelijk ander karakter heeft met be-trekking tot de ontwikkeling van de microbiële gemeenschap, de PHA-productiviteit en zelfs de PHA-samenstelling. Hoewel butyraat in bijna elk opzicht een superi-eur substraat is, toont dit onderzoek aan dat isobutyraatrijke afvalstromen een opmerkelijk PHA-productiepotentieel hebben. De belangrijkste bevinding is dat het dominante micro-organisme, een *Comamonas sp.*, is gekoppeld aan de pro-ductie van een uniek PHA-familielid, poly(3-hydroxyisobutyraat) (PHiB), tot 37% van het drooggewicht. Dit hoofdstuk is het eerste wetenschappelijke rapport dat de productie van microbieel PHiB identificeert en aantoont dat gemengde micro-biële gemeenschappen een krachtig hulpmiddel kunnen zijn voor het ontdekken van nieuwe metabole routes en nieuwe soorten polymeren.

In **Hoofdstuk 3** werd een ander ongebruikelijk vluchtig vetzuur onderzocht voor PHA-productie, octanoaat. Verschillende verrijkingsstrategieën werden ge-test om te selecteren voor een gemeenschap met een hoge opslagcapaciteit van PHA met middellange ketens (mcl-PHA). Op basis van de analyse van de meta-bole routes werd de hypothese geformuleerd dat de productie van mcl-PHA gun-stiger is onder zuurstof gelimiteerde omstandigheden dan PHA met een korte ketenlengte (scl-PHA). Deze hypothese werd bevestigd door bioreactorexperi-menten die aantoonden dat zuurstoflimitatie resulteerde in een hogere fractie van mcl-PHA ten opzichte van scl-PHA (d.w.z. een PHA-gehalte van 76% met een

mcl-fractie van 0.79 met zuurstoflimitatie, vergeleken met een PHA-gehalte van 72% met een mcl-fractie van 0.62 zonder zuurstoflimitatie). Fysisch-chemische analyse onthulde dat het geëxtraheerde PHA efficiënt kon worden gescheiden in een hydroxybutyraatrijke en een hydroxyhexanoaat/hydroxyoctanoaat-rijke fractie. De verhouding tussen de twee fracties kon worden aangepast door de omgevingsomstandigheden te veranderen. Bijna alle verrijkingen werden gedomineerd door *Sphaerotilus sp.* Dit hoofdstuk is het eerste wetenschappelijke rapport dat dit geslacht koppelt aan de productie van mcl-PHA, wat aantoont dat microbiële verrijking een krachtig hulpmiddel kan zijn om de biodiversiteit van mcl-PHA te onderzoeken en om industrieel relevante stammen te ontdekken. Bij oplosmiddelextractie van PHA heeft de keuze van het oplosmiddel een grote invloed op vele aspecten van het procesontwerp.

Hoofdstuk 4 biedt een raamwerk voor het uitvoeren van een systematische screening van oplosmiddelen voor PHA extractie. Eerst werd een database gebouwd met 35 oplosmiddelen die werden beoordeeld aan de hand van zes verschillende selectiecriteria. Vervolgens werden zes oplosmiddelen gekozen voor verdere experimentele analyse, waaronder 1-butanol, 2-butanol, 2-ethylhexanol (2-EH), dimethylcarbonaat (DMC), methylisobutylketon (MIBK) en aceton. De belangrijkste bevindingen zijn dat de extracties met aceton en DMC de hoogste opbrengsten (91-95%) opleverden met redelijk hoge zuiverheden (93-96%), waarbij aceton een belangrijk voordeel had van de mogelijkheid om water als anti-oplosmiddel te gebruiken. Bovendien gaven de resultaten nieuwe inzichten in de mechanismen achter PHA-extractie door erop te wijzen dat bij verhoogde temperaturen de extractie-efficiëntie minder wordt bepaald door de oplosbaarheidsparameters van het oplosmiddel en meer wordt bepaald door de grootte van het oplosmiddel. Hoewel specifieke factoren een rol zullen spelen bij de uiteindelijke oplosmiddelkeuze, zijn we van mening dat dit hoofdstuk een algemene strategie biedt voor het oplosmiddel selectieproces.

In **Hoofdstuk 5** wordt een nichetoepassing voor uit afval verkregen PHA voorgesteld en getest, waarbij het wordt gebruikt als bacterieel substraat in zelfhelend beton. Zelfhelend beton is een bestaande technologie die is ontwikkeld om het onvermijdelijke probleem van scheurvorming in betonnen constructies te verhelpen met een op bacteriën gebaseerd additief. Momenteel wordt deze technologie gehinderd door de kosten die gemoeid zijn met de bereiding van dit additief. Dit hoofdstuk biedt een proof-of-concept voor het gebruik van uit afval verkregen PHA als bacterieel substraat in dit additief. De resultaten laten zien dat een op PHA gebaseerd additief herstel van scheuren in betonmonsters kan induceren, waardoor de waterdoorlaatbaarheid van de scheuren aanzienlijk wordt verminderd in vergelijking met monsters zonder additief. Voor het eerst zijn deze twee opkomende gebieden van engineering, uit afval verkregen PHA en zelfhelend beton, beide gedreven door de behoefte aan duurzaamheid, met succes met elkaar verbonden. We voorzien dat deze nieuwe toepassing de industriële implementatie van de PHA-technologie zal verbeteren, terwijl tegelijkertijd

circulaire en mogelijk meer betaalbare grondstoffen voor zelfhelend beton worden geleverd.

Hoofdstuk 6 geeft een algemene discussie waarin overkoepelende onderwerpen zijn geselecteerd voor een grondige analyse. Ten slotte worden aanbevelingen voor verder onderzoek voorgesteld en wordt een toekomstvisie voor de sector geschetst.

1

INTRODUCTION

The universe is full of magical things patiently waiting for our wits to grow sharper.

Eden Phillpotts

1.1. TOWARDS A BIOBASED ECONOMY

Since the industrial revolution our society derives an increasing amount of its chemicals and materials from fossil feedstock. The world's economy became dependent on chemical products, including plastics, rubbers and fertilizer. Currently, the chemical industry is the sector with the largest energy consumption and the third largest emission of carbon dioxide (Levi *et al.*, 2018). Moreover, in the last decade, the destructive impact of the vast quantities of plastic, rubber and fertilizer residues in the environment became clear (Millican *et al.*, 2021;Ziajahromi *et al.*, 2020). To solve these problems, the chemical industry needs to become more energy-efficient, and needs to switch to renewable feedstock to produce biodegradable materials. (Meereboer *et al.*, 2020).

In the transition from a linear fossil-based economy to a circular biobased economy, the demand for biomass will increase. The utilization of the globally produced biomass (12.5 billion tons) in 2020 is shown in Fig. 1.1. Currently, the majority of the biomass (71%) is used for food and feed purposes. The remaining part (29%) is used for bioenergy (i.e., forestry and agricultural biomass, and solid municipal biowaste), biofuels (i.e., bioethanol and biodiesel) and biomaterials (i.e., wood for building, paper and board, textiles) (Millican *et al.*, 2021; Skoczinski *et al.*, 2021).

The fraction of biomass used for biobased polymers is still negligible with 0.038% (4.0 million tons) (Fig. 1.1). The size of the biobased polymer market is in sharp contrast to the total amount of polymers (including thermoplastics, thermosets, polyurethanes, elastomers, adhesives and coatings) produced by the chemical industry, which is the largest product group within the sector with a production of 369 million tons in 2020 (Levi *et al.*, 2018; Plastics Europe, 2015).
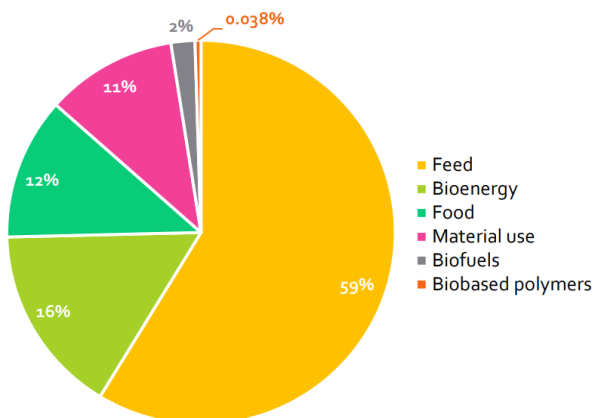
Figure 1.1.: Utilization of biomass globally in 2020 derived from Skoczinski *et al.*, 2021 All sectors add up to 12.5 billion tons biomass

1.2. BIOBASED POLYMER PRODUCTION FROM WASTE STREAMS

To produce more polymers in a biobased manner, the demand for biomass will increase. As a consequence the demand for arable land will grow, which puts an increasing pressure on natural systems and biodiversity. From the 4.0 million tons of biobased polymer, currently 49% is produced from feedstocks which are not competing with food or feed resources because non-edible parts or byproducts (e.g., glycerol) are used.

Fortunately, there is the potential to increase the use of biomass residues for biopolymer production. For example, the amount of crop residues produced annually was estimated at an additional 3.7 billion tons of biomass (Bentsen *et al.*, 2014). Furthermore, it is estimated that globally one third of the amount of food produced for human consumption is discarded (Schanes *et al.*, 2018). Currently, parts of these residues streams are already utilized for bioenergy or biofuels production. However, both from an economic and sustainability perspective, the recovery of chemicals and materials is to be preferred, because this has a higher added value and a higher position in the waste hierarchy than energy recovery (Marang, 2019).

Currently, the biobased polymer market contains, despite its small size, many different types of products. These can be subdivided in three main groups: modified natural polymers (e.g., cellulose-, lignin-, starch-, and casein-based polymers), polymers produced from chemically polymerized monomers (e.g., PLA, PEF, PE, PBS(x)), or polymers produced in microorganism or plants (polyhydroxyalkanoates, natural rubber, microbial cellulose). Out of the 28 types of biobased polymers depicted in Fig. 1.2, around 17 types are currently produced at commercial scale (Skoczinski *et al.*, 2021).

One type of biopolymer, polyhydroxyalkanoates (PHA), attracted widespread attention because it is one the few biobased polymers which is readily biodegradable in most environments (Emadian *et al.*, 2017;van den Oever *et al.*, 2017), thereby offering a solution for the pressing plastic pollution problem. Moreover, PHA can be produced by using a broad range of industrial and municipal organic waste streams as feedstock (Rodriguez-Perez *et al.*, 2018), as indicated by the red arrow in Fig. 1.2. For these reasons, PHA constitutes the focus of this thesis.

1
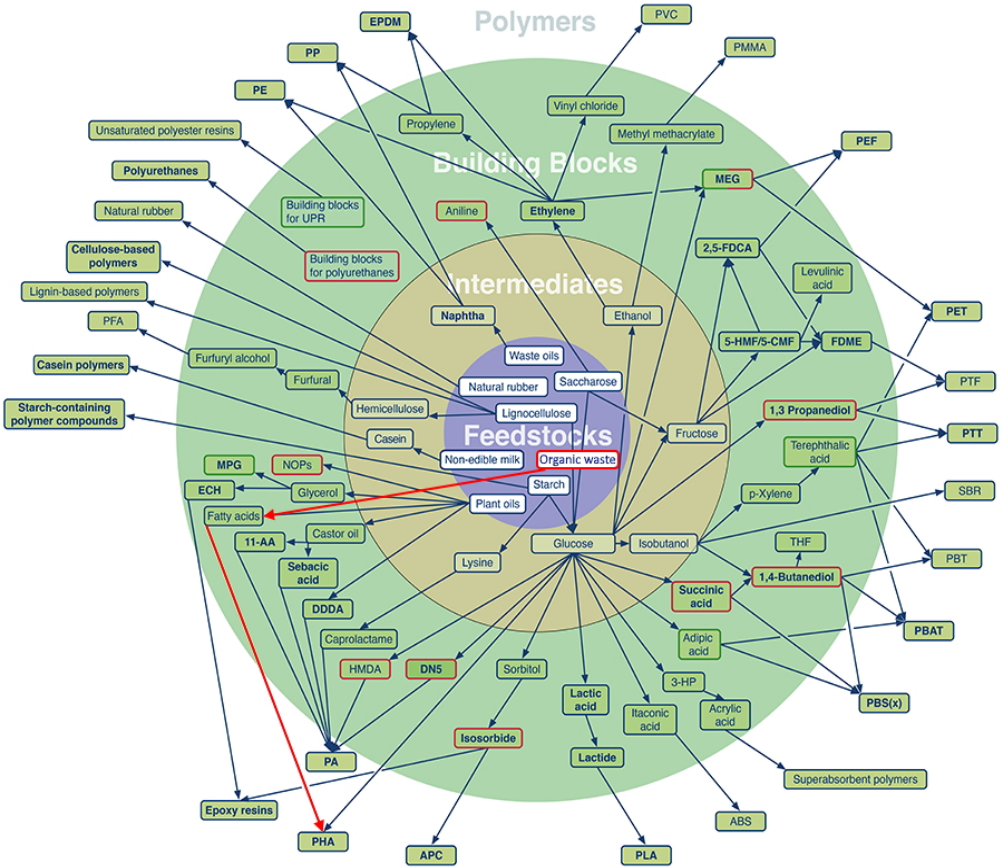
Figure 1.2.: Production routes from feedstocks to biobased building blocks and polymers adapted from Skoczinski *et al.*, 2021.The red arrows indicate the production route of PHA produced from organic waste, and constitutes the focus of this thesis.

1.3. THE FUNDAMENTALS OF POLYHYDROXYALKANOATES (PHA)

The PHA are a family of biobased polymers produced intracellularly in a broad range of bacteria as carbon and energy storage (Steinbüchel, 1991). The type of PHA monomer produced is determined by the substrate, the environmental conditions and the bacterial species. Currently, more than 150 different monomers have been discovered, where the vast majority is produced from unnatural substrates or genetically modified microorganisms (Steinbüchel *et al.*, 1995; Zheng *et al.*, 2020). PHA can be classified in two groups, short-chain length PHA (scl-PHA) with 3-5 carbons in the monomer, and medium-chain length PHA (mcl-PHA) with 6-14 carbons in the monomer (Fig. 1.3). The type and ratio of the monomers in the PHA polymers determines the physicochemical and mechanical properties of the final polymer product. Furthermore, the molecular weight (Mw), which typically ranges from 200 to 3000 kDa, is also determined by the process conditions, and also plays a role in the final polymer properties (Laycock *et al.*, 2013).
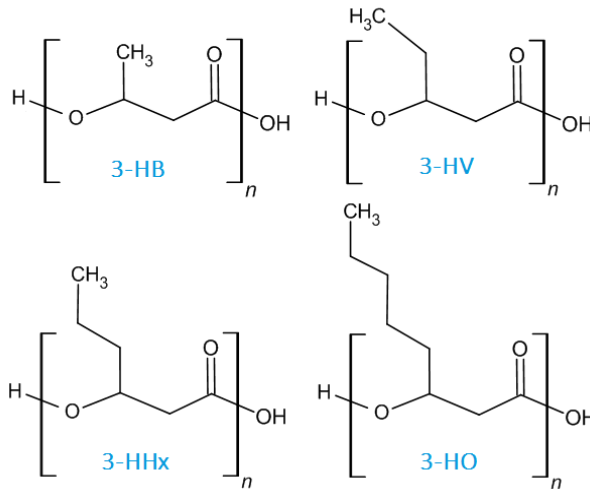
Figure 1.3.: Structure formula of the most common scl-PHA monomers, 3-hydroxybutyrate (3-HB) and 3-hydroxyvalerate (3-HV) and the often observed mcl-PHA monomers, 3-hydroxyhexanoate (3-HHx) and 3-hydroxyoctanoate (3-HO)

1.3.1. PHA BIOSYNTHESIS

The PHA which is currently commercially available is produced with pure culture processes, where costly, primary resources are used as substrate (Molenveld *et al.*, 2022). There are companies that produce different types of scl-PHA (PHBV, P3HB4HB), such as CjBio and Tianan. There are also companies that produce a mixture of scl-PHA and mcl-PHA (PHBH, PHBO, PHBD), such as Kaneka, Danimer,

PolyFerm Canadan, and RWDC.

An approach to produce PHA more cost-effective and more sustainable is by us-ing microbial enrichment cultures and organic waste streams as substrates. This technology diminishes a large part of the costs required for equipment steriliza-tion and raw materials, and consequently, removes part of the waste disposal costs (Fernández-Dacosta *et al.*, 2015 ; Kleerebezem *et al.*, 2007 and van den Oever *et al.*, 2017). To date, the upstream process for PHA production is reason-ably well-established. At least 19 different projects have successfully tested this technology at the pilot scale using a range of different organic waste streams (Estévez-Alonso *et al.*, 2021). Multiple companies are now trying to bring this technology to the market, such as Paques Biomaterials, Full Cycle Bioplastics, Bluepha, and Genecis (Molenveld *et al.*, 2022). Most, if not all, scale-up ef-forts are focused on the production of the short-chain length copolymer poly(3-hydroxybutyrate-co-3-hydroxyvalerate) (PHBV). The amount of research regard-ing mcl-PHA production from organic waste streams is still very limited (F. Silva *et al.*, 2022).

The bioprocess to biosynthesize PHA consists of three different steps. The first step is the anaerobic conversion of the waste streams to volatile fatty acids (VFAs) ranging from acetate to hexanoate. In a second step, the VFAs form the substrate for the enrichment of a PHA producing community. The enrichment is based on the principles on microbial community engineering, where micro-bial communities are selected with desired properties by engineering the envi-ronment of the microorganisms instead of the microorganisms themselves. In wastewater treatment, it has been found that when microorganisms are submit-ted to the alternating presence of substrate, they start producing storage poly-mers, mainly PHA (Van Loosdrecht *et al.*, 1997). The feast-famine regime is an example of an enrichment strategy where communities are aerobically submitted to short periods with carbon available and long periods without carbon available. This strategy appeared to be most successful in the enrichment of communities with a high PHA content and a high PHA production rate at both lab-scale and pilot-scale (Anterrieu *et al.*, 2014 ; Mulders *et al.*, 2020; Johnson, 2009a). In a third step, the PHA content of the enriched biomass can be maximized in a fed-batch bioreactor by feeding the same VFAs. By now, the process to biosynthesize PHA is reasonably well-established, however, the knowledge to convert it into a marketable product is still largely lacking.

1.3.2. PHA RECOVERY FROM BIOMASS

In recent years, research shifted from the biosynthesis of PHA more towards the recovery and the application of PHA (Estévez-Alonso *et al.*, 2021). There are two main methods to recover and purify PHA from the biomass. The first method aims at digesting or dissolving the cellular matrix with chemical agents in a water-based process while maintaining PHA in the solid phase. Various compounds can act as chemical agent: acids (e.g., H_2SO_4), alkalis (e.g., NaOH), oxidants (e.g. hypochlorite), surfactants (e.g., SDS, Triton X-100), or enzyme cocktails (Man-

nina *et al.*, 2020). The second method aims at selectively dissolving the PHA fraction with organic solvents at elevated temperatures. In literature, at least 26 different solvents are reported in relation to PHA extraction including, alcohols (e.g., 1-butanol), esters (e.g., ethyl acetate) carbonates (e.g., dimethyl carbonate), and ketones (e.g., acetone) (Alfano *et al.*, 2021; Pagliano *et al.*, 2021).

Both the cellular digestion method and the solvent extraction method have their advantages and disadvantages (Samorì *et al.*, 2015). In general, the cellular digestion method tends to result in a slightly higher yield, while the solvent-based method tends to result in a higher purity and higher molecular weight (Pagliano *et al.*, 2021). The chosen method also has a major influence on the process costs. The cellular digestion method does not involve an energy-intensive dewatering step after fermentation (Koller *et al.*, 2013). On the other hand, a large aqueous sludge stream exits the process which needs to be treated. Moreover, the added chemical agents in this stream are difficult to recover and to recycle (Kunasundari *et al.*, 2011). The solvent extraction method has a high energy requirement due to the evaporation of both the water and the solvent. On the other hand, solvents can be recovered and recycled more easily than chemical agents, although 100% recovery is unrealistic and contaminants must be removed at a certain point (Madkour *et al.*, 2013). Many publications assume that chlorinated solvents are the most effective approach for PHA extraction in terms of PHA yield and quality (Mannina *et al.*, 2020; Pagliano *et al.*, 2021). However, recent research shows that green solvents with a low impact on health, safety and environment (HSE) can be equally effective (Aramvash *et al.*, 2018; G. Jiang *et al.*, 2018). Nevertheless, it must be realized that most green solvents are flammable and still require strict safety measures.

When using organic waste streams as substrate and applying mixed cultures, it has been observed that the biomass consists of highly robust cells and extracellular substances. Moreover, a lower PHA content has been obtained in most waste-based pilot projects than in pure culture processes (Koller, 2020; Patel *et al.*, 2009). Therefore, digesting this relatively large fraction of strong cellular matrix becomes less favorable than solubilizing the PHA fraction with organic solvents (Molenveld *et al.*, 2022). In addition, solvents extractions tend to result in a high purity regardless of cultivation conditions (Pagliano *et al.*, 2021). This presumably benefits a waste-based production process, where compositional fluctuations and high concentrations of unknown pollutants will play a role. From this perspective, solvent extraction became the preferred method for the recovery of PHA in this thesis.

However, there are still many challenges regarding solvent extraction of PHA from biomass. There is still insufficient understanding to predict the relationship between raw material input, choice of solvent, process conditions, and final properties of the PHA. Moreover, the solvent extraction process is estimated to have a significant impact on the PHA production cost (almost 50%) mainly due to high energy and chemical demand (Saavedra del Oso *et al.*, 2021; Tamis, 2015; Valentino *et al.*, 2019)

1.3.3. APPLICATION OF PHA

A purified PHA polymer does not equal a marketable product. The last step in the PHA value chain towards an application is often overlooked or underestimated. The most often mentioned application for PHA is the usage as bioplastic, however, many challenges remain for this application. First of all, the estimated production cost of PHA is much higher than the cost of conventional plastics (Gurieff *et al.*, 2007). Second, due to the variable nature of organic waste streams it is challenging to produce a high and consistent quality bioplastic as required for commercially available plastics. Third, entering the conventional plastic market with a new product is a complicated procedure. The main reasons behind this are the small-scale at which PHA is currently produced compared to petrochemical plastics, and the lack of know-how and distribution channels for bioplastic processing (Bengsston *et al.*, 2017; Iles *et al.*, 2013).

In light of these challenges, the market entry of waste-derived PHA has presumably a higher chance of success if the initial objective is not an application as bioplastics. Instead, the focus should be on new applications where fluctuations in polymer characteristics, and small fractions of impurities are not regarded as problematic. These so-called niche applications can potentially boost the introduction of waste-derived PHA into the market, while avoiding the hurdles and the complexity of the conventional plastic industry. Moreover, these niche applications can potentially exploit the unique selling points of PHA (e.g. biodegradability) more effectively (Kleerebezem *et al.*, 2015; Tamis, 2015).

For PHA, some innovative niche applications have been explored already, such as bio-based paper coating (Lauzier *et al.*, 1993), bio-based glue (Pereira *et al.*, 2019), and slow-release fertilizer/herbicide (Boyandin *et al.*, 2017; Cao *et al.*, 2019). However, none of these applications are well-established yet. Therefore, this thesis introduces a new application for waste-derived PHA, using it as bacterial substrate in self-healing concrete.

1.4. SELF-HEALING CONCRETE

The technology of self-healing concrete was developed to overcome the almost inevitable problem of crack formation in concrete. Water aggressive substances which enter through cracks can deteriorate the concrete, and decrease the service life of constructions considerably (Yang *et al.*, 2004. Furthermore, concrete is today the most used construction material worldwide, and its production is accompanied by the emission of an enormous amount of carbon dioxide. Emissions in 2017 were estimated to be 8% of the global emissions (Quéré *et al.*, 2018). Therefore, self-healing concrete technology aims at decreasing maintenance costs and increasing service life of constructions, and reducing the environmental burden of concrete. Field trials of self-healing concrete structures have now demonstrated this technology at larger scale (Wiktor *et al.*, 2016).

To obtain concrete with self-healing properties, a granulated healing agent is mixed in the concrete before casting. This healing agent mainly consists of a bacterial substrate, and is supplemented with a small fraction of spores and other

essential nutrients. The bacterial substrate serves as carbon and energy source for bacterial growth. Once incorporated into the concrete, the spores become active after water intrusion due to the formation of cracks. Upon activation these bacteria are able to metabolize the organic substrate to carbon dioxide. Due to the alkaline (pH of 12-13) and calcium-rich environment of the concrete, the carbon dioxide reacts to calcium carbonate. This reaction results eventually in a physical barrier of mineral precipitates in the crack (Jonkers, 2007) (Fig. 1.4).

In previous research, different bacterial substrates have been investigated namely, urea (Wang *et al.*, 2015) various organic calcium acids (De Belie *et al.*, 2018), magnesium acetate (Palin *et al.*, 2017), and a lactic acid derivative (R. M. Mors *et al.*, 2015). Most of these substrates are obtained from valuable, primary biomass feedstocks, and therefore, presumably result in more costly and less sustainable self-healing concrete compared to substrates derived from waste streams.

In this thesis, two emerging fields of engineering, waste-derived PHA and self-healing concrete, both driven by the need for environmental sustainability, will be linked. We foresee that this new application of PHA will facilitate the implementation of waste-derived PHA technology, while simultaneously supplying circular and potentially more affordable raw materials for self-healing concrete.

© Richard van de Pol
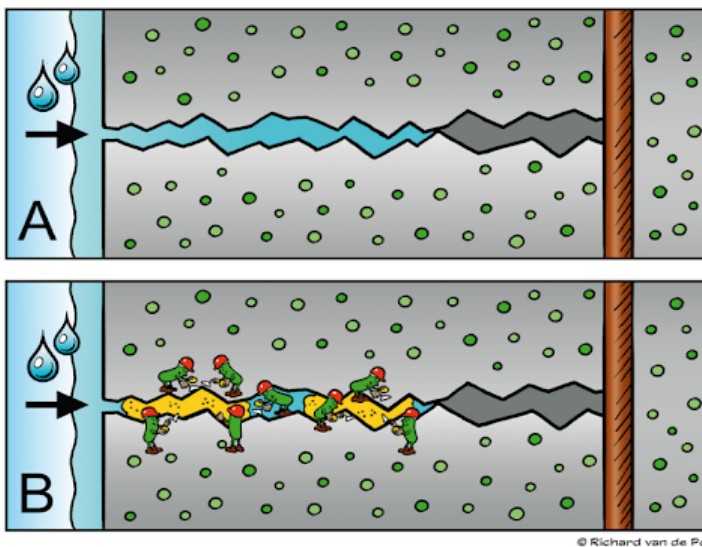
Figure 1.4.: Representation of the mechanism behind self-healing concrete copied from Betoniek edition 24 (2009).**A)** Water enters trough crack in concrete.**B)** Bacteria become active and 'heal' crack with mineral precipitation resulting in prevention of corrosion of steel reinforcement

1.5. AIM AND OUTLINE THESIS

The aim of this thesis is to optimize and balance waste-derived PHA biosynthesis with recovery, and to target for an application of PHA in self-healing concrete. The project that resulted in this thesis was part of the NWO program 'Closed Cycles – transition to a circular economy'.
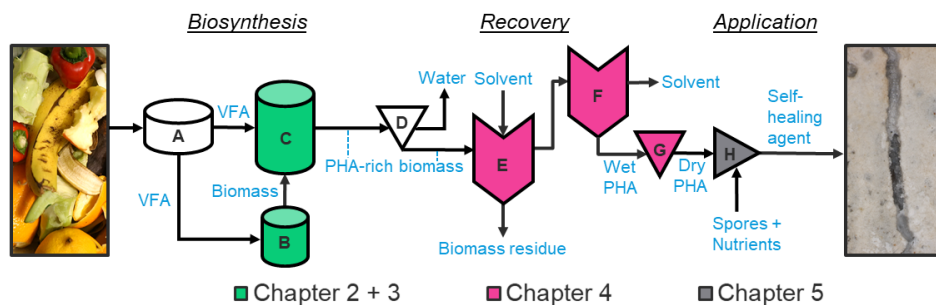
Figure 1.5.: An overview of this thesis from the perspective of the PHA production process from organic waste to an application in self-healing concrete. The focus of the four chapters is indicated with colors. The letters correspond to the different process steps including: **A)** Anaerobic fermentation, **B)** Microbial community enrichment, **C)** PHA accumulation, **D)** Dewatering, **E)** Extraction + S/L separation, **F)** Precipitation + S/L separation **G)** PHA drying, and **H)** Self-healing agent formation.

In the first two chapters, two uncommon VFAs were studied as carbon source for PHA biosynthesis, which resulted in the production of uncommon types of PHA (green process steps in Fig. 1.5).

1.6. CHAPTERS

Chapter 2 focuses on isobutyrate as substrate for PHA biosynthesis. Isobutyrate is a VFA which is present in many fermented waste streams, but has never been studied individually for PHA production. Because isobutyrate is an isomer of butyrate, the most preferred substrate for PHA production, this chapter aims to give insights into mechanism behind the high PHA productivity of butyrate. Interestingly, studying isobutyrate resulted in the discovery of a new PHA family member. In **Chapter 3**, octanoate is the substrate of interest for PHA biosynthesis. Medium-chain-length fatty acids as substrate can result in the enrichment of microbial communities that produce mcl-PHA. Mcl-PHA can form the next generation of biomaterials produced from waste streams. The selective advantage for mcl-PHA producing communities was optimized by carefully designing the operational conditions. The community was dominated by a microorganism which was not yet linked to mcl-PHA production.

Chapter 4 deals with the recovery of PHA from biomass via solvent extraction (pink process steps in Fig. 1.5). The choice of solvent has a large impact on the process design and the process cost. Solvent selection criteria were formulated and used to score a database of potential solvents. Six selected solvents were then experimentally assessed. The chapter offered a systematic approach for solvent selection and gave new insights in the desired properties of solvents.

Chapter 5 introduces and demonstrates a new application for PHA, as bacterial substrate in self-healing concrete (grey process steps in Fig. 1.5). It is envisioned that this application is less affected by the fluctuating and partly undefined properties of PHA derived from waste streams. In addition, the biodegradability of PHA is effectively used. The opportunities and challenges of this application are discussed from the perspective of the complete PHA value chain, and in relation to other waste-derived materials.

1

2

PRODUCTION OF A NEWLY DISCOVERED PHA FAMILY MEMBER WITH AN ISOBUTYRATE-FED ENRICHMENT CULTURE

Using microbial enrichment cultures for the production of waste-derived polyhydroxyalkanoates (PHA) is a promising technology to recover secondary resources. Volatile fatty acids (VFAs) form the preferred substrate for PHA production. Isobutyrate is a VFA appearing in multiple waste valorisation routes, such as anaerobic fermentation, chain elongation, and microbial electrosynthesis, but has never been assessed individually on its PHA production potential. This research investigates isobutyrate as sole carbon source for a microbial enrichment culture in comparison to its structural isomer butyrate. The results reveal that the enrichment of isobutyrate has a very distinct character regarding microbial community development, PHA productivity, and even PHA composition. Although butyrate is a superior substrate in almost every aspect, this research shows that isobutyrate-rich waste streams have a noteworthy PHA producing potential. The main finding is that the dominant microorganism, a *Comamonas sp.*, is linked to the production of a unique PHA family member, poly(3-hydroxyisobutyrate) (PHiB), up to 37% of the cell dry weight. This is the first scientific report identifying microbial PHiB production, demonstrating that mixed microbial communities can be a powerful tool for discovery of new metabolic pathways and new types of polymers.

2.1. INTRODUCTION

Polyhydroxyalkanoate (PHA) has attracted widespread attention as an alternative to petrochemical-based plastics (S. Y. Lee, 1996). PHA is completely biodegradable and biobased, and has thermoplastic properties. A broad range of bacteria are able to produce this biopolymer as an intracellular carbon and energy storage (Steinbüchel, 1991). The type of PHA monomer produced is determined by the substrate provided, the environmental conditions, and the microorganism, and in its turn will determine the physicochemical properties of the final polymer product. Currently, more than 150 different monomer units have been reported. Here, the vast majority is produced with metabolically engineered microorganisms or with substrates uncommon in the natural environment (Kumar *et al.*, 2018; Steinbüchel *et al.*, 1995; Zheng *et al.*, 2020).

An opportunity to produce PHA cost-effectively is by using mixed microbial communities and organic waste streams as feedstock. These technologies diminish the relatively large costs for sterilization and raw substrates (Kleerebezem *et al.*, 2007), and as a consequence, avoid part of the waste disposal expenses (Fernández-Dacosta *et al.*, 2015). To date, 19 pilot projects, using industrial or municipal organic waste streams as feedstock, have been operated (Estévez-Alonso *et al.*, 2021). Here, the most common type of PHA produced is the copolymer poly(3-hydroxybutyrate-co-3-hydroxyvalerate) (PHBV).

A three-step bioprocess is typically used for PHA production from organic waste streams. In the first step, the heterogeneous feedstock is fermented anaerobically, and primarily converted into volatile fatty acids (VFAs), ranging from acetate to hexanoate (Kleerebezem *et al.*, 2015; Serafim *et al.*, 2008). These VFAs form the preferred substrate for PHA production. In a second step, a microbial community is aerobically enriched with high PHA productivity by applying feast-famine conditions. This intermittent substrate feeding strategy generates a competitive advantage for bacteria that store PHA as reservoir of carbon and electrons inside their cell. In a successive accumulation step, the PHA content of the obtained enrichment can be maximized (Kourmentza *et al.*, 2017; M. A. Reis *et al.*, 2003.

Under laboratory conditions, the most abundant VFAs (acetate, propionate, butyrate) of fermented waste streams have been individually assessed on their PHA production potential (Jiang, 2011a; Lemos *et al.*, 2006 ; Marang, 2013). These studies reported microbial enrichments with high PHA production rates and were able to accumulate PHA up to 90% of the cell dry weight (Jiang, 2011a; Johnson, 2009a). Butyrate appeared to be the preferred VFA for PHA production, having the highest carbon uptake rate and the highest PHA yield, resulting in the highest PHA production rate (Marang, 2013). These laboratory studies in combination with modelling studies have resulted in an extensive understanding of the underlying PHA metabolism (Dias *et al.*, 2005; Johnson, 2009b; Van Aalst-Van Leeuwen *et al.*, 1997).

Besides linear volatile fatty acids, branched isomers like isobutyrate and isovalerate are regularly encountered products of anaerobic fermentations fed with organic waste (Dionisi *et al.*, 2005; Mulders *et al.*, 2020). For example,(Mechichi *et*

al., 2005) show that isobutyrate can constitute up to 12 wt% of total VFA stream when fermenting olive mill wastewater anaerobically. A possible contribution to the presence of isobutyrate is the activity of proteolytic anaerobic bacteria degrading valine (Tholozan *et al.*, 1988). The other, much more prevalent process is the isomerization of butyrate, which has been reported by multiple studies (Angelidaki *et al.*, 1995; Lovley *et al.*, 1982 ; Tholozan *et al.*, 1988). Although the precise ecological function needs to be elucidated, it is hypothesized that isomerization reduces the inhibitory effect of butyrate (W. S. Chen, Strik, *et al.*, 2017a. Despite its presence in the VFA stream of anaerobic fermentations, the PHA producing potential of isobutyrate has never been studied as sole carbon source. In addition, isobutyrate can be a major product of other waste valorization innovations, such as chain elongation (De Leeuw *et al.*, 2020), and microbial electrosynthesis (Levi *et al.*, 2018). Here, the aspiration is to produce isobutyrate as a platform chemical. Instead, a mixture of VFAs is produced at low concentrations, resulting in a complex and costly downstream processing (Menon *et al.*, 2020). The possibility to produce a solid substance, in the form of a PHA polymer, might facilitate purification and will expand the product spectrum of valorization routes focused on isobutyrate containing streams. Furthermore, n-butyrate has been identified as the preferred substrate for PHA production due to superior kinetics and product yield. Isobutyrate has an identical theoretical PHA yield (0.94 Cmol/Cmol), if energetically neutral isomerization to n-butyrate is assumed as first conversion step (Shi *et al.*, 1997). Studying the structural isomer of butyrate can give a better understanding of the mechanisms behind this high PHA productivity. Therefore, the aim of this research is to study the suitability of isobutyrate in relation to butyrate as substrate for PHA production with microbial enrichment cultures.

To this end, two sequencing batch reactors (SBRs) were operated with either isobutyrate or butyrate as substrate. For comparison, the operational parameters, which have been successfully applied in studies with acetate, propionate, lactate, and butyrate, were replicated from (Johnson, 2009a). During the whole enrichment phase the microbial community structure was monitored. At certain points, the performance of the enrichment was characterized, including its maximum PHA storage capacity by way of an accumulation experiment. Additionally, for 1 cycle of the SBR the substrates of both SBRs were exchanged. Finally, the stoichiometric and kinetic parameters of the enrichment in all experiments were derived from a modified version of a metabolic model originally developed by (Johnson, 2009b).

2.2. MATERIALS AND METHODS

2.2.1. ENRICHMENT IN SBRs

Two double-jacket glass bioreactors with a working volume of 1.4 L (Applikon Biotechnology, The Netherlands) were operated in parallel for the enrichment of a PHA-storing microbial culture on isobutyrate (SBR1) and butyrate (SBR2). The setup and operation of these bioreactors were based on the conditions as de-

scribed by Johnson, 2009a. The bioreactors were operated as non-sterile SBRs, subjected to a feast-famine regime with a cycle length of 12 h and a solids and hydraulic retention time (SRT and HRT) of 24 h, which implies that every cycle 50% of the SBR volume is replaced with fresh medium. The inoculum of the SBRs was aerobic activated sludge of a wastewater treatment plant (AWZI Harnaschpolder Delfluent, The Netherlands). Furthermore, the air flow rate to the bioreactors was set to 0.2 LN/min by means of a mass flow controller (MX4/4, DASGIP®, Eppendorf, Germany), and the stirring speed was set to 800 rpm (TC4SC4, DASGIP®, Eppendorf, Germany). The temperature in the bioreactor was controlled at 30 °C ± 0.5 °C with the water jacket around the bioreactor and an external thermostat bath (ECO RE 630 S, Lauda, Germany). The pH was maintained at 7.0 ± 0.1 by the addition of 1 M HCl and 1 M NaOH through an integrated revolution counter (MP8, DASGIP®, Eppendorf, Germany). The pumps for feeding, effluent removal, and pH control, the stirrer, and the airflow were controlled by a hardware abstraction layer (HAL; TU Delft, the Netherlands), which in turn was controlled by a PC using a custom scheduling software (D2I; TU Delft, the Netherlands). The D2I was also used for data acquisition of the online measurements: dissolved oxygen (DO), pH, temperature, acid and base dosage, in- and off-gas composition and feed/water balances. Moreover, the bioreactors were cleaned about twice per week to remove biofilms from the glass walls and the sensors of the bioreactor.

The medium consisted of a carbon and nutrient source with a composition as described by Marang, 2013. The carbon source concentration in the SBR was either 9.5 mM isobutyrate or butyrate.The nutrients concentrations in the SBR composed of 6.74 mM NH_4Cl, 2.49 mM KH_2PO_4,0.5 mM $MgSO_4H_2$, 0.72 mM KCl, 1.5 mL trace elements solution according to Vishniac *et al.*, 1957, and 5 mg/L allylthiourea (to prevent nitrification). To characterize the operational performance, the isobutyrate SBR was subjected three times to a cycle analysis experiment (SBR1-C1 = cycle 51; SBR1-C2 = cycle 111; SBR1-C3 = cycle 115) due to instability of the enrichment, while the butyrate SBR was subjected once to a cycle analysis experiment (SBR2-C = cycle 113).

2.2.2. EXCHANGE OF SUBSTRATES IN SBRS

After the cycle analysis experiments, both SBRs were operated for 1 cycle with exchanged substrate. This means that SBR1 received butyrate as carbon source (SBR1-E = cycle 127), and SBR2 received isobutyrate as carbon source (SBR2-E = cycle 128). During this cycle the operational performance was characterized. After this cycle the original carbon source was restored.

2.2.3. PHA ACCUMULATION IN FED-BATCH BIOREACTOR

The PHA accumulation experiments were performed in the same bioreactors as the enrichment, but operated in fed-batch mode. The stirring speed, pH, temperature, and aeration rate were kept at the same values as in the SBR. Half of the content of the SBR (700 ml) was used as seeding material for the accumulation experiment. In addition, 700 mL ammonium- and carbon-free medium

was supplied. After 30 minutes, to ensure a temperature of 30 °C, a pulse of 42 mmol isobutyrate or butyrate was supplied to each SBR (SBR1-A = cycle 136; SBR2-A = cycle 138). To prevent carbon source depletion throughout the PHA accumulation, isobutyric acid or butyric acid (1.5 M) and NaOH (1 M) were used to control the pH, ensuring a concentration of 10-30 mM of the carbon source in the bioreactor. Nitrogen was limited during most of the accumulation since no nitrogen source was supplied to the bioreactors and only a small amount (<0.8 mM of $NH4^+$) remained from the previous SBR cycle. In this way, growth in the fed-batch bioreactor was limited. If necessary, a few drops of (10x diluted) Antifoam C (Sigma-Aldrich, USA) were added to inhibit the formation of foam. The experiments were terminated after 11h.

2.2.4. ANALYTICAL METHODS

The performance of the cycle, exchange and accumulation experiments were characterized by online measurements (DO, pH, acid/base dosage, and in-/off-gas composition) with the equipment and software described above, and with offline samples (VFAs, ammonium, PHA, total and volatile suspended solids). The composition of the active biomass was assumed to be $CH_{1.8} O_{0.5} N_{0.2}$ (Beun *et al.*, 2002). A detailed description of the analytical methods is given by Johnson, 2009a. A modification has been made for the ammonium measurement. These samples were measured with a Gallery™ Plus Discrete Analyzer (Thermo-Fisher Scientific, USA).

The method to analyze the PHA composition of the biomass was also described in detail by Johnson, 2009a. In brief, the PHA in the biomass was hydrolyzed and esterified in the presence of concentrated HCl, propanol, and dichlorethane with a ratio of 1/4/5 (v/v/v) for 2 h at 100 °C. The formed propylesters, which accumulated in the organic phase, were analyzed by a gas chromatograph (model 6890N, Agilent, USA). The PHA analysis method was expanded to include the quantification of poly(3-hydroxyisobutyrate) (PHiB) by using methyl (S)-(+)-3-hydroxy-2-methylpropionate (Sigma-Aldrich, USA) as standard.

GC-MS analysis was carried out on a 7890A GC coupled to a 5975C Quadrupole MSD (both from Agilent, USA) to identify PHiB. A detailed description of the analytical protocol is described by Velasco Alvarez *et al.*, 2017.The same sample pre-treatment and the same standard as for GC quantification were used.

2.2.5. MICROBIAL COMMUNITY ANALYSIS

To analyze the microbial composition of the enriched cultures, 2 mL of biomass samples were collected in an Eppendorf tube. The samples were taken 2 times per week, and in addition during the cycle, exchange, and accumulation experiments. The tubes were centrifuged (13,300 g; 5 min.). The pellet was stored at -20 °C until analysis. After defrosting, genomic DNA was extracted using the DNeasy UltraClean Microbial Kit (Qiagen, Germany), following the manufacturer's instructions. DNA quantification was carried out using the Qubit® dsDNA Broad Range Assay Kit (Qubit® 2.0 Fluorometer, Thermo Fisher Scientific, USA), follow-

ing the manufacturer's instructions. Afterwards, about 50 μL of isolated (16S) DNA was sent to Novogene (China) for amplicon sequencing of the V3-4 region of the 16S rRNA gene. The sequence data have been deposited in GenBank with BioProject ID PRJNA766835.

2.2.6. METABOLIC MODEL AND PARAMETER IDENTIFICATION

A model, proposed by Johnson, 2009b and adapted towards butyrate by Marang, 2013 was used as starting point for this study. This model contains a set of metabolic and kinetic expressions which together describe the consumption and formation of the main compounds in the bioreactor, that is PHA, biomass, organic substrate, CO_2, O_2 and ammonium. The trends obtained by the model are fitted to the experimental data.

First, an extension of the model was proposed to include isobutyrate and PHiB (see Fig. 2.1). When feeding with isobutyrate, it was assumed that isobutyryl-CoA was converted to 3-hydroxyisobutyryl-CoA with the enzymes that are also active in valine metabolism (Massey *et al.*, 1976), and then polymerized with a PHA synthase to PHiB (R5 in Fig. 2.1). At the same time, it was assumed that HB monomers could be formed by isomerization of isobutyryl-CoA to butyryl-CoA (R2, R3 and R4 in Fig. 2.1). Similarly, it was assumed that PHiB is degraded towards isobutyryl-CoA and isomerized with the same enzyme (R8 and R3 in Fig. 2.1). In supplementary Table A.1 the entire reactions of Fig. 2.1 are displayed.

The obtained reactions were used to calculate the stoichiometric yields by balancing the conserved moieties (Ac-CoA, But-CoA, IBut-CoA, NADH, ATP). The stoichiometric yields and the kinetic expressions shown in supplementary Table A.2 and A.3 form the basis of the model. In accordance with the study of J. Tamis, 2014, the PHA degradation function was adapted. For this study, biomass specific rates and actual yields were derived from the model. The efficiency of the oxidative phosphorylation (P/O ratio) was assumed to be 2.0 mol ATP/mol NADH for all experiments (R11 in Fig. 2.1).

Throughout this work, the terms PHB and PHiB are defined as polymers consisting mainly of HB (3-hydroxybutyrate) monomers or HiB (3-hydroxyisobutyrate) monomers respectively. First, because the data suggest that the micro-organisms in the enrichment produce a mixture of homopolymers rather than a (P (3HB-co-3HiB)) copolymer. Second, because this improves the readability of the work. However, it is not excluded that in some of the experiments copolymers or homopolymers with significant amounts of other monomers were produced.
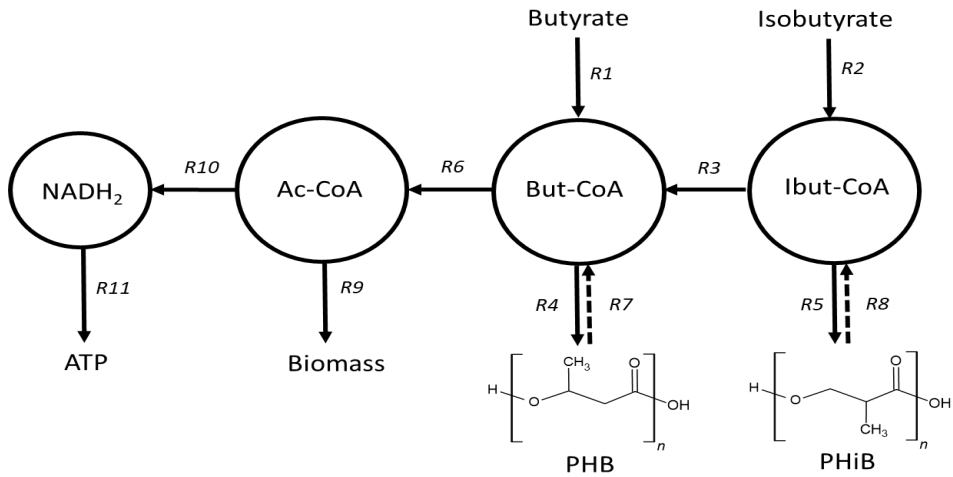
Figure 2.1.: A schematic representation of the proposed PHA metabolism. R1 and R2 represent substrate uptake reactions during the feast phase, depending on the substrate supplied. R3 represents the isomerization of isobutyryl-CoA to butyryl-CoA. R4 and R5 represent the PHB and PHiB production reactions respectively. When isobutyrate is supplied, both PHB and PHiB can be produced. R6 represents the conversion of butyryl-CoA to acetyl-CoA. R7 and R8 represent PHA degradation reactions and are active during the famine phase. R9 and R10 represent anabolic and catabolic reactions respectively. R11 represents the oxidative phosphorylation. Ac-CoA = acetyl-CoA, But-CoA = butyryl-CoA, Ibut-CoA = isobutyryl-CoA

2.3. Results

2.3.1. Overview enrichment and microbial community characterization

Two SBRs, pulse fed with either isobutyrate or butyrate, were operated for 136 and 138 cycles respectively in this study. The sequencing batch regime was started after the substrate was depleted from the initial batch incubation. SBR1, fed with isobutyrate, had a longer lag phase, and was started when SBR2, fed with butyrate, was operated for 2 cycles already.

The addition of nutrients and carbon source at the beginning of a cycle resulted in a relatively short feast phase, which was succeeded by a relativity long famine phase. The feast phase was characterized by a high oxygen uptake rate, and its duration could therefore be extracted from the DO data (Stouten *et al.*, 2019). In Fig. 2.2(a)and 2.2(c), the duration of the feast phase of SBR1 and SBR2 respectively is plotted for the complete enrichment. Although in both systems a clear downward trend can be observed, the feast time in SBR1 remained at a significantly higher value than SBR2, indicating a low isobutyrate uptake rate and a high butyrate uptake rate. Moreover, the feast length of SBR1 displayed much variability over time, while SBR2 showed a much more stable system in terms of feast length. The microbial community data, measured by 16S amplicon sequencing, confirms that the stability of the enrichment is low in SBR1 and high in SBR2 (Fig. 2.2and 2.2(c)). In SBR1, a *Comamonas sp.* is the dominant species, but its presence is highly dynamic. When *Comamonas sp.* becomes abundant, the feast time decreases for most cycles. Its decrease in relative abundance appears to coincide with an increase in feast time and the temporary emergence of *Camelimonas sp.* and *Zoogloea sp.* From the moment that *Comamonas sp.* becomes abundant (cycle 51-135) the average feast time is 167±53 min. SBR2 reveals a very distinct pattern, where 2 stable phases can be distinguished. In the first phase (cycle 27-56) *Zoogloea sp.* is dominant with an average cycle length of 71±7 min, while in the second phase (cycle 62-137) *Plasticicumulans acidivorans* is dominant with an average feast time of 27±5 min. During the enrichment, the performance of both SBRs was characterized in the form of a cycle analysis experiments, substrate exchange experiments, and accumulation experiments. Fig. 2.2 highlights these key moments in the enrichment and displays the corresponding feast time and microbial community.

2.3.2. Identification of poly(3-hydroxyisobutyrate)

During PHA analysis a peak appeared on the chromatogram which did not match with the propyl ester of 3-hydroxybutyrate or 3-hydroxyvalerate. Nevertheless, its formation and degradation during the SBR cycle resembled a typical PHA shape, a rapid increase during the feast phase and a decrease during the famine phase. Mass spectrometry analysis through GC-MS revealed that the unknown peak had a similar mass spectrum as 3-hydroxybutyrate (data not shown). Then,
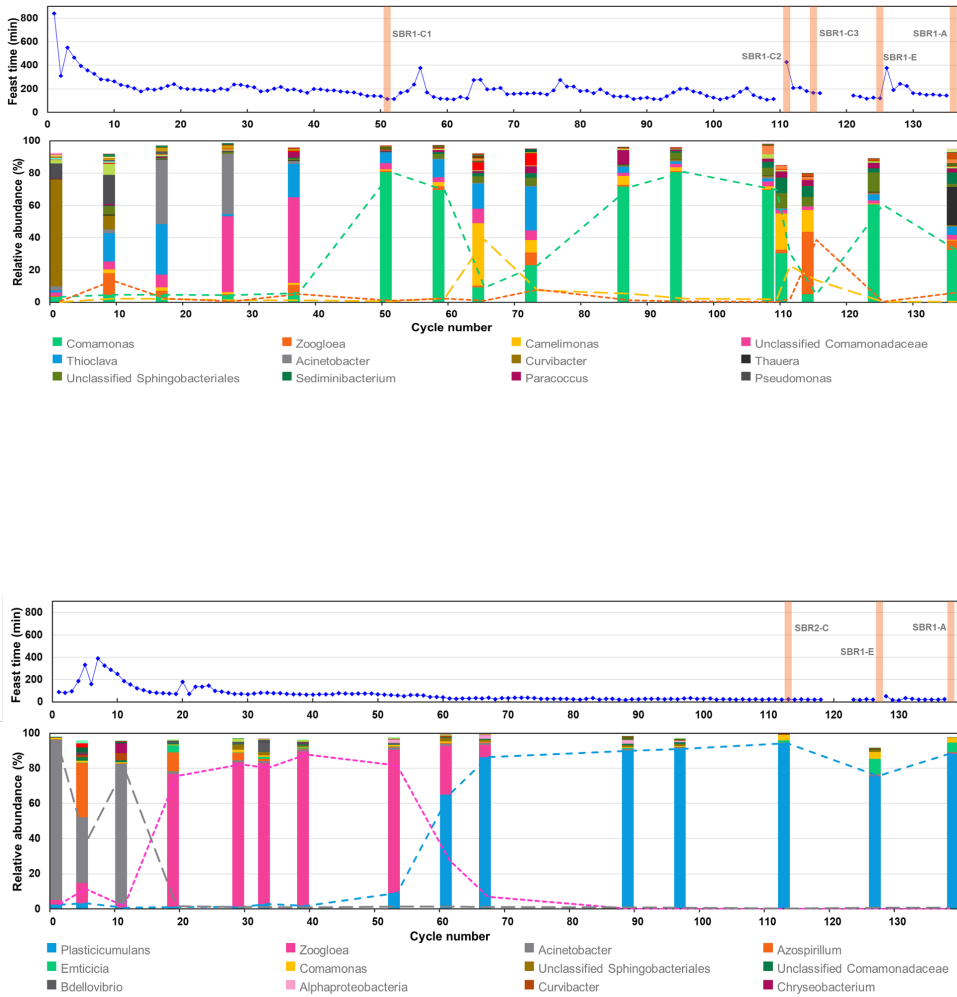
Figure 2.2.: Overview of the feast length and the community structure for the whole enrichment of SBR1 and SBR2. **a and c:** Feast length of SBR 1 and 2 respectively. The vertical bars represent the different experiments conducted. The gaps in the curve are caused by failure of the data acquisition, not by failure of the SBR performance. **b and d:** Relative abundance of genera derived from 16S amplicon analysis of SBR 1 and 2 respectively. Only genera reaching a relative abundance higher than 1% are shown in graph. The three most abundant genera are depicted with both stacked columns and lines..

methyl 3-hydroxy-2-methylpropionate, the methyl ester of the 3-hydroxy vari-
ant of isobutyrate, was used as standard. Before analysis, the methyl ester was
converted to a propyl ester in the same way as the conventional standard. It ap-
peared that this new standard had the same retention time (Fig. 2.3a-b) and the
same mass spectrum (Fig. 2.3c-d) as the unknown peak. This demonstrates that
the unknown peak represents poly(3-hydroxy-2-methylpropionate), also known
as poly(3-hydroxyisobutyrate)(PHiB).
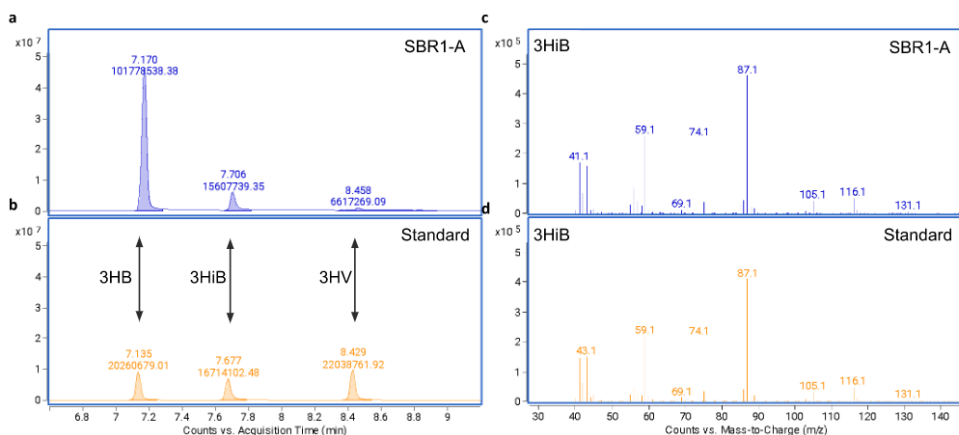
Figure 2.3.: GC-MS analysis of sample from SBR1-A (a and c) in comparison with stan-
dards (b and d). a and b: The chromatogram of the GC analysis reveals the
three PHA monomers identified in the biomass, that is 3-hydroxybutyrate
(3HB), 3-hydroxyisobutyrate (3HiB), and 3-hydroxyvalerate (3HV). c and d:
The mass spectra of the MS analysis reveal a very high degree of similarity
of the mass-to-charge ratio of the monomer 3-hydroxyisobutyrate (3HiB), be-
tween the sample and the standard.

2.3.3. SBR CYCLE PERFORMANCE

A more detailed insight of the performance of the SBR's was obtained by an ex-
tensive analysis of specific operational cycles. For SBR1, multiple cycles were
analyzed due to a variation of the functional performance during the enrichment,
illustrated by the feast times in Fig. 2.2a.

The main experimental and modelled results of the cycle measurements are de-
picted in Fig. 2.4a-d and Table. 2.1. In supplementary Fig. A.1, a complete
version of the experimental results fitted with the metabolic model is shown, in-
cluding biomass, ammonium and off-gas data.

The first cycle analysis, SBR1-C1, showed the highest substrate uptake rate
(feast time is 125 min), the highest relative abundance of *Comamonas sp.* (81%),
and the highest PHA content (41.1 wt%) at the end of the feast phase. Surpris-
ingly, the monomer composition of the PHA was strongly dominated by the newly
discovered PHiB (37 out of 41 wt%).
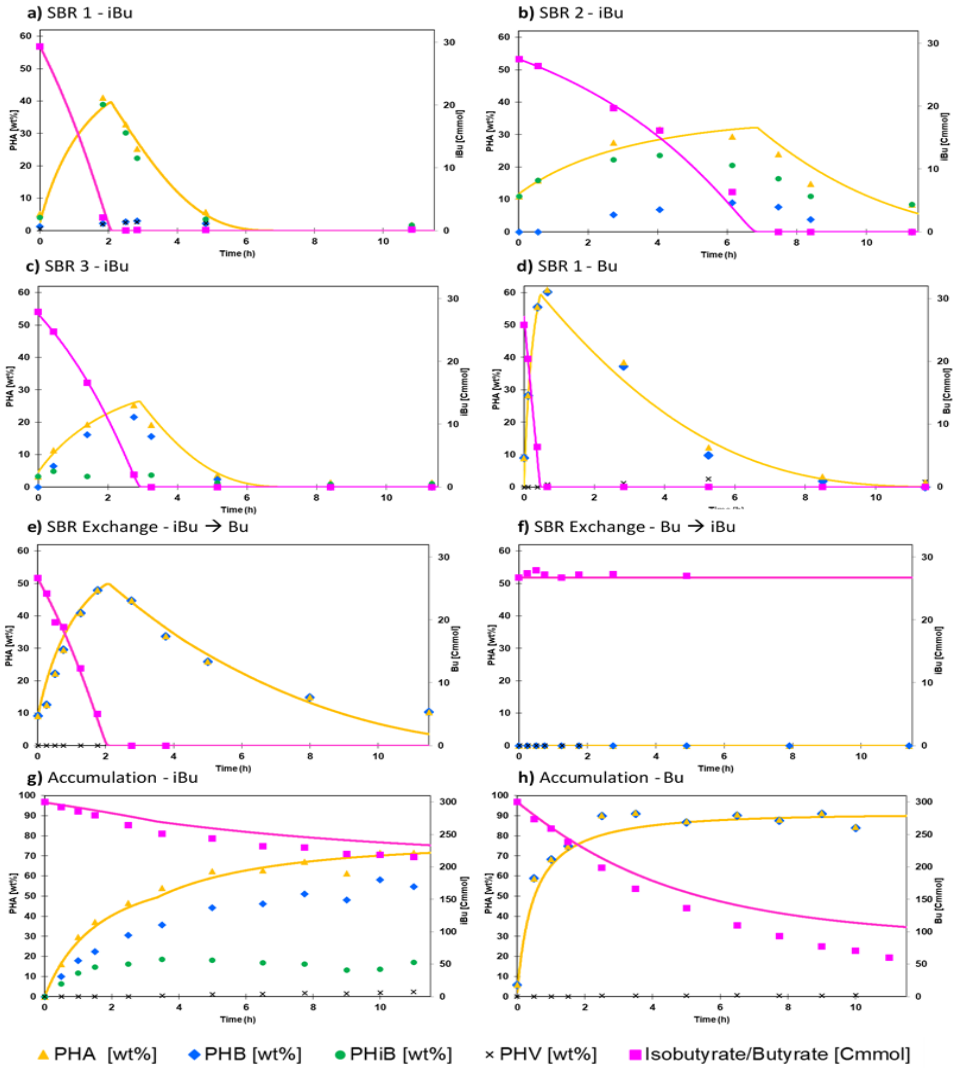
Figure 2.4.: Overview of PHA and substrate analysis of the cycle experiments **(a-d)**, substrate exchange experiments **(e-f)**, and accumulation experiments **(g-h)**. The symbols represent the observed data. Here, the yellow triangles represent the total PHA content, which is a sum of the individual monomers measured (HB, HiB, HV) represented by the remaining symbols. The pink solid line represent the modelled substrate amount in the bioreactor [Cmmol] and the yellow solid line represents the modelled total PHA content [wt%], calculated with equation 16 in supplementary Table. A.3. In the graphs of SBR1 (**a, b, c, e, g**) the substrate is isobutyrate, in the graphs of SBR2 (**d, f, h**) the substrate is butyrate (indicated on secondary axes).

However, this seemingly competitive functionality appeared to be unstable over the cycles. At certain moments in the enrichment, the community collapses as reflected in the increase in the length of the feast phase, and different dominant strains appear.

	Unit	Isobutyrate					Butyrate		
		SBR1-C1	SBR1-C2	SBR3-C3	SRR1-E	SBR1-A	SBR2-C3	SBR2-E	SBR2-A
Type of experiment		Cycle	Cycle	Cycle	Exch.	Accu.	Cycle	Exch.	Accu.
Measured data									
Length feast phase /time to 60 wt% PHA	h	125	429	166	120	264	25	-	30
PHB max. feast	%	3	9	22	48	58	61	0	91
PHiB max. feast	%	37	24	5	0	16	0	0	0
PHV max. feast	%	3	1	0	0	3	3	0	0
Total PHA max. feast	%	41	32	25	48	72	62	0	92
PHA:X	[gPHB/1gX]	0.7	0.5	0.3	0.9	2.6	1.6	0	11.2
Microbial community data									
Comamomas / Plasticicumulans	(%)	81	30	5	66	35	94	88	76
Other most abundant					Zoogl. (39%)				
Second most abundant		Thiocl. (7%)	Camel. (23%)	Camel. (14%)	Unc. Sphingo. (13%)	Thauera (26%)	Emtic. (2%)	Emtic. (5%)	Emtic. (9%)
Model derived yields (first 2.5h of accumulation)									
$q_{s,max}$	[Cmmol/Cmmol/h]	1.09	0.51	0.74	1.28	0.79	5.48	0	2.48
μ_{max}	[Cmmol/Cmmol/h]	0.3	0.2	0.31	0.31	0.14	0.02	0	0
$q_{PHA,max}$	[Cmmol/Cmmol/h]	0.58	0.18	0.2	0.81	0.49	5.15	0	2.3
$Y_{X,S}$	[Cmmol/Cmmol]	0.27	0.39	0.41	0.24	0.19	0	-	0
$Y_{PHA,S}$	[Cmmol/Cmmol]	0.54	0.34	0.34	0.58	0.6	0.96	-	0.92
Model derived (famine phase)									
k_d	$[Cmmol^{1/3}/Cmmol^{1/3}/h]$	-0.8	-0.4	-0.75	-0.27	0	-0.3	0	0

Table 2.1.: Overview of the main measured data, microbial community data (16S amplicon sequencing), and model derived yields and biomass specific rates of the different cycle analysis, substrate exchange, and accumulation experiments. *Unc. Sphingo = Unclassified Sphingobacteriales, Exch = exchange, Accu. = accumulation, Thiocl. = Thioclava, Camel. = Camelimons, Zoogl. = Zoogloea, Emtic. = Emticicia*

The second cycle analysis, SBR1-C2, was conducted at the time of such a collapse. Here, the substrate uptake rate and the PHA production rate of the community dropped abruptly; the feast time becomes 429 min and the $q_{PHA,max}$ is 3.2 times lower than SBR1-C1. Although *Comamonas sp.* is still abundant (30%), a side population of *Camelimonas sp.* appears (23%). This duality is also reflected in the PHA productivity, which is a mixture of PHiB and PHB, as shown in Fig. 2.4b. The third cycle analysis, SBR1-C3, was conducted four cycles after the collapse represented by SBR1-C2. According to the feast time, the community had returned to a moderately stable phase, although the feast time was higher than during SBR1-C1 (166 min compared to 125 min). The 16S amplicon sequencing data revealed that the presence of *Comamonas sp.* and *Camelimonas sp.* had decreased and a new dominant species appeared, *Zoogloea sp.* Fig. 2.4c shows that this well-known PHA producer (Fang *et al.*, 2019; Stouten *et al.*, 2019) was mainly associated with PHB production, rather than with PHiB production, although the PHA content at the end of the feast phase was low (25 wt%).

The contrast of isobutyrate-fed SBR1 with butyrate-fed SBR2, couldn't be larger. The cycle analysis, SBR2-C, reveals a highly enriched community (94% rel. abundance of P. acidivorans), a very high substrate uptake rate (feast time is 25 minutes), and a very high PHA production rate, as shown in Fig. 2.4 d. In SBR1 a

large share of the isobutyrate is used in the feast phase to sustain growth reactions ($Y_{X,S,feast}$ is 0.27 to 0.41). Butyrate use for growth in the feast is negligible in SBR2-C ($Y_{X,S,feast}$ is 0.01).

2.3.4. Substrate exchange

For 1 cycle, the carbon substrates of SBR1 and SBR2 have been exchanged (SBR1-E and SBR2-E). The main results of this experiment are shown in Fig. 2.4e-f and Table. 2.1. At the time, SBR 1 was dominated by *Comamonas sp.* (rel. abundance of 66%). Therefore, SBR1-E can best be compared to SBR1-C1. It is observed that when SBR1 was fed with butyrate, there was no lag-phase in substrate uptake and the PHA production completely shifted towards PHB production. The total PHA content at the end of the feast phase is slighter higher in SBR1-E (48 wt%) than in SBR1-C1 (41 wt%). The qs,max and qPHA,max have increased slightly, while the other variables remained remarkably comparable. The main difference was that the degradation of PHB in the famine phase is significantly slower in SBR1-E than the degradation of PHiB in SBR1-C1 (k_d is -0.27 and -0.80 $Cmmol^{1/3}/Cmmol^{1/3}$/h respectively).

At the time of the SBR2-E experiment, the SBR2 bioreactor was highly enriched with P. acidivorans. Remarkably, this butyrate-enriched community did not possess the capability to metabolize isobutyrate at all. During the 12 h duration of the experiment no substrate, ammonium or O_2 consumption was observed, and no biomass, PHA or CO_2 production was observed (see Fig. 2.4 f and supplementary Fig. A.1).

2.3.5. Maximum PHA accumulation capacity

To evaluate the maximum PHA accumulation capacity, an ammonium limited fed-batch experiment was conducted. Results are shown in Fig. 2.4 g-h and table 2.1. At the time, *Comamonas sp.* was not very dominant in SBR1 (rel. abundance of 32%). It seemed that *Thauera sp.*, a known PHA producer (M. Reis *et al.*, 2011; Tamang *et al.*, 2021), had entered the microbial community (rel. abundance of 24%) (Fig. 2.2b). As in SBR1-C2, the presence of this side population was reflected in the PHA productivity, resulting in a combination of PHiB and PHB. In the first 2 hours, the production of both polymer types occurred at a similar rate. Later, it seemed that the production rate of PHiB decreased faster than the production rate of PHB, resulting in a product dominated by PHB at the end of the experiment (55 out of 72 wt%).

SBR2 revealed again a distinct functionality than SBR1. As expected, PHB is the prevailing polymer type. As in the cycle experiments, the PHA production rate and the PHA yield are much more favorable in the butyrate-fed SBR than in the isobutyrate-fed SBR. Additionally, this experiment demonstrates that the PHA accumulation capacity is substantially higher for the microbial community enriched on butyrate than the community enriched on isobutyrate (92 wt% compared to 72 wt%). The carbon and electron balances of the cycle and exchange experiments closed for 100±3%. For the accumulation experiments, a gap in the mass

balance develops, resulting in a closure of 84±3%. This gap has been observed before, and is presumably due to the formation of unknown extracellular compounds over time in accumulation experiments (Marang, 2013). In supplementary Table. A.4, the values for each individual experiment are displayed.

2.4. DISCUSSION

2.4.1. A NEW PHA FAMILY MEMBER

To our knowledge, this is the first scientific article that reports the finding of poly(3-hydroxyisobutyrate). No scientific publications have been found that describe the production of this compound with microbial communities, metabolically engineered organisms, or chemical synthesis. One patent on the production of 3-hydroxyisobutyrate with a metabolically engineered strain mentions poly(3-hydroxyisobutyrate) and proposes the possibility that this polymer is produced by the cultivated bacterium (Marx *et al.*, 2015). However, no measurements were reported to verify this statement. Furthermore, the chemical synthesis of the closely related poly(2-hydroxyisobutyrate) has been described (Kricheldorf *et al.*, 2008; Pittman *et al.*, 1978).

Although PHiB has not been described yet, it is known that environments with a high microbial diversity and a diverse carbon supply have the capacity to produce a broad range of uncommon PHAs. Reports from sewage treatment plants have revealed the presence of PHA consisting of 3-hydroxyhexanoate, 3-hydroxyheptanoate, 3-hydroxyoctanoate, and the branched monomers, 3-hydroxy-2-methylbutyrate and 3-hydroxy-2-methylvalerate (Odham *et al.*, 1986; Wallen *et al.*, 1974). In addition, in the sediments of an estuarine, PHAs consisting of 3-hydroxy-6-methylheptanoic acid and 3-hydroxy-7-methyloctanoate were discovered (Findlay *et al.*, 1983). These examples confirm that environmental communities can possess the metabolic capacity to produce uncommon and branched PHAs, and that 3-hydroxy-2-methylpropionate (PHiB) fits this pattern.

2.4.2. PUTATIVE PHiB METABOLISM

The presence of *Comamonas sp.* showed a clear correlation with PHiB production (see Fig. 2.5). PHiB is the dominant polymer when the relative abundance of *Comamonas sp.* is high, and PHB is the dominant polymer when the relative abundance of *Comamonas sp.* has reached a minimum and other species become dominant. Therefore, it is believed that the different micro-organisms in the enrichment produce homopolymers rather than a (P (3HB-co-3HiB)) copolymer.

According to literature, *Comamonas acidivorans* is capable of producing another uncommon PHA consisting completely of 4-hydroxybutyrate (4-HB) monomers, when supplied with the corresponding substrates (W. H. Lee *et al.*, 2004; Saito *et al.*, 1994). This unique feature makes it more plausible that the *Comamonas sp.* found in this study is responsible for the production of PHiB as homopolymer.
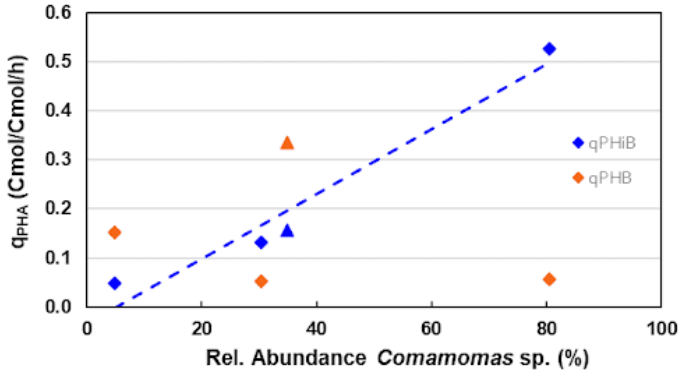
Figure 2.5.: Relative abundance of Comamomas sp. versus biomass specific production rate of PHiB and PHB for SBR1 -C1 to C3 (◆), and SBR1-A (of first 2.5h) (▲). The trendline accentuates the correlation between rel. abundance of *Comamonas sp.* and qPHiB.

Moreover, Sudesh *et al.*, 1998 suggests that this competence of *Comamonas acidivorans* was not due to the PHA synthase having a high specificity to incorporate 4-HB monomers, but rather the presence of an efficient metabolic pathway to produce 4-hydroxybutyryl-CoA from related precursors, such as 4-HB and 1,4-butanediol. A comparable principle might be responsible for PHiB production in this study, a *Comamonas sp.* possessing an effective machinery to convert isobutyrate into 3-hydroxyisobutyryl-CoA.

The results of the exchange experiment (SBR1-E) give some additional insights in the metabolic reactions underlying PHiB production. The instant response to this new substrate, butyrate, suggests that the metabolic pathways of PHA production, growth and catabolism from isobutyrate have overlap with the pathways from butyrate. Moreover, all yields shown in supplementary Table. A.4 hardly change when the substrate switched from isobutyrate to butyrate.

This advocates for the pathway proposed in Fig. 2.1, because here the carbon and electron stoichiometry is identical, whether PHiB is produced from isobutyrate, PHB from isobutyrate, or PHB from butyrate. In addition, the instant increase of $q_{s,max}$ and $q_{PHA,max}$ in butyrate-fed SBR1-E compared to isobutyrate-fed SBR1-C1, while µ remains very similar, indicates that the uptake of isobutyrate or the production of PHiB is rate-limiting (R2 and R5 in Fig. 2.1).

The major difference between SBR1-C1 and SBR1-E is the degradation rate of PHiB and PHB in the famine phase respectively, which is slower in SBR1-E than SBR1-C1 (k_d is -0.27 and -0.80 Cmmol/Cmmol/h respectively). Notably, the k_d of SBR1-E is very comparable to the k_d of the PHB-producing community of SBR2 (k_d is -0.3 Cmmol/Cmmol/h). These observations make it plausible that a different pathway is used for PHB degradation (R7 in Fig. 2.1 than for PHiB degradation (R8, R3 & R6 in Fig. 2.1). This pathway for PHB degradation with acetoacetyl-CoA

as intermediate (R7 in Fig. 2.1 and supplementary Table A.1) has been widely accepted in literature as most prevalent pathway (Oeding *et al.*, 1973; Senior *et al.*, 1973).

2.4.3. PHiB PRODUCTION AS SELECTIVE STRATEGY

Pulse-fed sequencing batch reactors with long periods of substrate depletion are well studied systems which are known to select for communities with high substrate uptake rates. Hoarding the substrate in the form of PHA via a small number of enzymatic steps is a productive strategy compared to the complex and relatively slow formation of biomass (Kleerebezem *et al.*, 2007). This line of reasoning can be extended to the formation of PHiB compared to PHB when isobutyrate is supplied as carbon source. PHiB is the type of PHA most closely related to isobutyrate, and the formation requires, according to Fig. 2.1, less enzymatic steps than the formation of PHB, and is, therefore, presumably faster. This idea is confirmed by our results which showed that the smallest feast time (i.e. highest substrate uptake rate) corresponds to the highest fraction of PHiB compared to PHB (e.g. SBR1-C1).

However, our results also showed that possessing the highest substrate uptake rate is not the only factor required to endure as a dominant community. At five moments in the enrichment of SBR1 the feast time increased up to 2 to 8-fold of the minimum feast time of 108 minutes. From two of these events the community dynamics were captured by 16S amplicon analysis. It revealed that the dominant *Comamonas sp.* washes out as can been seen from the decrease in relative abundance, and other species take over. These opportunistic species appeared rapidly, and disappeared almost with the same pace. Here, the question appears, what caused the fluctuations in community in SBR1?

According to Hibbing *et al.*, 2010, microbial competition for a limiting resource, carbon in our study, can been classified in two different strategies, exploitation and interference competition. Exploitation competition is a passive form of competition, focused on the rapid uptake of the limiting nutrient. Interference competition is an active form of competition, which involves direct antagonistic interaction with the opponent.

The data suggest that in SBR2 around the 60th cycle an example of exploitation competition manifested itself. Here, P. acidivorans slowly but steadily gained ground against *Zoogloea sp.* until it is washed out. It seems that the competitive strategy of P. acidivorans based on very fast substrate uptake coupled to PHA production in absence of growth in the feast phase, is very effective in washing out competitive strains.

The fluctuations in community in SBR1 revealed a very different pattern, and could be explained by interference competition. *Camelimonas sp.* or another species could have secreted an antimicrobial which inhibited the growth of *Comamonas sp.* In addition, there are a range of different microbial interactions difficult to uncover (e.g. viral infections, predation, cross feeding) which may also play a role in the competition of SBR1 (Conthe Calvo, 2018).

2.4.4. COMPARISON OF BUTYRATE TO ISOBUTYRATE IN RELATION TO OTHER CARBON SOURCES

The laboratorial research on PHA substrates has reached a level that many different carbon sources (acetate, propionate, lactate, butyrate, isobutyrate) have been assessed on their PHA production potential under virtually identical conditions (Jiang, 2011a, Jiang, 2011b; Marang, 2013).All enrichments except isobutyrate were dominated by Plasticicumulans acidvorans (acetate, propionate, butyrate), or a close relative (lactate). Butyrate reveals the highest potential in terms of PHA production rate ($q_{PHA,max}$), isobutyrate among the lowest (see Fig. 2.6a).

However, it appears that isobutyrate scores slightly higher than the frequently encountered substrate propionate. Part of this results could be explained by the length of the metabolic pathway from substrate towards PHA, which is for example shorter for butyrate then for acetate, lactate, and propionate. On the other hand, according to Fig. 2.1, the number of enzymatic steps for isobutyrate and butyrate towards PHA is the same. Therefore, other factors, such as enzyme kinetics, enzyme expression levels, and cell morphology, will also play a role.

Fig. 2.6b displays the PHA yield as a fraction of the maximal theoretical yield as estimated using the metabolic pathways described $Y_{PHA,S}/Y_{PHA,S}^{max}$. Here, it appears that butyrate, acetate, and lactate maximize their PHA yield by channelling almost all substrate towards PHA, while minimizing growth. Interestingly, although the propionate enrichment is dominated by *P. acidivorans*, the growth reaction is not eliminated like in the butyrate or acetate enrichments. This would suggest a substrate-related explanation for the poor PHA yield in the propionate enrichment.
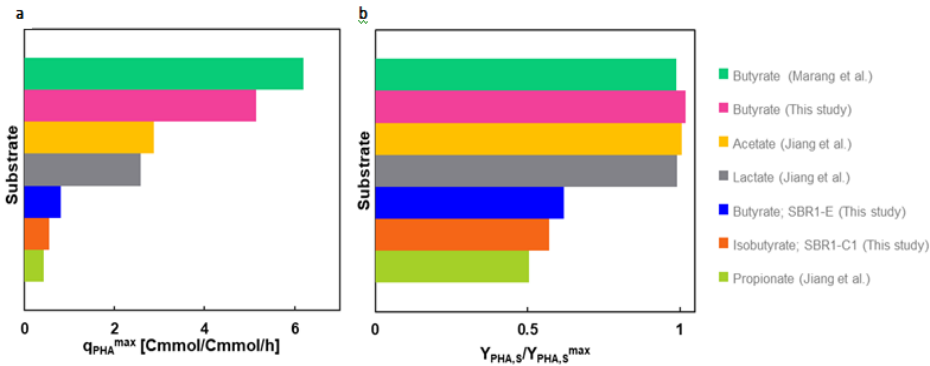
Figure 2.6.: Comparison of this study and other single-carbon studies with virtually identical experimental settings, including acetate and propionate (Jiang, 2011a), lactate (Johnson, 2009a), and butyrate (Marang, 2013). a) q_{PHA}^{max} in the feast phase of the SBR cycle. b) the PHA yield as a fraction of the maximal theoretical yield $Y_{(HA,S)}/Y_{PHA,S}^{max}$ in the feast of the SBR cycle.

It is presumed that for propionate and isobutyrate, that are both characterized by a lower substrate uptake rate and longer feast phase, a relatively large portion of the substrate is used for growth reactions, and PHA production yields are therefore much lower than the predicted maximum. On the other hand, when the isobutyrate enrichment is fed with butyrate (SBR1-E), no significant increase is observed of the PHA yield. This would suggest that community-related factors also play a role in the poor PHA yield of the isobutyrate enrichment (i.e. although the enriched community is capable of metabolizing isobutyrate, it is not capable of reaching high PHA yields).

When you assume that butyrate or acetate are more abundant in natural environments than isobutyrate, then it could be argued that it makes evolutionary sense to develop a high PHA productivity trait for butyrate and acetate, but not for isobutyrate. The fact that an all-round PHA champion like *P. acidivorans* completely lacks the capability to take up and/or process isobutyrate, as shown in experiment SBR2-E, supports this idea.

2.4.5. OUTLOOK

The experimental outcomes of structural isomers isobutyrate and butyrate reveal a very distinct behavior in terms of ecological stability, PHA productivity, and PHA composition. Although butyrate is superior from a bioprocess development point of view, this research shows that isobutyrate-rich streams can produce unique PHA polymers, although a lower maximum PHA content can be established in comparison with most other VFAs. This is the first scientific report identifying bacterial PHiB production. It supports the idea that selective environments are a powerful tool to discover new metabolic pathways and new type of polymers. Studying the physicochemical properties of this polymer, would be an interesting topic for future research, and might be the onset for a research area to produce PHA specialties by using microbial enrichments.

A

A<small>PPENDIX</small>-C<small>HAPTER</small> 2

	Reaction	Stoichiometry
1.	Butyrate uptake	1 Cmol But + 0.75 mol ATP → 1 Cmol But-CoA
2.	Isobutyrate uptake	1 Cmol IBut + 0.75 mol ATP → 1 Cmol IBut-CoA
3.	Isomerase of IBut-CoA to But-CoA	1 Cmol IBut-CoA → 1 Cmol But-CoA
4.	PHB production	1 Cmol But-CoA → 1 Cmol PHB + 0.25 mol $NADH_2$
5.	PHiB production	1 Cmol IBut-CoA → 1 Cmol PHiB + 0.25 mol $NADH_2$
6.	But-CoA to Ac-CoA	1 Cmol But-CoA → 1 Cmol Ac-CoA + 0.5 mol $NADH_2$
7.	PHB consumption	1 Cmol PHB + 0.25 mol ATP → 1 Cmol Ac-CoA + 0.25 mol $NADH_2$
8.	PHiB consumption	1 Cmol PHiB + 0.25 mol ATP + 0.25 mol $NADH_2$ → 1 Cmol IBut-CoA
9.	Growth on Ac-CoA	1.267 Cmol Ac-CoA + 0.2 mol NH_3 + 2.16 mol ATP → 1 Cmol $CH_{1.8}O_{0.5}N_{0.2}$ + 0.267 mol CO_2 + 0.434 mol $NADH_2$
10.	Catabolism	1 Cmol Ac-CoA → 1 mol CO_2 + 2 mol $NADH_2$
11.	Oxidative phosphorylation	1 Cmol $NADH_2$ + 0.5 mol O_2 → δ mol ATP

Table A.1.: Metabolic reactions. The metabolic reactions proposed for the isobu-
tyrate and butyrate model are on a carbon-mole base (per Cmol),
adapted from Marang, 2013. The origin and derivation of the stoichio-
metric reactions can be found in Van Aalst-Van Leeuwen *et al.*, 1997.
Later the model was optimized by Johnson, 2009b, and adapted to-
wards butyrate by Marang, 2013. The efficiency of the oxidative phos-
phorylation (δ) was assumed to be 2.0 for all experiments. But-CoA =
Butyryl-CoA, IBut-CoA = Isobutyryl-CoA, Ac-CoA = Acetyl-CoA.

2

Feast Phase/ (Butyrate/Isobutyrate)			
Growth	$Y_{CO_2,X}^{feast,max} = -\frac{40\delta-291}{250\delta-75}$	$Y_{O_2,X}^{feast,max} = -\frac{279}{200\delta-60}$	$Y_{X,S}^{feast,max} = -\frac{250\delta-75}{210\delta+216}$
	$Y_{N(Ac),X}^{feast,max} = -0.2$		
PH(i)B production	$Y_{CO_2,PH(i)B}^{feast,max} = -\frac{\delta-3}{10\delta-3}$	$Y_{O_2,PH(i)B}^{feast,max} = -\frac{27}{80\delta-24}$	$Y_{PH(i)B,S}^{feast,max} = -\frac{10\delta-3}{9\delta}$
Maintenance	$Y_{CO_2,Ac}^{feast,max} = -1$	$Y_{O_2,Ac}^{feast,max} = -1.25$	$Y_{ATP,S}^{feast,max} = -0.75 - 25\delta$
Famine phase (PHB, PHiB)			
Growth	$Y_{CO_2,X}^{famine,max} = -\frac{15\delta-241}{225\delta-25}$	$Y_{O_2,X}^{famine,max} = -\frac{1077}{900\delta-100}$	$Y_{X,PHO}^{famine,max} = -\frac{225\delta-25}{210\delta+216}$
	$Y_{N,X}^{famine,max} = -0.2$		
Maintenance	$Y_{CO_2,PH(i)B}^{famine,max} = -1$	$Y_{O_2,PH(i)B}^{famine,max} = 1.125$	$Y_{ATP,PH(i)B}^{famine,max} = -0.25 - 2.25\delta$

Table A.2.: Overview of stoichiometric yields. In the feast phase, growth, PH(i)B production and maintenance reactions take place, which are driven by substrate consumption. In the famine phase, only growth and maintenance reactions take place, which are driven by PH(i)B consumption. The yields are derived from the metabolic reactions (A.1) and balances for the conserved moieties (NADH, ATP, AcCoA, But-CoA, Ibut-CoA). The method for this derivation is described in detail by Van Aalst-Van Leeuwen *et al.*, 1997. The yields are expressed as a function of the efficiency of the oxidative phosphorylation (P/O ratio, symbol δ). All yields are on carbon-mole base (Cmol/Cmol).

Feast

PHA production	$q_{PHA,1}^{\text{feast}}(t) = \left(q_S(t) - \mu^{\text{feast}}(t) \cdot \frac{1}{Y_{X,S}^{\text{feast}}} - m_S\right) \cdot Y_{PHA,S}^{\text{feast}}$	if $q_{PHA,1}^{\text{feast}} \leq q_{PHA,2}^{\text{feast}}$	eq.1

With PHA inhibition $\quad q_{PHA,2}^{\text{feast}}(t) = q_{PHA}^{\max} \cdot \frac{C_S(t)}{K_S + C_S(t)} \cdot \left[1 - \left(\frac{f_{PHA,X}(t)}{f_{PHA,X}^{\max}}\right)^a\right] \qquad$ if $q_{PHA,1}^{\text{feast}} \geq q_{PHA,2}^{\text{feast}} \quad$ eq.2

Substrate uptake $\quad q_{S,1}(t) = q_S^{\max} \cdot \frac{C_S(t)}{K_S + C_S(t)} \qquad\qquad\qquad$ if $q_{PHA,1}^{\text{feast}} \leq q_{PHA,2}^{\text{feast}} \quad$ eq.3

With PHA inhibition $\quad q_{S,2}(t) = \mu^{\text{feast}}(t) \cdot \frac{1}{Y_{X,S}^{\text{feast}}} + q_{PHA}^{\text{feast}} \cdot \frac{1}{Y_{PHA,S}^{\text{feast}}} + m_S \qquad$ if $q_{PHA,1}^{\text{feast}} \geq q_{PHA,2}^{\text{feast}} \quad$ eq.4

Growth $\quad \mu^{\text{feast}}(t) = \mu^{\max} \cdot \frac{C_{NH_3}(t)}{K_{NH_3} + C_{NH_3}(t)} \cdot \frac{C_S(t)}{K_S + C_S(t)} \qquad\qquad\qquad$ eq.5

Maintenance $\quad m_S = \frac{m_{ATP}}{Y_{ATP,S}^{\text{feast}}} \qquad\qquad\qquad$ eq.6

CO$_2$ evolution $\quad q_{CO_2}^{\text{feast}}(t) = \mu^{\text{feast}}(t) \cdot Y_{CO_2,X}^{\text{feass}} + q_{PHA}^{\text{feast}}(t) \cdot Y_{CC_2,PHA}^{\text{feast}} + m_S \cdot Y_{CO_2,S}^{\text{feast}} \qquad$ eq.7

O$_2$ uptake $\quad q_{O_2}^{\text{feast}}(t) = \mu^{\text{feast}}(t) \cdot Y_{O_2,X}^{\text{feast}} + q_{PHA}^{\text{feast}}(t) \cdot Y_{O_2,PHA}^{\text{feast}} + m_S \cdot Y_{O_2,S}^{\text{feast}} \qquad$ eq.8

NH$_3$ uptake $\quad q_{NH_3}^{\text{feast}}(t) = \mu^{\text{feast}}(t) \cdot Y_{NH_3,X}^{\text{feast}} \qquad\qquad\qquad$ eq.9

Famine Phase

Growth $\quad \mu^{\text{famine}}(t) = Y_{X,PHA}^{\text{famine}} \cdot \left(q_{PHA}^{\text{famine}}(t) - m_{PHA}\right) \qquad\qquad\qquad$ eq.10

PHA degradation $\quad q_{PHA}^{\text{famine}}(t) = k \cdot \left(\frac{C_{x0}}{C_x(t)}\right)^{1/3} f_{PHA,X}(t)^{2/3} \qquad\qquad\qquad$ eq.11

Maintenance $\quad m_{PHA} = \frac{m_{ATP}}{Y_{ATP,PHA}^{\text{famine}}} \qquad\qquad\qquad$ eq.12

CO$_2$ evolution $\quad q_{CO_2}^{\text{famine}}(t) = \mu^{\text{famine}}(t) \cdot Y_{CO_2,X}^{\text{famine}} + m_S \cdot Y_{CO_2,PHA}^{\text{famine}} \qquad\qquad\qquad$ eq.13

O$_2$ uptake $\quad q_{O_2}^{\text{famine}}(t) = \mu^{\text{famine}}(t) \cdot Y_{O_2,X}^{\text{famine}} + m_S \cdot Y_{O_2,PHA}^{\text{famine}} \qquad\qquad\qquad$ eq.14

NH$_3$ uptake $\quad q_{NH_3}^{\text{famine}}(t) = \mu^{\text{famine}} \cdot Y_{NH_3,X}^{\text{famine}} \qquad\qquad\qquad$ eq.15

Overall

PHA content of cell dry weight $\quad PHAwt\%(t) = \frac{C_{PHA}(t) \cdot Mw_{PH(i)B}}{C_{PHA}(t) \cdot Mw_{PH(i)B} + \left(C_X(t) \cdot Mw_X / \left(1 - \tilde{f}_{\text{ash}}\right)\right)} * 100\% \qquad$ eq.16

Table A.3.: Model Kinetics.The kinetic expressions that describe the evolution of most essential compounds in the system. During the feast phase there are six compounds ($PHA, substrate, biomass, CO_2, O_2$, NH$_3$). During the famine there is no substrate, so only 5 compounds remain ($PHA, substrate, biomass, CO_2, O_2$, NH$_3$). The derivation of the expressions originated in the work of Van Aalst-Van Leeuwen *et al.*, 1997 and Johnson, 2009a.
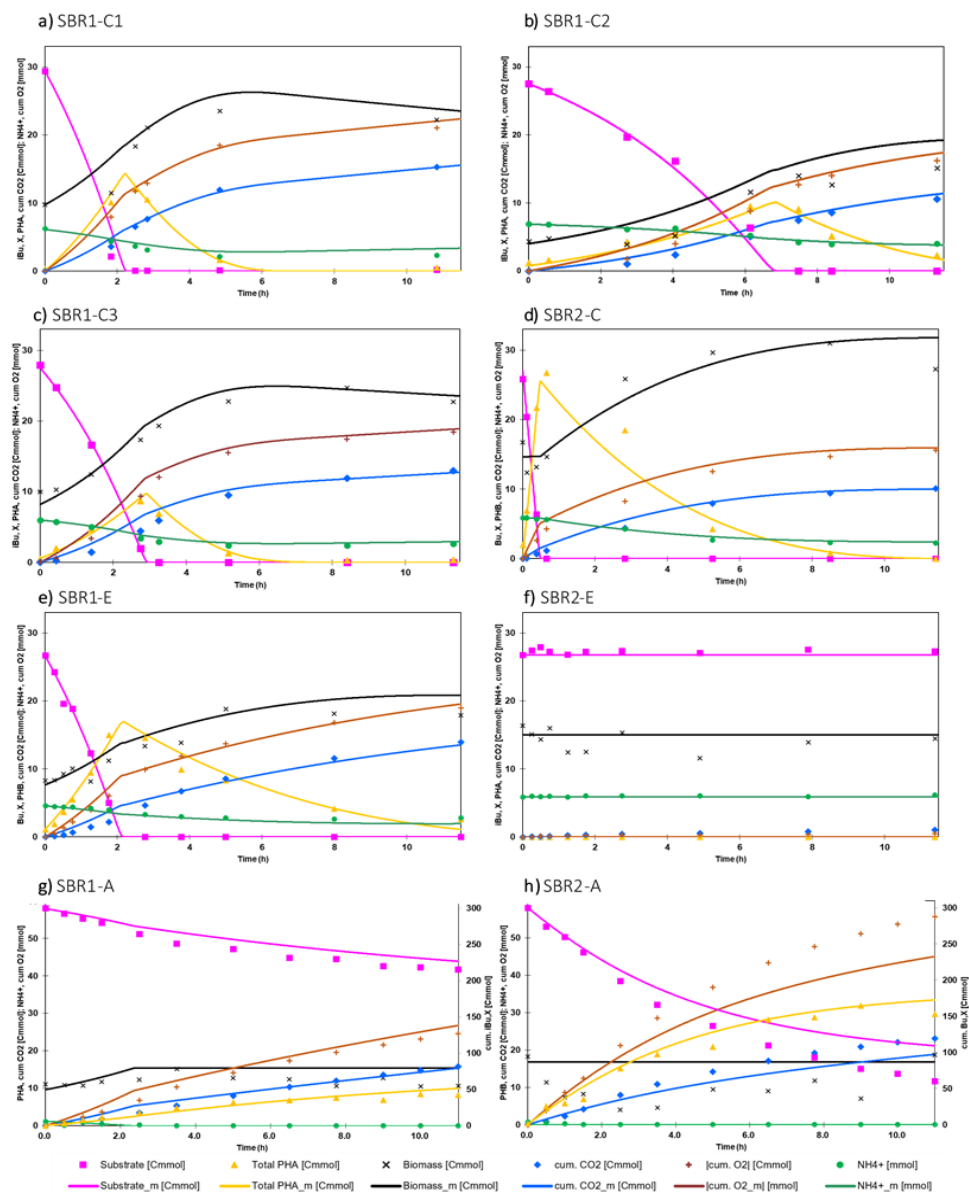
Figure A.1.: Modelled and observed results of experiments of the cycle experiments **(a-d)**, substrate exchange experiments **(e-f)**, and accumulation experiments (g-h). The symbols represent the observed data. The solid lines represent the modelled data (indicated with _m in legend), calculated with the kinetic expressions depicted in table A.3. In the SBR1 graphs (**a, b, c, e, g**) the substrate is isobutyrate, in the SBR2 graphs (**d, f, h**) the substrate is butyrate (indicated on axes). For both CO_2 and O_2 the cumulative values are shown. As O_2 is consumed, the absolute value of the cumulative values is depicted.

	Unit	Isobutyrate					Butyrate		
		SBR1-C1	SBR1-C2	SBR3-C3	SRR1-E	SBR1-A	SBR2-C3	SBR2-E	SBR2-A
Type of experiment		Cycle	Cycle	Cycle	Exchange	Accumulation	Cycle	Exchange	Accumulation
Carbon and electron balance									
C-Balance	%	2.33	2.63	2.23	-3.04	-11.92	-4.01	-0.47	-19.95
e-balance	%	1.15	2.58	2.09	-2.01	-13.80	-5.13	-0.38	-17.77
Model derived yields (first 2.5h of accumulation)									
Y_{X,S_feast}	[Cmmol/Cmmol]	0.27	0.39	0.41	0.24	0.19	0.004	-	0.00
Y_{PHA,S_feast}	[Cmmol/Cmmol]	0.54	0.34	0.34	0.58	0.60	0.96	-	0.92
Y_{CO_2,S_feast}	[Cmmol/Cmmol]	0.19	0.26	0.25	0.18	0.21	0.06	-	0.08
Y_{O_2,S_feast}	[mmol/Cmmol]	0.37	0.45	0.44	0.35	0.37	0.19	-	0.21
Y_{X,PHA_famine}	[Cmmol/Cmmol]	0.56	0.52	0.53	0.44	-	0.67	-	-
Y_{CO_2,PHA_famine}	[Cmmol/Cmmol]	0.63	0.48	0.73	0.56	-	0.33	-	-
Input parameters model									
mATP (fitted)	mmol/Cmmol/h	0.11	0.10	0.08	0.13	0.25	0.00	0.00	0.20
P/O ratio	-	2.00	2.00	2.00	2.00	2.00	2.00	2.00	2.00

Table A.4.: Outcome of the carbon and electron balance analysis, additional model derived yields, and input parameters of the model. The carbon balances and the electron (degree of reduction) balances were set up for all 7 experiments as an indication of the accuracy of the measurements. Here, the flux of carbon and electrons into the system was subtracted from the flux out of the system. mATP represents the amount of ATP required per Cmol biomass per unit of time, and was fitted to the data for every individual experiment. The P/O ratio reflects the efficiency of the oxidative phosphorylation and was assumed to be 2 mol ATP/mol NADH for all experiments (Beun *et al.*, 2000).

3

PRODUCTION OF MEDIUM-CHAIN-LENGTH PHA IN OCTANOATE-FED ENRICHMENTS DOMINATED BY *Sphaerotilus sp.*

Medium-chain-length polyhydroxyalkanoate (mcl-PHA) production by using microbial enrichments is a promising but largely unexplored approach to obtain elastomeric biomaterials from secondary resources. In this study, several enrichment strategies were tested to select for a community with a high mcl-PHA storage capacity when feeding octanoate. Based on the analysis of the metabolic pathways, the hypothesis was formulated that mcl-PHA production is more favorable under oxygen limited conditions than short-chain-length PHA (scl-PHA). This hypothesis was confirmed by bioreactor experiments showing that oxygen limitation during the PHA accumulation experiments resulted in a higher fraction of mcl-PHA over scl-PHA (i.e., a PHA content of 76 wt% with a mcl-fraction of 0.79 with oxygen limitation, compared to a PHA content of 72 wt% with a mcl-fraction of 0.62 without oxygen limitation). Physicochemical analysis revealed that the extracted PHA could be separated efficiently into a hydroxybutyrate-rich fraction with a higher M_w and a hydroxyhexanoate/hydroxyoctanoate-rich fraction with a lower M_w. The ratio between the two fractions could be adjusted by changing the environmental conditions, such as oxygen availability and pH. Almost all enrichments were dominated by *Sphaerotilus sp.* This is the first scientific report that links this genus to mcl-PHA production, demonstrating that microbial enrichments can be a powerful tool to explore mcl-PHA biodiversity and to discover novel industrially relevant strains.

3.1. INTRODUCTION

Polyhydroxyalkanoate (PHA) has attracted widespread attention as a biobased and biodegradable alternative to petrochemical-based materials. A broad range of bacteria are able to produce this biopolymer as an intracellular storage compound (Steinbüchel, 1991). The type of PHA monomer produced is determined by the substrate provided, the environmental conditions, and the microorganism. In its turn, the type of PHA polymer will determine the physicochemical properties of the final product. (Steinbüchel *et al.*, 1995; Zheng *et al.*, 2020).

PHA can potentially be produced cost-effectively by using microbial enrichments cultures and organic waste streams as feedstock. This approach diminishes the relatively large expenses for sterilization and raw substrates as required for pure culture production (Kleerebezem *et al.*, 2007), and avoids part of the waste disposal costs (Fernández-Dacosta *et al.*, 2015). To date, at least 19 pilot studies have been conducted, using municipal or industrial organic waste streams as feedstock (Estévez-Alonso *et al.*, 2021). In all these studies, the predominant type of PHA produced was the copolymer poly(3-hydroxybutyrate-co-3-hydroxyvalerate) (PHBV).

For thermoplastic applications, the mechanical properties of PHBV are already superior to the homopolymer, polyhydroxybutyrate (PHB) (Jain *et al.*, 2015). However, incorporating medium-chain-length PHA (mcl-PHA) monomers in the polymer is required for elastomeric applications. Mcl-PHA consists of larger monomers ranging from 6 to 14 carbons, while short-chain-length PHA (scl-PHA) consists of monomers with 3 to 5 carbons. Increasing the mcl-PHA monomer composition in the polymer will result in a lower melting temperature, a lower degree of crystallinity, a lower tensile strength, and a higher extension to break (Anjum *et al.*, 2016; Rai *et al.*, 2011). The production of these elastomers can expand the product utilization spectrum of PHA in the future, thereby potentially targeting rubber-like materials or adhesives (Elbahloul *et al.*, 2009; Pereira *et al.*, 2019).

The microbial metabolism to produce mcl-PHA is much less widespread than the metabolism for scl-PHA. In general, mcl-PHA production is linked to a special class of PHA synthases (PhaC Class II) possessed by a small number of organisms such as the well-studied *Pseudomonas sp.* or *Comamonas sp.*(Rai *et al.*, 2011; Tortajada *et al.*, 2013). However, some studies assert that in rare cases other classes of PHA synthases (class I and III) can incorporate hydroxyhexanoate (HHx) or hydroxyoctanoate (HO) monomers in the polymer (Quillaguamán *et al.*, 2010; Sudesh *et al.*, 2000). Because mcl-PHA metabolism appears to be sparse in the microbial world and because the available knowledge is incomplete, applying enrichment techniques offers an adequate approach to explore the microbial diversity (Stouten *et al.*, 2019).

The vast majority of the mcl-PHA research has been conducted with pure cultures. Nevertheless, a small number of laboratorial studies focused on using microbial enrichments with feast-famine conditions.This intermittent substrate feeding strategy generates a competitive advantage for bacteria that store PHA as carbon and electron reservoir inside their cell. A proof-of-principle was already established with C8, C9, C12 and C18 fatty acids (Alaux *et al.*, 2022; Z. Chen

et al., 2018; S. H. Lee *et al.*, 2011; Shen *et al.*, 2015), where it was found that medium-chain fatty acids form a suitable substrate for the enrichment of mcl-PHA producers. The mcl-PHA fractions of the total PHA content ranged from 0.06 to 0.88. However, the maximal obtained PHA contents were still rather low (23 to 49 wt%) compared to scl-PHA enrichment studies (Johnson, 2009a). In addition, an approach to understand and control the ratio between scl-PHA and mcl-PHA is still lacking.

PHA production from organic waste streams typically starts with the anaerobic fermentation of the feedstock where volatile fatty acids (VFAs) are formed, ranging from acetate to hexanoate (Kleerebezem *et al.*, 2015; F. Silva *et al.*, 2022). Via a chain elongation step, the carbon chain of these VFAs can be extended to synthesize octanoate (Angenent *et al.*, 2016; Kucek, 2016). In this research, octanoate was used as sole carbon source because octanoate is regarded as one of the optimal substrates for mcl-PHA biosynthesis (Li *et al.*, 2021; Sun *et al.*, 2007). Therefore, the aim of this research is to study which enrichment strategies result in a community with a high mcl-PHA storage capacity when feeding octanoate.

To this end, sequencing batch reactors (SBRs) were operated with octanoate as substrate. Analysis of the PHA metabolic pathways revealed that the production of mcl-PHA requires less oxygen respiration than scl-PHA production. This resulted in the hypothesis that mcl-PHA production has a competitive advantage over scl-PHA production in an oxygen limited environment. Therefore, the dissolved oxygen concentration was varied to understand and modify the enrichment process in terms of PHA content and composition. In addition, the pH of the SBRs was varied to study the effect of the toxicity of undissociated octanoic acid. For every operational steady state, the performance of the enrichments was characterized, including the maximum PHA storage capacity by means of accumulation experiments. An existing metabolic and kinetic model was adapted towards octanoate to derive the stoichiometric and kinetic parameters of all experiments (Johnson, 2009b). Finally, physicochemical polymer properties were determined to reveal information about the microbial origin of the produced polymer.

3.2. Materials and Methods

3.2.1. Enrichment in SBRs

Two double-jacket glass bioreactors with a working volume of 1.4 L (Applikon Biotechnology, The Netherlands) were operated for the enrichment of a PHA-storing microbial culture on octanoate. The setup and operation of these bioreactors were based on the conditions as described by Johnson, 2009a. The bioreactors were operated as non-sterile SBRs, subjected to a feast-famine regime with a cycle length of 12 h and a solids and hydraulic retention time (SRT and HRT) of 24 h, which implies that every cycle 50% of the SBR volume is replaced with fresh medium. The inoculum of the SBRs was aerobic activated sludge of a wastewater treatment plant (WWTP) (Harnaschpolder Delfluent, The Netherlands). Furthermore, the air flow rate to the bioreactors was set to 0.2 LN/min by means of a

mass flow controller (MX4/4, DASGIP®, Eppendorf, Germany), and the stirring speed was set to 800 rpm (TC4SC4, DASGIP®, Eppendorf, Germany). The temperature in the bioreactor was controlled at 30 °C ± 0.5 °C with the water jacket around the bioreactor and an external thermostat bath (ECO RE 630 S, Lauda, Germany). The pumps for feeding, effluent removal, and pH control, the stirrer, and the airflow were controlled by a hardware abstraction layer (HAL; TU Delft, the Netherlands), which in turn was controlled by a PC using a custom scheduling software (D2I; TU Delft, the Netherlands). The D2I was also used for data acquisition of the online measurements: dissolved oxygen (DO), pH, temperature, acid and base dosage, in- and off-gas composition and feed/water balances. Moreover, the bioreactors were cleaned about twice per week to remove biofilms from the glass walls and the sensors of the bioreactor. The medium consisted of a separate carbon and nutrient source. The carbon source concentration in the SBR was 4.75 mM octanoate. The nutrients concentrations in the SBR were composed of 6.74 mM NH_4Cl, 2.49 mM KH_2PO_4, 0.55 mM $MgSO_4.H_2O$, 0.72 mM KCl, 1.5 mL/L trace elements solution according to Vishniac *et al.*, 1957, and 5 mg/L allylthiourea (to prevent nitrification). To characterize the operational performances, the SBRs were subjected to multiple cycle analysis experiments.

3.2.2. PHA ACCUMULATION IN FED-BATCH BIOREACTOR

The PHA accumulation experiments were performed in the same bioreactors as the enrichment, but operated in fed-batch mode. The pH, temperature, and aeration rate were copied from the corresponding SBR. Half of the content of the SBR (700 ml) of the final cycle was used as seeding material for the accumulation experiment. In addition, 700 mL ammonium- and carbon-free medium was supplied. After 30 min, to ensure a temperature of 30 °C, a pulse of 6.7 mmol octanoate was supplied to each bioreactor. To prevent carbon source depletion throughout the PHA accumulation, octanoic acid (undiluted) and NaOH (1 M) were used to control the pH. In addition, pulses of 0.67 mmol octanoate were supplied every 2 h from t = 4 h to the end of the experiment. One accumulation was performed by replacing octanoate and octanoic acid by hexanoate and hexanoic acid. Nitrogen was limited during most of the accumulation since no nitrogen source was supplied to the bioreactors and only a small amount (< 1.7 mM of NH4+) remained from the previous SBR cycle. In this way, growth in the fed-batch bioreactor was limited. If necessary, a few drops of (10x diluted) Antifoam C (Sigma-Aldrich, USA) were added to inhibit the formation of foam. The experiments were terminated after 24 h.

3.2.3. VARYING pH IN THE BIOREACTOR

The pH was maintained by the addition of 1 M HCl and 1 M NaOH through an integrated revolution counter (MP8, DASGIP®, Eppendorf, Germany). During the first enrichment (S7), the set point of the SBR and the accumulation bioreactor were 7.0 ± 0.1. The set point was increased to 8.0 ± 0.1 and 9.0 ± 0.1 in the second (S8) and third enrichment (S9) respectively, and the corresponding accumula-

tions (A8 and A9) (Fig. 3.1). The microbial community of the first enrichment was used as inoculum for the second enrichment, and the microbial community of the second enrichment was used as inoculum for the third enrichment. In addition, every new enrichment was supplemented with fresh aerobic activated sludge from the WWTP. The oxygen transfer limitation experiments (Section 3.2.4) and hexanoate accumulation were conducted at pH 8.0 ± 0.1. All different operational states in this study were enriched for at least 70 cycles.

3.2.4. Dissolved oxygen limitation

In aerobic feast-famine SBRs, oxygen consumption is a key indicator of the PHA production behavior of the community (Stouten *et al.*, 2019). The fraction of the cumulative amount of oxygen consumed in the feast phase (O_2feast) was calculated several SBR cycles by using equation 3.1.

$$O_2 \text{ feast } (\%) = \frac{\text{Cum. } o_{2 \text{ feast}} (\text{mol})}{\text{Cum. } o_{2 \text{ feast}} (\text{mol}) + \text{Cum. } o_{2 \text{ famine}} (\text{mol})} \tag{3.1}$$
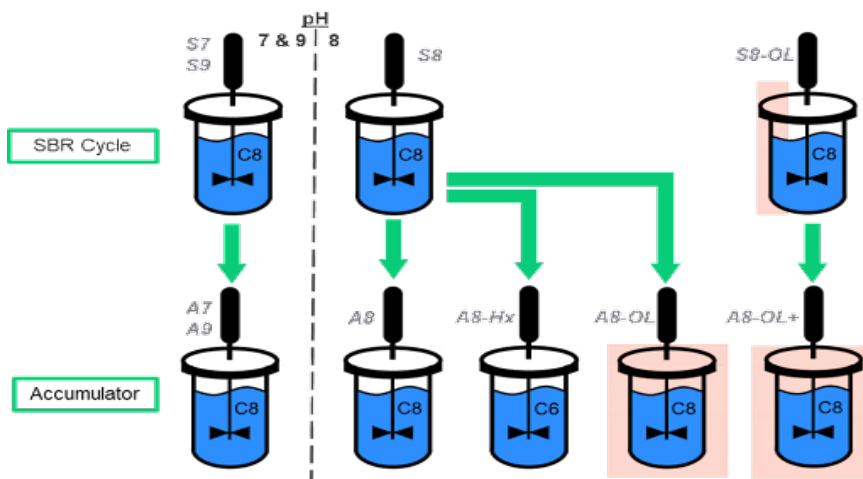
Figure 3.1.: Experimental overview of this study. C8 refers to octanoate and C6 refers to hexanoate as substrate. The name of each experiment is displayed in grey. Experiments under oxygen limitation (OL) are indicated by the pink areas.

Moreover, the influence of the dissolved oxygen concentration, and the corresponding oxygen consumption rate, on the PHA composition was investigated. Dissolved oxygen limitation was achieved by lowering the stirrer speed from 800 to 200 rpm when substrate was available. This means that during the enrichment the stirrer speed was automatically lowered during the feast phase (S8-OL Fig. 3.1). For both enrichment S8 and S8-OL, an oxygen limited accumulation

experiment was conducted to test the maximum PHA storage capacity (A8-OL and A8-OL+ respectively). During the oxygen limited accumulation experiments the stirrer speed was at all times at 200 rpm. The microbial community of the enrichment at pH 8 was used as starting material for the oxygen limited enrichment, again supplemented with fresh aerobic activated sludge from the WWTP. The volumetric mass transfer coefficient ($k_L a$) for a stirrer speed of 200 and 800 rpm was determined by using the dynamic gassing out method (Garcia-Ochoa *et al.*, 2009; van 't Riet, 1979) under the operational conditions of the experiment.

3.2.5. PHA EXTRACTION AND FRACTIONATION

During the accumulation experiments, 50 ml cell suspension was collected from the bioreactor after 12 h. After centrifuging and freeze-drying, ±350 mg of the dried biomass was mixed with 12.5 ml chloroform. The suspension was incubated for 3 h at 60 °C while manually shaken every 30 min. Then, the suspension was filtered (0.45 µm filter). Lastly, the chloroform was evaporated in a fume hood to obtain purified PHA.

Part of the purified PHA from the accumulation at pH 8 (A8) was fractionated by selective precipitation. To this end, the PHA was divided in 5 parts of ±20 mg and redissolved in 0.8 ml chloroform. Different volumes of antisolvent (1-heptane) were added (0.9, 1.1, 1.4, 1.6, and 15). After 15 min incubation, the tubes were centrifuged and the supernatant was decanted into another tube. Only the tube with 15 volumes of 1-heptane was incubated for 48 hours. Then, the solvent-antisolvent mixture in all tubes was evaporated in a fume hood. The obtained PHA fractions were analyzed by gas chromatography.

3.2.6. ANALYTICAL METHODS

The performance of the cycle and accumulation experiments were characterized by online measurements (DO, pH, acid/base dosage, and in−/off-gas composition) with the equipment and software described above, and with offline samples (VFAs, ammonium, PHA, total and volatile suspended solids). The composition of the active biomass was assumed to be $CH_{1.8}O_{0.5}N_{0.2}$ (Beun *et al.*, 2002. A detailed description of the analytical methods is given by Johnson, 2009a. A modification has been made for the ammonium measurement. These samples were measured with a Gallery™ Plus Discrete Analyzer (Thermo-Fisher Scientific, USA).

The method to analyze the PHA composition of the biomass by gas chromatography (GC) was also modified to include mcl-PHA. In brief, the PHA in the biomass was hydrolyzed and esterified in the presence of concentrated acid, propanol, and dichloroethane with a ratio of 1/4/5 (v/v/v) for 3 h at 100 °C. In this research, H2SO4 was used as acid instead of HCl. The formed propylesters, which accumulated in the organic phase, were analyzed by a gas chromatograph (model 6890N, Agilent, USA). The PHA analysis method was expanded to include the quantification of poly(3-hydroxyhexanoate) (PHHx) and poly(3-hydroxyoctanoate) (PHO) by using methyl 3-hydroxyhexanoate (Sigma-Aldrich, USA) and methyl 3-hydroxyoctanoate (Santa Cruz Biotechnology, USA) as standard. Furthermore, the method

for measuring volatile suspended solids was substituted by a thermogravimetric analysis (TGA) using a Perkin Elmer TGA 8000. Around 2 mg of freeze-dried biomass sample was heated from 35 °C to 105 °C (10 °C/min), followed by an isothermal step (100 min), followed by a second heating run from 105 °C to 550 °C (10 °C/min), followed by a second isothermal step (60 min). All steps were under a nitrogen atmosphere, while in the last isothermal step the nitrogen gas was switched to air. The TGA data was also applied as alternative method to determine the PHA weight percentage of the biomass (W. S. Chen, Strik, *et al.*, 2017b). A differential scanning calorimeter (DSC) measurement was performed to measure the melting (Tm) temperature of the extracted PHA (section 3.2.4) using a Perkin Elmer DSC−7.

First, the PHA sample was cooled from 25 to −70 °C at a rate of 20 °C/min. Then, the PHA sample was heated from −70 to 180 °C at the same rate. After 10 min at 180 °C, the sample was quench cooled to −70 °C at a rate of 100 °C/min. In a second heating run, the sample was heated again to 140 °C at a rate of 20 °C/min. This run was used for Tm determination. All steps were performed under a nitrogen atmosphere. A PHBVHx poly(3-hydroxybutyrate-co-3-hydroxyvalerate- co-3-hydroxyhexanoate) (94%/2%/4%) reference sample (Sigma-Aldrich, USA) was measured for comparative purposes. A gel permeation chromatography (GPC) measurement was performed to measure the molecular weight distribution of the extracted PHA (section 3.2.4) using a Shimadzu Prominence GPC system equipped with a Shodex LF−804 column. Dimethyl furan (DMF) was used as the eluent at a flow rate of 1 mL/min at 40 °C. Before injection, the PHA sample was first dissolved in chloroform at a concentration of 30 mg/mL, then diluted with 9 volumes of DMF, and subsequently filtered. Data of the refractive index detector was quantified with a universal calibration of monodisperse polystyrene standards with the help of LabSolutions software.

3.2.7. MICROBIAL COMMUNITY ANALYSIS

To analyze the microbial composition of the enriched cultures, 2 mL of bioreactor content was collected in an Eppendorf tube. These samples were taken approximately 2 times per week during the enrichment phase, and in addition during the cycle and accumulation experiments. The tubes were centrifuged (13,300 g; 5 min). The pellet was stored at −20 °C until analysis. After defrosting, genomic DNA was extracted using the DNeasy UltraClean Microbial Kit (Qiagen, Germany), following the manufacturer's instructions. DNA quantification was carried out using the Qubit® dsDNA Broad Range Assay Kit (Qubit® 2.0 Fluorometer, Thermo Fisher Scientific, USA), following the manufacturer's instructions. Afterwards, about 50 µL of isolated (16S) DNA was sent to Novogene Ltd. (Hongkong, China) for amplicon sequencing of the V3-4 region of the 16S rRNA gene and for metagenomic sequencing. A description of the procedure for metagenomic sequencing is presented by Pabst *et al.*, 2021. Various genomic fragments were aligned with published sequences from GenBank using NCBI BLAST tool to find related genes and strains (Altschul *et al.*, 1990). All sequence data of this study have been deposited in GenBank with BioProject ID PRJNA831682

3

3.2.8. METABOLIC MODEL AND PARAMETER IDENTIFICATION

A metabolic and kinetic model proposed by Johnson, 2009b was used as starting point for this study. The previous model was transformed from acetate uptake and PHB production to octanoate (and hexanoate) uptake and PHB, PHHx, and PHO production (Fig. 3.2). The model contains a set of metabolic and kinetic expressions which together describe the consumption and formation of the main compounds in the bioreactor, that is PHA (PHB, PHHx, PHO), biomass, organic substrate, CO_2, O_2, and ammonium.
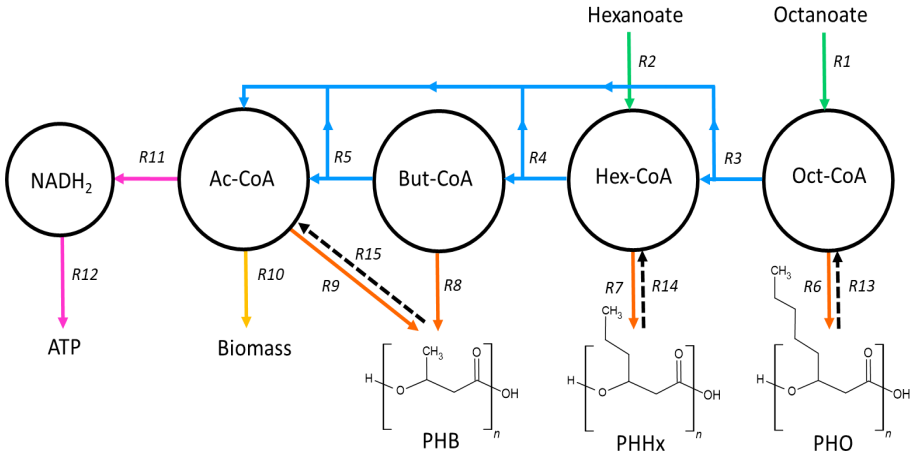
Figure 3.2.: A schematic representation of the proposed PHA metabolism. R1 and R2 represent the uptake reactions when substrate is present. R3, R4, R5 represent different stages of the beta-oxidation pathway. R6 to R9 represent the PHA production routes, while R13 to R15 represent the PHA degradation routes. R10 represent anabolic reactions, while R11 and R12 represent catabolic reactions. Ac-CoA = Acetyl-CoA, But-CoA = Butyryl-CoA, Hex-CoA = Hexanoyl-CoA, Oct-CoA = Octanoyl-CoA.

It was assumed that octanoate is taken up and activated to octanoyl-CoA at the cost of 3 ATP (R1). Then, octanoyl-CoA can be converted to PHO via part of the beta-oxidation pathway (R6) Alternatively, octanoyl-CoA can complete the beta-oxidation pathway one (R3) or two (R3 + R4) times, and subsequently form PHHx (R7) and PHB (R8). Every time the beta-oxidation is completed acetyl-CoA is formed, which can be funneled into PHB (R9), into growth (R10) or into catabolism (R11 and R12). When the external substrate is depleted (famine phase), the different types of PHA are degraded (R13, R14 and R15) to sustain growth and catabolic reactions. When hexanoate is supplied as carbon source (R2), the same set of reactions apply except for R1, R3, R6 and R13. The entire reactions of Fig. 3.2 are displayed in Table B.1.

The obtained reactions were used to calculate the stoichiometric yields by bal-

ancing the conserved moieties (Octanoyl-CoA, Hexanoyl-CoA, Butyryl-CoA, Acetyl-CoA, NADH, ATP). The stoichiometric yields and the kinetic expressions shown in Table B.2 and B.3 form the basis of the model. The stoichiometric yields that encompassed PHA were calculated by multiplying the stoichiometric yield of the specific PHA type by the fraction of this type of PHA at the moment the cellular PHA content was maximal, as shown in the example of PHA yield on substrate ($YPHA_S$ in Cmol/Cmol) in equation 3.2.

$$Y_{PHA,S} = Y_{PHB,S} \cdot \frac{PHB_{\max}}{PHA_{\max}} + Y_{PHHx,S} \cdot \frac{PHHx_{\max}}{PHA_{\max}} + Y_{PHO,S} \cdot \frac{PHO_{\max}}{PHA_{\max}} \tag{3.2}$$

Here, $Y_{PHB/PHHx/PHO,S}$ (Cmol/Cmol) describe the stoichiometric yield of the specific type of PHA on substrate, and $\frac{PHB/PHHx/PHO_{\max}(Cmol)}{P_{HA_{\max}}(Cmol)}$ describe the fraction of this type of PHA measured by GC analysis. In accordance with the study of J. Tamis, 2014, the PHA degradation function was adapted. The efficiency of the oxidative phosphorylation (P/O ratio) was assumed to be 2.0 mol ATP/mol NADH for all experiments (R12 in Fig. 3.2). FADH2, produced in the TCA cycle and the beta-oxidation pathway, was assumed to be a NADH equivalent in terms of ATP yield. The trends obtained by the model are fitted to the experimental data. Then, the biomass specific rates and actual yields were derived from the model.
Throughout this work, PHO, PHHx or PHB are defined as monomers of HO, HHx, or HB embedded in a polymer respectively, regardless of whether this is a copolymer or a homopolymer.

3.3. RESULTS

3.3.1. START ENRICHMENT

An SBR, pulse-fed with octanoate, was operated for 80 cycles at pH 7. During this enrichment, online data (e.g., O_2 in off-gas) and offline data (e.g., PHA and 16S amplicon analysis) were examined. The addition of nutrients and carbon source at the beginning of each cycle was followed by a phase of a high oxygen uptake rate, of which the duration and the magnitude were extracted from the off-gas data. As the experiment proceeded, both the duration of the feast phase (feast time) and the fraction of oxygen consumed in the feast phase (O_2feast, as calculated by equation 3.1) showed a downward trend (Fig. 3.3a). The shift in both variables suggested that the community shifted from a growth-oriented strategy towards a PHA hoarding strategy. The PHA analysis data confirmed this hypothesis by revealing that PHA production in the form of PHB was low in the first cycles, but significantly increased between the 10th and 24th cycle (Fig. 3.3b). Then, the first stable phase commenced (cycle 22-38) which was characterized by PHB production (42 wt% at the end of the feast phase), an average feast time of 81 ± 18 min, and an average O_2feast of 59 ± 3%. The amplicon sequencing data revealed that *Acinetobacter sp.* or *Zoogloea sp.* are likely to be responsible for this functionality (Fig. 3.3c).

3
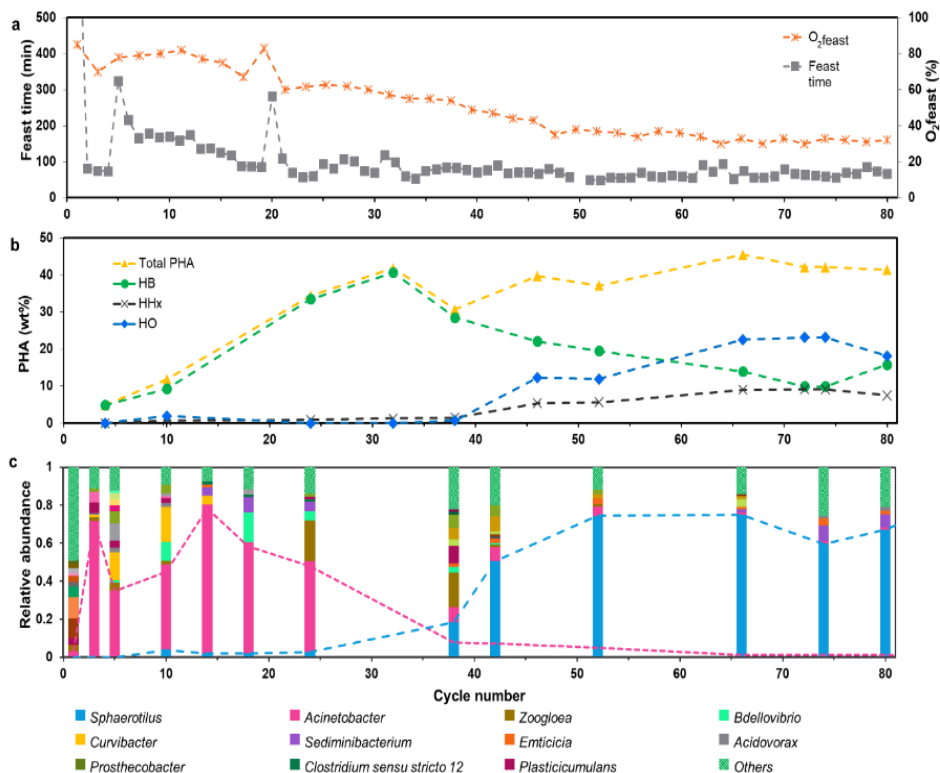
Figure 3.3.: Overview of online and offline data of the enrichment at pH 7. **a:** the length of the feast phase (feast time) and the fraction of O2 consumed in the feast phase (O$_2$feast) both derived from the off-gas data. **b:** the PHA content at the end of the feast phase, including specification of the different monomers. **c:** the relative abundance of genera derived from 16S amplicon sequencing. The two most abundant genera are shown both with stacked columns and lines. Only genera with a relative abundance of more than 1% are depicted in the graph.

After the 38th cycle, another shift in functionality and community structure occurred followed by a second stable phase (cycle 48-80). This phase is characterized by the production of PHA (42 wt%) consisting of hydroxyoctanoate (HO) (23 wt%), hydroxyhexanoate (HHx) (9 wt%), but also hydroxybutyrate (HB) (10 wt%) monomers. This phase revealed a significantly lower average value for the O_2feast (34 ± 3%) compared to the first stable phase (59 ± 3%). In addition, the feast times also showed a slight decrease (65 ± 11 min). A clear link with the 16S amplicon sequencing data is observed where *Sphaerotilus sp.* became abundant from the 38th cycle onwards and remained the dominant species during the second stable phase (Fig. 3.3).

3.3.2. PERFORMANCE OF ENRICHMENT AT VARYING pH

The pH of the bioreactor was increased from pH 7 to pH 8 and pH 9 in two consecutive enrichment experiments. At each pH, a detailed insight of the performance of the enrichment was obtained by the analysis of an SBR cycle and an accumulation experiment. The main experimental results are presented in Fig. 3.4 and Fig. 3.3 a & c (pH = 8). More detailed information can be found in Table 3.1, and Fig. B.1 and Table B.4 in the supplementary online materials.
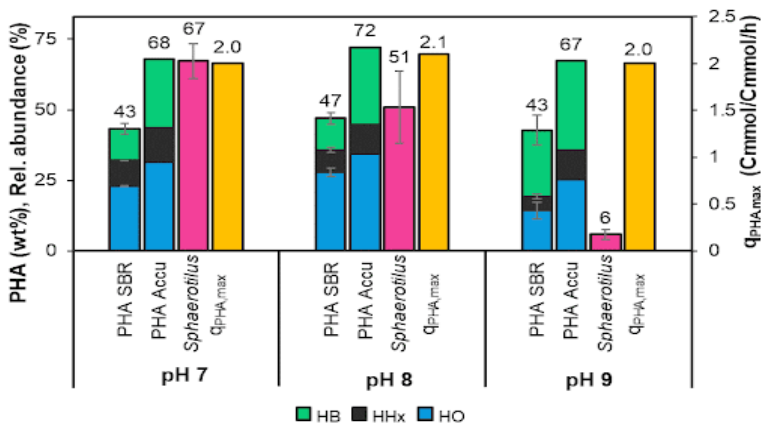
Figure 3.4.: Main results of the enrichment experiments at varying pH. 'PHA SBR' is the average PHA wt% at the end of the feast phase over the last three samples of the SBR enrichment. 'PHA Accu.' is the PHA wt% of the maximal value in the accumulation experiment. 'Sphaerotilus' is the relative abundance of this genus in the 16S amplicon data over the last three samples of in the enrichment. $q_{PHA,max}$ is calculated from the SBR cycle analysis in the enrichement. In supplementary Fig. B.1, all experimental results fitted with the metabolic model are shown, including off-gas, ammonium and biomass.

The PHA content at the end of the feast phase appeared to be slightly higher for the enrichment at pH 8 (S8), than for the enrichment at pH 7 (S7) and pH 9 (S9). The PHA monomer composition was reasonably similar in S7 and S8, while in S9

more PHB was produced. For the maximum PHA content in the accumulation experiments a similar trend was observed. The accumulation at pH 8 (A8) obtained the highest PHA content with 72 wt% PHA (HO fraction of 0.49, HHx fraction of 0.14, HB fraction of 0.38). The biomass specific PHA production rate ($q_{PHA,max}$) remained fairly constant regardless of pH value. Interestingly, *Sphaerotilus sp.* was dominant at pH 7 and pH 8, while it was outcompeted at pH 9 as revealed by both 16S amplicon data and microscopic observations (data not shown). It was decided to continue the following experiments at pH 8, as the results at pH 8 appeared to be most favorable in terms of PHA production. Nevertheless, it must be noted that the community at pH 8 was enriched for more cycles than the community in S7.

3.3.3. THE IMPACT OF OXYGEN LIMITATION

The oxygen supply rate was decreased in the bioreactor to test the hypothesis that oxygen limitation favors the production of mcl-PHA over scl-PHA. This was achieved by lowering the stirrer speed during the feast phase of the SBR and during the whole accumulation. This resulted in a decrease of the kLa from 93.5 h^{-1} to 5.3 h^{-1} and a decrease in dissolved oxygen concentration from 5.7 mg/L to below 0.1 mg/L. A significant increase in feast time was observed in the SBR with oxygen limitation (S8-OL) compared to the standard SBR (S8) (1.7 h instead of 1 h), indicating that the biomass specific rates are impacted by the oxygen limited environment (Fig. 3.5 and Table 3.1). Aside from the difference in feast time, the PHA trends of the two cycle analyses showed a similar profile (Fig. 3.6 a & b). No significant difference in the ratio of PHA monomers produced was observed. However, a slightly larger fraction of the substrate is directed towards PHA production under oxygen limitation indicated by a higher YPHA,S, and resulting in a higher PHA content at the end of the cycle in S8-OL (55 wt%) compared to S8 (46 wt%). Interestingly, the oxygen limited regime did not cause a major shift in the microbial community structure; *Sphaerotilus sp.* remained the dominant genus.

Two accumulation experiments were performed under oxygen limited conditions. A8-OL was inoculated with biomass from the SBR at pH 8 without oxygen limitation (S8). A8-OL+ was inoculated from the oxygen limited SBR (S8-OL) (see experimental overview in Fig. 3.1). The results were compared to the standard accumulation at pH 8 (A8) (Fig. 3.6 c-e and Table 3.1). Although all biomass specific rates decreased when oxygen limitation was imposed, the total amount of PHA after 12 h accumulation and the final PHA content were remarkably identical to non-oxygen limited conditions (all experiments between 81.4 and 82.2 mCmol and between 71.9 and 76.5 wt% respectively). Again, the yield values expressed that PHA production is slightly more efficient, and growth is slightly less efficient when oxygen is limited. A significant difference was detected in PHA composition when comparing the oxygen limited accumulations (A8-OL and A8-OL+) to the standard accumulations (A8). The PHB content decreased significantly, the PHHx content remained fairly constant, and the PHO content increased significantly. Oxygen limited conditions resulted in a higher mcl-fraction of the PHA,
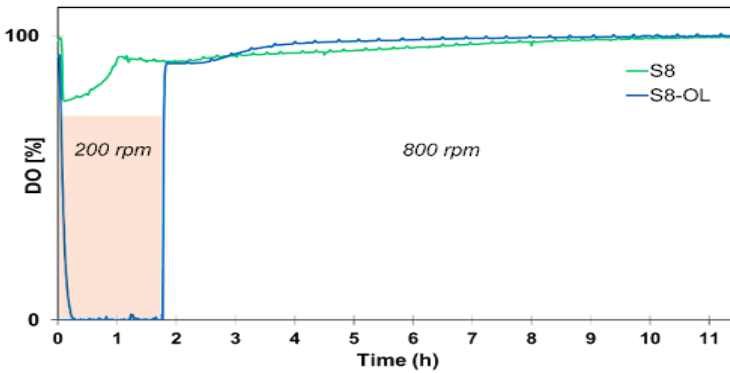
Figure 3.5.: Dissolved oxygen profile during one cycle of the standard SBR at pH 8 (S8) and of the SBR under oxygen limitation (S8-OL). For S8-OL, stirrer speed is lowered to 200 rpm in the feast phase indicated by the pink area.

from 0.62 in A8 to 0.79 in A8-OL and 0.76 in A8-OL+. The difference between the two oxygen limited accumulations (A8-OL and A8-OL+) is small in every aspect suggesting that the influence of enriching under oxygen limitation is minimal as was already expected from the analysis of the SBRs.

3.3.4. ACCUMULATION WITH HEXANOATE

One accumulation experiment was performed with hexanoate (A8-Hx) as sole carbon source inoculated with biomass enriched on octanoate (S8). Fig. 3.6 f reveals that the biomass demonstrated an instant response towards this new substrate. However, the biomass specific rates as well as the final PHA amount and content were lower than in the standard accumulation (A8) (Table 3.1). Moreover, the PHA consisted predominantly of PHB while PHO was absent. The PHHx content was again very similar to A8.

3.3.5. BIOREACTOR DATA VALIDATION

The carbon and electron balances of the SBR cycles closed on average for 99.9 ± 5.3%. For the accumulation experiments, a gap in the mass balance developed over time, resulting in an average closure of 66.5 ± 13%. Although these gaps have been observed in accumulation experiments of previous research (Marang, 2016; Vermeer et al., 2022), the gaps in this study are larger. A possible explanation for the large size of these gaps forms the feeding method during the accumulation which entails the addition of undiluted octanoic or hexanoic acid. It was hypothesized that the undiluted acid was not able to dissolve completely in the medium. To confirm this hypothesis, undiluted octanoic acid was fed to a

3

		SBR Cycles				Accumulations					
	Unit	S7	S8	S9	S8-OL	A7	A8	A9	A8-OL	A8-OL+	A8-Hx
Number of cycles enriched		80	99	70	70	80	89	70	93	70	99
Length feast phase	h	1.1	1.0	1.2	1.7	5.3	1.5	1.1	1.8	2.6	1.9
Total PHA max.	%	42	46	49	54	68	72	67	73	76	57
HB max.	%	10	12	24	14	24	27	32	18	16	49
HH max.	%	9	7	7	9	12	10	10	10	11	8
HO max.	%	23	26	18	31	32	35	25	45	49	0
TGA	%	51.0	52	53	55	70	77	68	74	73	61
mcl-fraction		0.76	0.73	0.51	0.73	0.64	0.62	0.53	0.76	0.79	0.15
Fraction O2 feast/ O2 consumed total (mmol)		0.28	0.33	0.27	0.26	55.4	39.3	40.5	32.3	27.8	39.1
Sphaerotilus natans		60%	43%	3%	77%	72%	43%	3%	64%	77%	70%
Other most abundant				*Thau (39%)*				*Thau (39%)*			
Second most abundant		*Sedim (8%)*	*Dechl (4%)*	*Phrea (20%)*	*Ferru (10%)*	*Zoo (4%)*	*Dechl (4%)*	*Phrea (20%)*	*Phrea (6%)*	*Ferru (10%)*	*Lead (4%)*
$q_{s,max}$	mCmol/mCmol/h	-2.30	-2.10	-2.00	-2.30	-0.70	-1.40	-1.4	-1.00	-0.8	-1.10
μ_{max}	mCmol/mCmol/h	0.40	0.22	0.07	0.10	0.10	0.30	0.20	0.15	0.15	0.11
$q_{PHA,max}$	mCmol/mCmol/h	2.00	2.10	2.00	2.30	0.80	1.30	1.30	0.90	0.67	0.90
$Y_{X,S}$	mCmol/mCmol	0.19	0.11	0.04	0.05	0.15	0.20	0.22	0.16	0.13	0.13
$Y_{PHA,S}$	mCmol/mCmol	0.77	0.88	0.96	0.94	0.75	0.70	0.72	0.76	0.77	0.74
$Y_{O2,PHA}$	mmol/mCmol	0.19	0.19	0.14	0.16	0.40	0.43	0.39	0.34	0.34	0.47
$Y_{O2,S}$	mmol/mCmol	0.21	0.16	0.13	0.15	0.30	0.30	0.28	0.26	0.26	0.35

Table 3.1.: Overview of the main measured data, microbial community data (16S amplicon sequencing), and model derived yields and biomass specific rates of the cycle and accumulation experiments. *Thau = Thauera sp., Sedim = Sediminibacter sp., Dechlo = Dechloromonas sp., Zoo = Zoogloea sp., Phre = Phreatobacter sp., Ferru = Ferruginibacter sp., Leadb = Leadbetterella sp.*
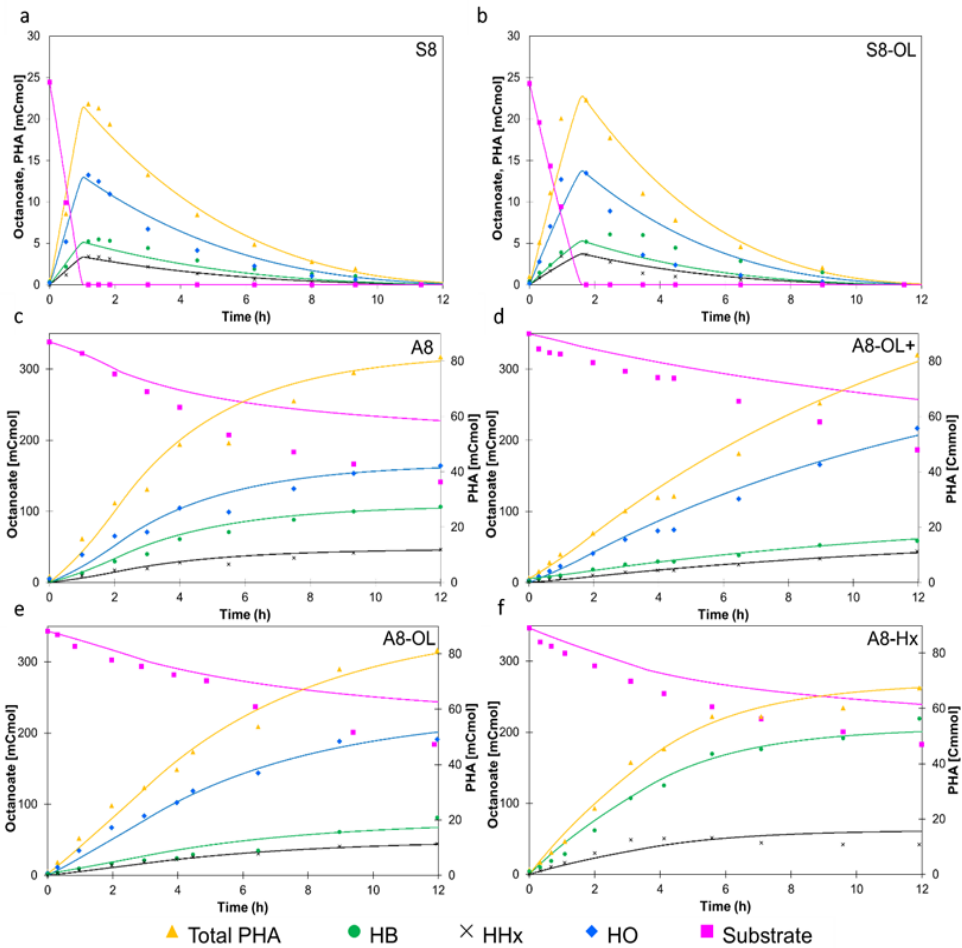
Figure 3.6.: Overview of PHA and substrate analysis of S8 (a), S8-OL (b), A8 (c), A8-OL+
(d), A8-OL (e), and A8-Hx (f). The symbols represent the measured data,
while the lines represent the modeled data. The yellow data points represent
the total amount of PHA in the bioreactor, which is a sum of the individual
monomers (HO, HHx, HB). For the accumulations, the substrate consumption
is presented as a cumulative curve starting and ending at an arbitrary value.
In supplementary Fig. B.1, all experimental results fitted with the metabolic
model are shown, including off-gas, ammonium and biomass

bioreactor without biomass to aim for a concentration of 500 mg/L. Nevertheless, measurements showed that the medium contained 420 ± 6 mg/L after 2 h of incubation with a stirrer speed of 800 rpm at pH 8, a difference of 17%. This result makes it plausible that part of the octanoic acid did not dissolve in the above-described accumulation experiments as well.

Thermogravimetric analysis (TGA) was used as a secondary PHA quantification method to validate the PHA analysis results of the GC (Chan et al., 2017). On average, the TGA measured 3.0 ± 2.6 wt% higher than the GC which confirms that the applied GC method is reliable for mcl-PHA quantification (Table 3.1).

3.3.6. METAGENOMIC ANALYSIS

One biomass sample, taken at the time of the cycle analysis of pH 7 (S7), was subjected to metagenomic analysis. The outcome revealed a relative abundance of 54% *Sphaerotilus natans*, which is in accordance with the 16S amplicon results. The remaining microbial community is very fractionated with the second most abundant microorganism only having a relative abundance of 0.6%. The genome of S. natans displays the highest similarity with the subspecies *S. natans subsp. sulfidivorans* D-507 (accession: CP035708.1).

Two copies of the PHA synthase gene were found both in the genomic data of this study and in the online available genome of *S. natans subsp. sulfidivorans* D-507. The first synthase gene has 100% similarity with a PhaC class I synthase found in *S. natans* (McCool *et al.*, 2001). The second PHA synthase is classified as alpha/beta fold hydrolase in *S. natans* (Ollis *et al.*, 1992), but it reveals a high similarity with PHA synthases in other microorganisms which are not assigned to a specific class of PHA synthases (e.g. 96% identities with PHA synthase in *Leptothrix sp. C29)* (Whitman *et al.*, 2015). Although both PHA synthases have roughly the same size (1200 nucleotides), the similarity between the two genes is low. Only two fragments of the genes revealed reasonable similarity. The first alignment had 154/271 (71%) identities, while the second alignment had 166/251 (66%) identities.

3.3.7. PHYSICOCHEMICAL PROPERTIES

PHA from the accumulation experiments was purified from the biomass via solvent extraction and subsequently analyzed for its physicochemical properties. The GPC chromatograms disclosed one PHA peak for each accumulation experiment with an average polydispersity index of 2.4 ± 0.4. The value of the molecular weight (M_w) showed substantial variation between the experiments ranging from 263 to 1358 kDa. A trend was observed between the degree of polymerization and the monomer fraction of HB and HO in the monomer Fig. 3.7 a). The degree of polymerization instead of M_w is plotted in this figure to exclude the effect of the differently sized monomers. A larger fraction of HB monomers and a smaller fraction of HO monomers correlate to a higher degree of polymerization. The HHx monomer fraction was fairly constant in all measurements regardless of the degree of polymerization.

3
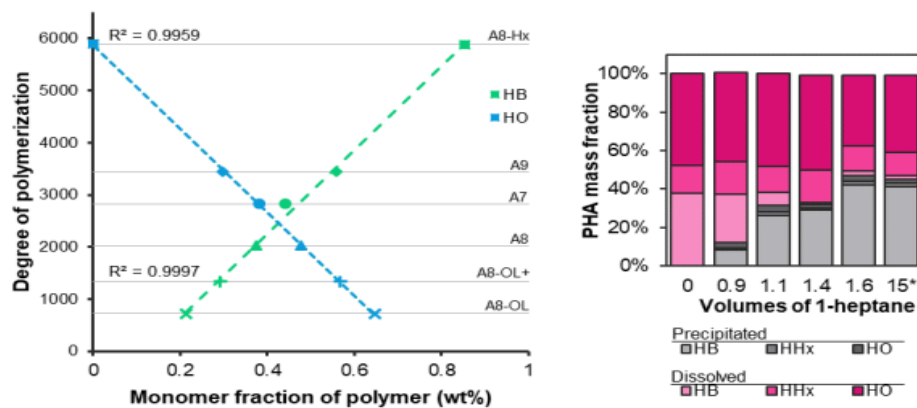
Figure 3.7.: Determination of polymer structure **a**: The degree of polymerization versus monomer composition for all accumulation experiments. A trendline was drawn through both the HB and HO data points. **b**: PHA fractionation test. Different volumes of 1-heptane were added to chloroform with PHA dissolved from the accumulation at pH 8 at 12 h (S8). PHA was measured in both the pellet (precipitated) and supernatant (dissolved). *The tubes with 15 volumes were incubated for 48 h instead of 15 min.

Part of the extracted PHA of the accumulation at pH 8 (A8) was redissolved in chloroform and fractionated through precipitation with different volumes of 1-heptane. It appeared that the PHA separated into an HB-rich fraction (91 wt% HB) and an HHx/HO-rich fraction (96 wt% HHx/HO) by adding 1.4 or more volumes of 1-heptane. Precipitation of the HHx/HO-rich fraction was not achieved, even after 15 volumes of 1-heptane and 48 h of incubation time at RT (Fig. 3.7 b). The M_w of the HB-rich fraction was 657 kDa (PDI = 3.0), while the M_w of the HHx/HO-rich fraction was 265 kDa (PDI = 1.7). This demonstrates that the PHA produced by the community in A8 with an average M_w of 497 kDa comprises a mixture of polymer chains differing both in size and monomeric composition.

The DSC curves revealed a high degree of similarity between all samples. Two melting temperature (T_m) peaks were measured in each sample with an average value of 143 ± 6 °C and 157 ± 4 °C. A higher HB content seems to result in a slightly higher Tm, although the trend is not very distinct (Fig. B.2). A8-Hx forms an exception: it does not follow this trend and has only 1 peak. A reference sample consisting mainly of HB monomers (94%) with a small fraction of HV (2%) and HH (4%) monomers also gave two melting peaks at slightly lower temperatures (137 °C and 152 °C).

3.4. DISCUSSION

3.4.1. ENRICHMENT WITH A HIGH PHA STORAGE CAPACITY

In this study, we demonstrated that enrichments cultures can be deployed for the selection of communities with a high mcl-PHA storage capacity. Accumulation under oxygen limitation resulted in a maximal PHA content of 76 wt%, where the mcl-PHA monomers were dominant (i.e., an HHx fraction of 0.14 and an HO fraction of 0.65). This is considerably higher than the 34 wt% reported in previous research investigating octanoate-fed enrichments, although the mcl-PHA fraction was similar (i.e., HHx fraction of 0.08 and HO fraction of 0.62) (Z. Chen *et al.*, 2018; Li *et al.*, 2021 also obtained a lower PHA content (53 wt%) when enriching with octanoate as co-substrate, which also resulted in a significantly lower mcl-PHA fraction (i.e., HHx fraction of 0.08 and HO fraction of 0.26).

Study	Substrate	Number of cycles per SRT	PHA content after accumulation (wt%)
S. H. Lee *et al.*, 2011	Nonanoate	5.2	34
Z. Chen *et al.*, 2018	Octanoate	3	49
This study	Octanoate	2	76

Table 3.2.: Number of SBR cycles per SRT and PHA content for studies enriching with medium-chain length fatty acids. Other studies do not display a value for the SRT.

In scl-PHA studies, it was established that minimizing the number of SBR cycles per SRT is a crucial factor for the enrichment of communities with a high PHA productivity. The reason is that the substrate to biomass ratio is increased leading to a higher PHA content at the end of the feast phase provided that substrate is predominantly used for PHA production (Jiang, 2011c. In this study, the number of SBR cycles per SRT was deliberately set at a low value of 2 which is lower than the value extracted from other mcl-PHA studies whenever data was available (Table 3.2). Therefore, we argue that the low number of SBR cycles per SRT in this study was key for the high final PHA content compared to other studies where mcl-PHA is produced with enrichments.

3.4.2. MCL-PHA PRODUCTION AS SELECTIVE STRATEGY

Analysis of the pathways for octanoate metabolism revealed that an active beta-oxidation pathway is accompanied with the production of reduced electron carries such as NADH (and $FADH_2$) (R3-5 in Fig. 3.2). For PHB production, more cycles of the beta-oxidation are required and, therefore, more NADH is produced than for PHHx and PHO production. The production of biomass from octanoate also results in a net NADH production. NADH can be regenerated via the oxidative phosphorylation resulting in the production of ATP (R12 in Fig. 3.2). When the degree of reduction of the substrate is high compared to the storage polymer, oxidative regeneration of NADH is coupled to more ATP production than is actually needed in storage polymer production. Alternatively, ATP can be used in

maintenance reactions of the bacteria. However, under feast-famine conditions, the biomass specific PHA production rates are relatively high compared to the biomass specific maintenance reaction rates when substrate is present (Table 3.1 and B.4). Therefore, maintenance reactions offer a relatively small sink for the surplus of ATP.

In Fig. 3.8, the modelled surplus of ATP is shown for a hypothetical community that produces 100% PHB but with the kinetic parameters found in the enrichment at pH 8 (S8). The ATP surplus is positive in the feast phase, while it becomes negative in the famine. In reality, the bacteria have possibly several adaptations to eliminate a surplus of ATP such as lowering the substrate uptake rate, the dissipation of energy in futile cycles, increasing in ATP requirements for maintenance, and decreasing the efficiency of the oxidative phosphorylation. However, implementation of those adaptations will reduce the competitiveness of the community in the SBR.

When solely PHO is produced hypothetically, a shortage of ATP instead of a surplus can be reached in the feast phase, as can be seen by the blue line in Fig. 3.8. This shortage of ATP can be replenished by the complete oxidation of substrate via the TCA cycle. A third scenario is the production of a mixture of PHO, PHHx and PHB as has been found in the experimental results of this study (S8). In this scenario indicated by the yellow line in Fig. 3.8, the ATP surplus is minimal compared to the 100% PHB scenario. Overall, it appears that the scenario's with mcl-PHA production do not result in a large energy surplus. Therefore, this theory suggests that mixed PHO, PHHx and PHB production may be the direct resultant from the electron distribution between energy consuming product formation pathways and respiration driven energy production.
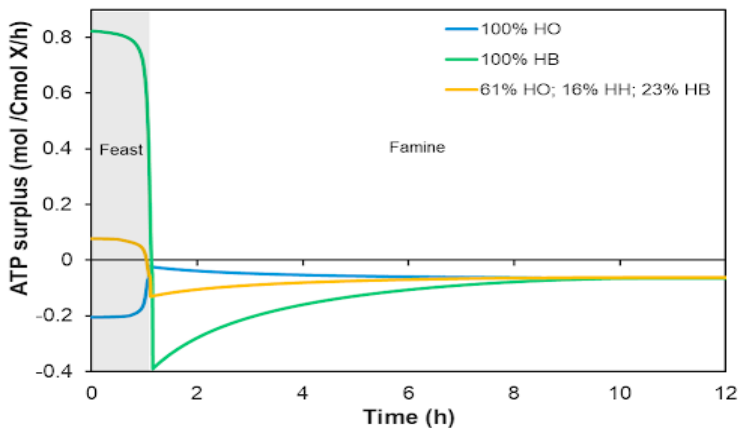

Figure 3.8.: Modelled ATP surplus (in mol $ATP/CmolX/h$) for two hypothetical scenarios (blue and green line), and for SBR cycle at pH 8 (S8) (yellow line). The kinetic parameters $(q_{s,max}, max, q_{PHA,max}, m_{ATP}, k_d)$ were copied from the S8.

3.4.3. OXYGEN LIMITATION AS TOOL TO ENHANCE MCL-PRODUCTION

In aerobic feast-famine SBRs, the oxygen uptake rate profile during the cycle is a key indicator of the functional performance of the microbial community. When the community predominantly converted the substrate directly into biomass, the majority of the oxygen (±80%) was consumed in the feast phase (Fig. 3.3 b). A smaller fraction (±60%) of the oxygen was consumed in the feast phase, when a scl-PHA production strategy was adopted by the community. The reason is that the produced PHA was oxidized in the famine phase to support growth. As explained in the previous section, mcl-PHA production in the feast phase results in a smaller surplus of ATP than scl-PHA production. Therefore, the oxidative phosphorylation can be operated at a lower rate, thereby consuming less oxygen. This was confirmed in the first enrichment where an even smaller fraction (±30%) of the oxygen was consumed in the feast phase when mcl-PHA was produced. First, this makes oxygen consumption an important process performance indicator. Second, limiting oxygen supply becomes a potential selective tool to increase the mcl-PHA fraction.

Although this tool has been successfully employed for enhancing mcl-PHA production in pure cultures (Blunt *et al.*, 2017; Fernández *et al.*, 2005) and for enhancing PHA yields in scl-PHA producing enrichments (Pratt *et al.*, 2012; Third *et al.*, n.d.), it has never been demonstrated as selective strategy to enhance mcl-PHA production in microbial enrichments. This study demonstrated that the mcl-fraction of the maximal PHA content increased from 0.62 to 0.79 when oxygen limitation was applied. Interestingly, another advantage of oxygen limitation is a 20% decrease in the PHA yield on oxygen (Y_{PHA,O_2}) under oxygen limitation compared to no oxygen limitation (Table 3.1). This indicates that less substrate is oxidized to reach same quantity of PHA. It is difficult to determine this directly from the substrate uptake curve due to the unusual large gap in the mass balance.

3.4.4. *Sphaerotilus sp.* AS MCL-PHA PRODUCER

Microscopic observations, 16S amplicon and metagenomic sequencing established that *Sphaerotilus natans subsp. sulfidivorans* was dominant in all enrichments except at pH 9. Although *Sphaerotilus sp.* has been linked to PHB production (Takeda *et al.*, 2017), this is, to our knowledge, the first report that links this genera to mcl-PHA production. Furthermore, *Sphaerotilus natans* is known to grow relatively well under conditions of low oxygen concentration (Pellegrin *et al.*, 1999), which could explain why this species was also dominant in the oxygen limited SBR (S8-OL).

In a recent study by Grabovich *et al.*, 2021 , a comparative genome analysis was conducted on *S. natans subp. sulfidivorans and S. natans subsp. natans.* It was proposed that the two bacteria should be reclassified as separate species, *S. sulfidivorans sp. nov. and S. natans*, based on a significant difference in genome characteristics and metabolic versatility. A difference is that *S. natans* can probably only grow as organoheterotroph, while *S. sulfidivorans sp. nov.* can also grow

as lithoautotroph, indicating the large variability in metabolism between the two species.

3.4.5. Polymer structure and microbial origin

The PHA fractionation experiment revealed that the enrichments in this study produced at least an HB-rich polymer, which could be effectively separated from the mcl-PHA fraction. For this reason, the polymer properties of the produced PHA are likely to be highly customizable. A study by Furrer et al. (2007) showed that PHHxO (poly(3-hydroxyhexanoate-co-octanoate) can solubilize reasonably well in 1-hexane, which presumably also explains why the HHx/HO-rich fraction did not precipitate when 15 volumes of 1-heptane were added in this study. The DSC data also suggests the presence of an HB-rich polymer, because a high melting temperature was found similar to the PHBVHx reference. From literature, it is known that mcl-PHA exists predominantly in an amorphous state (Cai *et al.*, 2009; Fernández *et al.*, 2005; Ruiz *et al.*, 2019). Therefore, no clear melt transition exists when heat is applied, which could explain why no independent melting peaks appear on the DSC spectrum corresponding to the mcl-PHA. The low PDI of 1.7 of the HHx/HO-rich fraction suggests that the HHx and HO monomers are embedded in one copolymer.

In the genome of *S. sulfidivorans sp. nov.*, two PhaC genes were found with significant differences. Alvarez-Santullano *et al.*, 2021 states that members of the order Burkholderia, which is the order where *Sphaerotilus sp.* belongs to, generally possess two or more different copies of the PhaC gene. It was also proposed that PhaC classification is more diverse than was previously known with the existence of additional classes. For *S. sulfidivorans sp. nov.*, it is possible that one PhaC gene encodes for a PHA synthase that produces mainly PHB, while the other encodes for a PHA synthase that produces mainly PHHxO resulting in two different polymers instead of one copolymer in one microorganism. Both synthases will presumably have different characteristics, which may contribute to explaining the relation between the monomer content and the degree of polymerization (Fig. 3.7 a). Different physiological conditions results in differences in the activity of the two PHA synthases and subsequently different values of the overall M_w. Nevertheless, it is also possible that a second microbial species is responsible for part of the produced PHA.

3.4.6. Outlook

To date, octanoate is present in most chain elongation studies and processes as minor component (Holtzapple *et al.*, 2022). However, in recent years, the octanoate yield in these studies increased (Kucek, 2016), and it is expected that this trend will continue. Therefore, it is believed that octanoate valorization routes such as described in this study will become more relevant in the future. Alternatively, the findings from this study (e.g., a low number of cycles per SRT or oxygen limitation) can possibly be extrapolated towards platform chemicals that are currently omnipresent in waste valorization routes such as hexanoate (W. S.

A

Chen, Huang, *et al.*, 2017). The bacterial species that were enriched at pH 7 and 8 (*S. sulfidivorans sp. nov*) and at pH 9 (*Thauera sp. or Phreatobacter sp.*) were not yet linked to mcl-PHA production. This illustrates that large parts of the mcl-PHA biodiversity are still unexplored, and that microbial enrichments can be a powerful tool to explore these parts and to seek for novel industrially relevant strains.

B

	Reaction	Stoichiometry
R1	Octanoate uptake	1 Octanoate + 0.38 ATP → 1 Oct-CoA
R2	Hexanoate uptake	1 Hexanoate + 0.5 ATP → 1 Hex-CoA
R3	β-oxidation 1	1 Oct-CoA → 0.25 NADH + 0.75 Hex-CoA + 0.25 Ac-CoA
R4	β-oxidation 2	1 Hex-CoA → 0.33 NADH + 0.67 But-CoA + 0.33 Ac-CoA
R5	β-oxidation 3	1 But-CoA → 0.5 NADH + 1 Ac-CoA
R6	PHO production	1 Oct-CoA → 0.13 NADH + 1 PHO
R7	PHHx production	1 Hex-CoA → 0.17 NADH + 1 PHHx
R8	PHB production 1	1 But-CoA → 0.25 NADH + 1 PHB
R9	PHB production 2	1 Ac-CoA + 0.25 NADH → 1 PHB
R10	Growth on Ac-CoA	1.27 Ac-CoA + 0.2 NH_3 + 2.16ATP → 1 $CH_{1.8}O_{0.5}N_{0.2}$ + 0.27 CO_2 + 0.43 NADH
R11	Catabolism	1 Ac-CoA → 1 CO_2 + 2 NADH
R12	Ox. phosphorylation	1 NADH + 0.5 O_2 → δ ATP
R13	PHO consumption	1 PHO + 0.13 ATP + 0.13 NADH → 1 Oct-CoA
R14	PHHx consumption	1 PHHx + 0.17 ATP + 0.17 NADH → 1 Hex-CoA
R15	PHB consumption	1 PHB + 0.25ATP → 1 Ac-CoA + 0.25 NADH

Table B.1.: Metabolic reactions. The metabolic reactions proposed for the octanoate and hexanoate model are on a carbon-mole base (per Cmol). The origin and derivation of the stoichiometric reactions can be found in Van Aalst-Van Leeuwen *et al.*, 1997. Later the model was optimized by Johnson, 2009b. The efficiency of the oxidative phosphorylation (δ) was assumed to be 2.0 for all experiments. But-CoA = Butyryl-CoA, Hex-CoA = Hexanoyl-CoA, Oct-CoA = Octanoyl-CoA, Ac-CoA = Acetyl-CoA. In the model, there is no dissipation reaction for a surplus of NADH/ATP. Instead, the flux through the TCA is reversed to eliminate the surplus of NADH/ATP, thereby hypothetically converting CO_2 into acetyl-CoA. Although the reverse TCA cycle exist in some bacteria, it is not expected in an oxidative environment found in the SBRs of this study.

3

Feast Phase/ Accumulation(octanoate)			
Growth	$Y_{CO_2,X}^{feast,max} = -\frac{130\delta-507}{550\delta-75}$	$Y_{O_2,X}^{feast,max} = -\frac{2691}{2200\delta-300}$	$Y_{X,S}^{feast,max} = -\frac{550\delta-75}{420\delta+432}$
PHO production	$Y_{CO_2,PHO}^{feast,max} = -\frac{\delta-3}{22\delta-3}$	$Y_{O_2,PHO}^{feast,max} = -\frac{63}{352\delta-48}$	$Y_{PHO,S}^{feast,max} = -\frac{22\delta-3}{21\delta}$
PHHx production	$Y_{CO_2,PHHx}^{feast,max} = -\frac{2\delta-3}{22\delta-3}$	$Y_{O_2,PHHx}^{feast,max} = -\frac{15}{88\delta-66}$	$Y_{PHHx,S}^{feast,max} = -\frac{22\delta-3}{20\delta}$
PHB production	$Y_{CO_2,PHB}^{feast,max} = -\frac{4\delta-3}{22\delta-3}$	$Y_{O_2,PHB}^{feast,max} = -\frac{27}{176\delta-24}$	$Y_{PHB,S}^{feast,max} = -\frac{22\delta-3}{18\delta}$
Maintenance	$Y_{CO_2,S}^{feast,max} = -1$	$Y_{O_2,S}^{feast,max} = -\frac{11}{8}$	$Y_{ATP,S}^{feast,max} = -\frac{3}{8-\frac{11}{4}\delta}$
Feast phase/ Accumulation (Hexanoate)			
Growth	$Y_{CO_2,X}^{feast,max} = -\frac{85\delta-399}{400\delta-75}$	$Y_{O_2,X}^{feast,max} = -\frac{2043}{1600\delta-300}$	$Y_{X,S}^{feast,max} = -\frac{400\delta-75}{315\delta+324}$
	$Y_{N,X}^{feast,max} = -0.2$		
PHHx production	$Y_{CO_2,PHHx}^{feast,max} = -\frac{\delta-3}{16\delta-3}$	$Y_{O_2,PHHx}^{feast,max} = -\frac{15}{64\delta-12}$	$Y_{PHHx,S}^{feast,max} = -\frac{16\delta-3}{15\delta}$
PHB production	$Y_{CO_2,PHB}^{feast,max} = -\frac{5\delta-6}{32\delta-6}$	$Y_{O_2,PHB}^{feast,max} = -\frac{27}{128\delta-24}$	$Y_{PHB,S}^{feast,max} = -\frac{32\delta-6}{27\delta}$
Maintenance	$Y_{CO_2,S}^{feast,max} = -1$	$Y_{O_2,S}^{feast,max} = -\frac{4}{3}$	$Y_{ATP,S}^{feast,max} = \frac{1}{2} - \frac{8}{3}\delta$
Famine phase (PHB, PHHx, PHO)			
Growth on PHO	$Y_{CO_2,X}^{famine,max} = -\frac{105\delta-457}{525\delta-25}$	$Y_{O_2,X}^{famine,max} = -\frac{2373}{2100\delta-100}$	$Y_{X,PHO}^{famine,max} = -\frac{525\delta-25}{420\delta+432}$
	$Y_{N,X}^{famine,max} = -0.2$		
Growth on PHHx production	$Y_{CO_2,X}^{famine,max} = -\frac{60\delta-349}{375\delta-25}$	$Y_{O_2,X}^{famine,max} = -\frac{69}{60\delta-4}$	$Y_{X,PHH}^{famine,max} = -\frac{375\delta-25}{375\delta+315}$
	$Y_{N,X}^{famine,max} = -0.2$		
Growth on PHB production	$Y_{CO_2,X}^{famine,max} = -\frac{15\delta-241}{225\delta-25}$	$Y_{O_2,X}^{famine,max} = -\frac{1077}{900\delta-100}$	$Y_{X,PHB}^{famine,max} = -\frac{225\delta-25}{210\delta+216}$
	$Y_{N,X}^{famine,max} = -0.2$		
Maintenance on PHO	$Y_{CO_2,PHO}^{famine,max} = -1$	$Y_{O_2,PHO}^{famine,max} = \frac{21}{16}$	$Y_{ATP,PHO}^{famine,max} = -\frac{1}{8-\frac{21}{8}\delta}$
Maintenance on PHHx	$Y_{CO_2,PHHx}^{famine,max} = -1$	$Y_{O_2,PHHx}^{famine,max} = \frac{5}{4}$	$Y_{ATP,PHHx}^{famine,max} = -\frac{1}{6-\frac{5}{2}\delta}$
Maintenance on PHB	$Y_{CO_2,PHB}^{famine,max} = -1$	$Y_{O_2,PHB}^{famine,max} = \frac{9}{8}$	$Y_{ATP,PHB}^{famine,max} = -\frac{1}{4-\frac{9}{4}\delta}$

Table B.2.: Overview of stoichiometric yields. In the feast phase and in the accumulation, growth, PHA production and maintenance reactions take place, which are driven by substrate consumption. In the famine phase, only growth and maintenance reactions take place, which are driven by PHA consumption. The yields are derived from the metabolic reactions (Table B.1) and balances for the conserved moieties (NADH, ATP, AcCoA, But-CoA, Hex-CoA, Oct-CoA). The method for this derivation is described in detail by Van Aalst-Van Leeuwen *et al.*, 1997. The yields are expressed as a function of the efficiency of the oxidative phosphorylation (P/O ratio, symbol δ). All yields are on carbon-mole base (Cmol/Cmol).

Feast

PHA production	$q_{PHA,1}^{feast}(t) = \left(q_S(t) - \mu^{feast}(t) \cdot \frac{1}{Y_{X,s}^{fest}} - m_S \right) \cdot Y_{PHA,S}^{feast}$	if $q_{PHA,1}^{feast} \leq q_{PHA,2}^{feast}$	eq.1

$$q_{PHA\,A,2}^{feast}(t) = q_{PHA}^{max} \cdot \frac{c_s(t)}{K_s + C_s(t)} \cdot \left[1 - \left(\frac{f_{PHAX}(t)}{f_{PHAX}^{max}} \right)^a \right]$$

With PHA inhibition, if $q_{PHA,1}^{feast} \geq q_{PHA,2}^{feast}$ eq.2

Substrate uptake $q_{S,1}(t) = q_S^{max} \cdot \frac{c_s(t)}{K_s + C_s(t)}$ if if $q_{PHA,1}^{feast} \leq q_{PHA,2}^{feast}$ eq.3

With PHA inhibition $q_{S,2}(t) = \mu^{feast}(t) \cdot \frac{1}{Y_{x,s}^{feust}} + q_{fHA}^{feast}(t) \cdot \frac{1}{Y_{frAst}^{fest}} + m_s$ if $q_{PHA,1}^{feast} \geq q_{PHA,2}^{feast}$ eq.4

Growth $\mu^{feast}(t) = \mu^{max} \cdot \frac{C_{NH_2}(t)}{K_{NH_1} + C_{NH_3}(t)} \cdot \frac{C_s(t)}{K_s + C_s(t)}$ eq.5

Maintenance $m_S = \frac{m_{ATP}}{Y_{ATP,S}^{feast}}$ eq.5

CO$_2$ evolution $qq_{CO_2}^{feast}(t) = \mu^{feast}(t) \cdot Y_{Co}^{feast} + q_{PHA}^{feast}(t) \cdot Y_{C_{CO},PHA}^{feast} + m_S \cdot Y_{CO_2,S}^{feast}$ eq.7

O$_2$ uptake $q_{O_2}^{feast}(t) = \mu^{feast}(t) \cdot Y_{O_2,X}^{feast} + q_{PHA}^{feast}(t) \cdot Y_{O_2,PHA}^{feast} + m_S \cdot Y_{O_2,S}^{feast}$ eq.8

NH$_3$ uptake $q_{NH_3}^{feast}(t) = \mu^{feast}(t) \cdot Y_{NH_3,X}^{feast}$ eq.9

TCA flux $q_{TCA}^{feast}(t) = \mu_{feast}(t) * \frac{1}{Y_{X,TCA}^{feast}} + q_{PHA}(t) * \frac{1}{Y_{PHA,TCA}^{feast}} + m_S * Y_{TCA,S}^{feast}$ eq.10

Famine Phase

Growth $\mu^{famine}(t) = Y_{X,PHA}^{famine} \cdot \left(q_{PHA}^{famine}(t) - m_{PHA} \right)$ eq.11

PHA degradation $q_{PHA}^{famine}(t) = k \cdot \left(\frac{Cx0}{Cx(t)} \right)^{1/3} f_{PHA,X}(t)^{2/3}$ eq.12

Maintenance $m_{PHA} = \frac{m_{ATP}}{Y_{ATP,PHA}^{famine}}$ eq.13

CO$_2$ evolution $q_{CO_2}^{famine}(t) = \mu^{famine}(t) \cdot Y_{CO_2,X}^{famine} + m_S \cdot Y_{CO_2,PHA}^{famine}$ eq.14

O$_2$ uptake $q_{O_2}^{famine}(t) = \mu^{famine}(t) \cdot Y_{O_2,X}^{famine} + m_S \cdot Y_{O_2,PHA}^{famine}$ eq.15

NH$_3$ uptake $q_{NH_3}^{famine}(t) = \mu^{famine} \cdot Y_{NH_3,X}^{famine}$ eq.16

TCA$flux$ $q_{TCA}^{famine}(t) = \mu_{famine}(t) * \frac{1}{Y_{x,rCA}^{famine}} + m_s^* Y_{TCA,S}^{famine}$ eq.17

Table B.3.: Model Kinetics. The kinetic expressions that describe the evolution of most essential compounds in the system. During the feast phase there are six compounds (PHA, substrate, biomass, CO_2, O_2, NH_3). During the famine there is no substrate, so only 5 compounds remain (PHA, substrate, biomass, CO_2, O_2, NH_3). The values for $q_s^{max}, u^{max}, q_p^{max}, and m_{ATP}$ are fitted to the model. The yields containing PHA are derived by **eqn. 1** in the Materials and Methods. The derivation of the expressions originated in the work of Van Aalst-Van Leeuwen *et al.*, 1997 and Johnson, 2009b

3
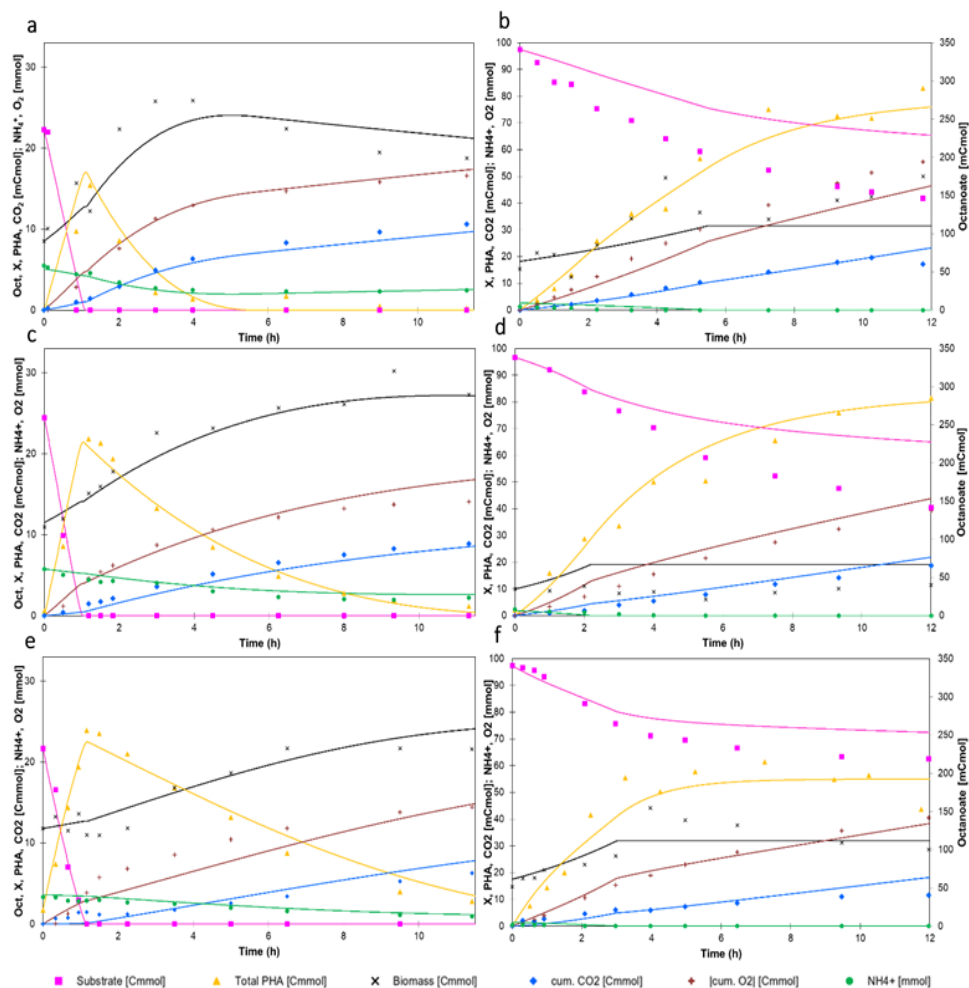
Figure B.1.: Modelled and observed results of experiments of the cycle experiments and accumulation experiments at pH 7 **(a-b)**, pH 8 **(c-d)**, and pH 9 **(e-f)**. The symbols represent the observed data. The solid lines represent the modelled data, calculated with the kinetic expressions depicted in Table B.3. For both CO_2 and O_2 the cumulative values are shown. As O_2 is consumed, the absolute values of the cumulative values is depicted.
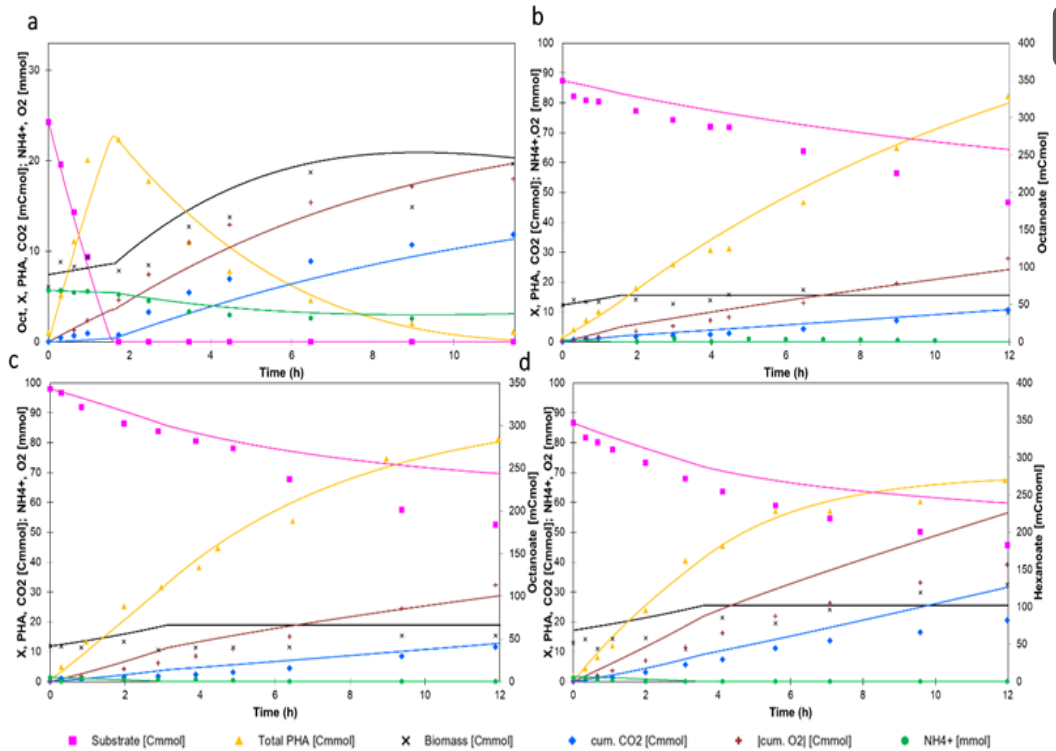
Figure B.2.: Modelled and observed results of experiments of the cycle experiments and accumulation experiments. S8-OL **(a)**, A8-OL+ **(b)**, A8-OL **(c)**, A8-Hx **(d)**. The symbols represent the observed data. The solid lines represent the modelled data, calculated with the kinetic expressions depicted in Table B.3. For both CO_2 and O_2 the cumulative values are shown. As O_2 is consumed, the absolute values of the cumulative values is depicted.

3

		SBR Cycles					Accumulations				
Type of experiment	Unit	S7	S8	S9	S8-OL	A7	A8	A9	A8-OL	A8-OL+	A8-Hx
Measured data											
Number of cycles enriched		80	99	70	70	80	89	70	70	93	99
C-Balance	%	1.6	-5.7	6.17	-7.1	17.6	49.5	33.4	37.7	46	35.4
e-balance	%	7.1	4.9	-2.10	-4.4	27.9	48.6	14.7	34.1	43	37.8
Model derived parameters for feast phase or first 2.5h of accumulation											
Y_{CO_2,S_feast}	[mmol/mCmol]	0.05	0.02	0.01	0.02	0.11	0.10	0.07	0.09	0.10	0.13
Y_{X,PHA_famine}	[mmol/mCmol]	0.53	0.63	0.61	0.55	-	-	-	-	-	-
Y_{CO_2,PHA_feast}	[mmol/mCmol]	0.02	0.02	0.02	0.02	0.03	0.03	-0.05	0.01	0.01	0.04
Y_{CO_2,PHA_famine}	[mmol/mCmol]	0.47	0.37	0.40	0.45	-	-	-	-	-	-
Input parameters model											
$m_{ATP}(fitted)$	mmol/Cmmol/h	0.13	0.08	0.10	0.20	0.34	0.52	0.25	0.29	0.30	0.34
P/O ratio	-	2.0	2.0	2.0	2.0	2.0	2.0	2.0	2.0	2.0	2.0
k_d	$[Cmmol^{1/3}/Cmmol^{1/3}/h]$	-0.70	-0.26	-0.12	-0.35	-	-	-	-	-	-

Table B.4.: Outcome of the carbon and electron balance analysis, additional model derived yields, and input parameters of the model. The carbon balances and the electron (degree of reduction) balances were set up for all 7 experiments as an indication of the accuracy of the measurements. Here, the flux of carbon and electrons into the system was subtracted from the flux out of the system. mATP represents the amount of ATP required for maintenance per Cmol biomass per unit of time, and was fitted to the data for every individual experiment. The P/O ratio reflects the efficiency of the oxidative phosphorylation and was assumed to be 2 mol ATP/mol NADH for all experiments (Beun *et al.*, 2000

3
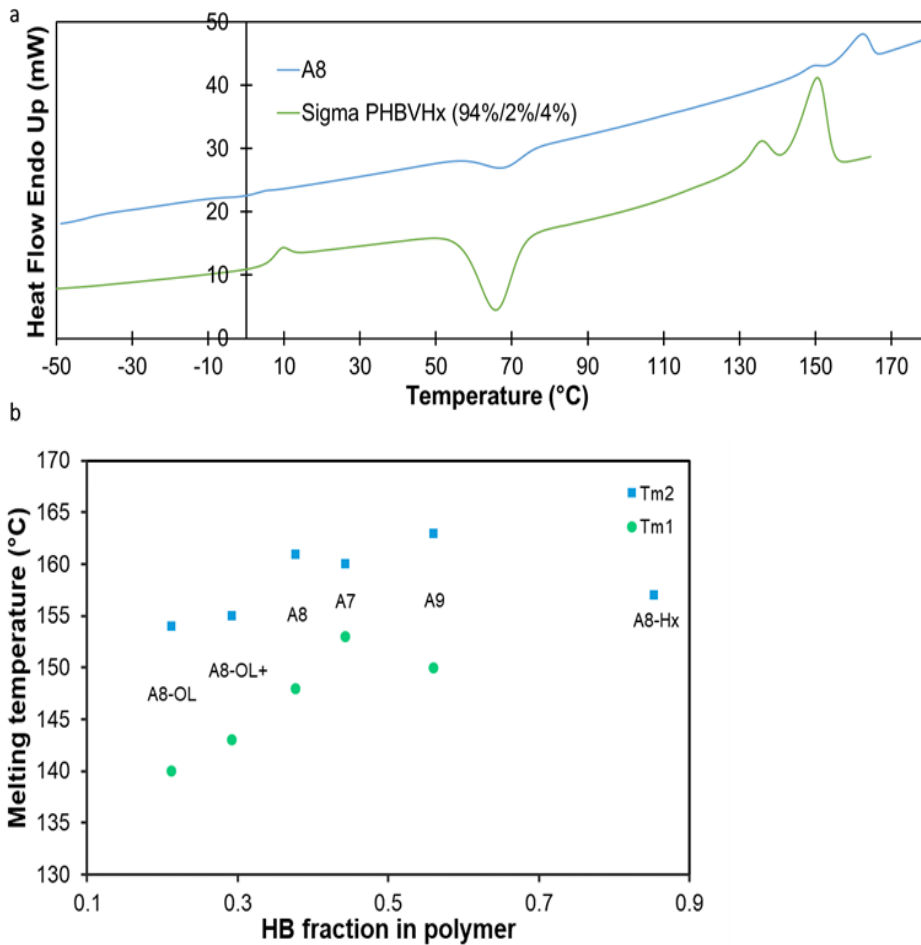
Figure B.3.: Overview of DSC data. **a**: Example of DSC spectrum of accumulation at pH 8. The reference is PHBVHx (Sigma Aldrich, USA). Both samples show an exothermic cold crystallization peak around 67 °C. **b**: Melting temperature peak 1 and 2 (T_{m1} and T_{m2}) of all accumulation experiments in relation to HB fraction of polymer.

4

SYSTEMATIC SOLVENT SCREENING AND SELECTION FOR POLYHYDROXYALKANOATES (PHBV) RECOVERY FROM BIOMASS

The biotechnological production of poly(3-hydroxybutyrate-co-3-hydroxyvalerate) (PHBV) derived from organic waste streams by mixed microbial communities is well established at the pilot-level. However, there is limited research on the recovery of the biopolymer from the microbial biomass, while its impact on product quality and product costs is major. When applying solvent extraction, the choice of solvent has a profound influence on many aspects of the process design. This study provides a framework to perform a systematic solvent screening for PHBV extraction. First, a database was constructed of 35 solvents that were assessed according to six different selection criteria. Then, six solvents were chosen for further experimental analysis, including 1-butanol, 2-butanol, 2-ethyl hexanol (2-EH), dimethyl carbonate (DMC), methyl isobutyl ketone (MIBK), and acetone. The main findings are that the extractions with acetone and DMC obtained the highest yields (91-95%) with reasonably high purities (93-96%), where acetone had a key advantage of the possibility to use water as anti-solvent. Moreover, the results provided new insights in the mechanisms behind PHBV extraction by pointing out that at elevated temperatures the extraction efficiency is less determined by the solvent's solubility parameters and more determined by the solvent size. Although case-specific factors play a role in the final solvent choice, we believe that this study provides a general strategy for the solvent selection process.

4.1. INTRODUCTION

Polyhydroxyalkanoate (PHA) has attracted widespread attention as an alternative to petrochemical-based plastics (S. Y. Lee, 1996). PHA is completely biodegradable, biobased, and has thermoplastic properties. A wide range of bacteria are able to produce this biopolymer as an intracellular carbon and energy storage (Steinbüchel, 1991). The substrate, the environmental conditions, and the microorganisms will determine the type of PHA monomer produced. The PHA monomer composition will influence the physicochemical properties of the final polymer product.

An opportunity to produce PHA cost-effectively is by using mixed microbial communities (MMC) and organic waste streams as feedstock. These technologies diminish the relatively high costs for raw substrates and sterilization of equipment (Kleerebezem et al., 2007), and as a consequence, avoid part of the waste disposal expenses (Fernández-Dacosta et al., 2015). To date, at least 19 pilot projects have been reported, using either industrial or municipal organic waste streams as feedstock (Estévez-Alonso et al., 2021). Here, the most common type of PHA produced is the random copolymer poly(3-hydroxybutyrate-co-3-hydroxyvalerate) (PHBV).

While the biotechnological process to produce PHA from low-value feedstock is reasonably well-established, the knowledge to convert it into an affordable thermoplastic is still largely lacking (De Donno Novelli et al., 2021; Estévez-Alonso et al., 2021). Yet the downstream processing step is a crucial part of the process because of its large impact on the final product quality, and because of its significant contribution to the production costs (almost 50%) (Saavedra del Oso et al., 2021; Samorì et al., 2015; Tamis, 2015; Valentino et al., 2019).

Currently, there are two main methods for the recovery of PHA-rich biomass, digesting the cellular matrix with chemical agents in a water-based process or solubilizing the PHA itself with organic solvents. In general, the cellular digestion method results in a slightly higher yield, while the solvent-based method results in a higher purity and higher molecular weight (Pagliano et al., 2021). MMC are known to form biomass consisting of highly robust cells and extracellular substances, and have in most cases a somewhat lower PHA content than industrial pure culture processes. (Koller, 2020; Mannina et al., 2020; Patel et al., 2009). From this point of view, it can be argued that digesting this relatively large fraction of strong cellular matrix becomes less favorable than solubilizing the PHA fraction with organic solvents (Molenveld et al., 2022). In this work, we therefore focused on a solvent-based extraction of PHA from biomass obtained from a MMC process.

The choice of solvent is important for SHE (safety, health, and environment) considerations, solvent pricing, and certainly for the obtained product yield and quality. However, the solvent selection also has a major impact on the overall process design. For economic and sustainability reasons, it is key that the solvent is efficiently recyclable (removal of contaminants and water), and readily recoverable from the depleted biomass and the PHA product. Furthermore, the selected solvent determines what kind of PHA precipitation strategy can be em-

ployed (cooling, addition of antisolvent, evaporation). These latter factors can be equally important as product yield, or solvent pricing in determining the final PHA production costs, and are not considered in existing PHA downstream processing literature.

The number of publications focusing on solvent selection for extraction of PHA from MMC is low, especially when waste-based pilot plants are involved. The majority of the research has been done with chlorinated solvents, however, recent studies focused on assessment of greener solvents. Regarding MMC, dimethyl carbonate has been tested on lab-scale biomass produced with a synthetic feed (de Souza Reis *et al.*, 2020; Samorì *et al.*, 2015). Furthermore, Alfano *et al.*, 2021 tested three different ethyl esters on pilot plant biomass derived from an actual waste source, where ethyl acetate revealed the most promising results. The available research has in common that the focus is on one solvent or one solvent family. Due to a wide variation in the specifications of the PHA-rich biomass between the publications (microbial composition and structure, PHA content, monomer composition, molecular weight, type of contaminants), it is difficult to compare the solvents. Therefore, we argue that for a good comparison a diverse range of solvents must be tested under similar conditions with the same input biomass.

To this end, we conducted an extensive solvent screening for the extraction of PHBV derived from a pilot plant fed with leachate from the organic fraction of municipal solid waste (OFMSW). First, a solvent database was constructed containing all solvents described in academic literature in relation to PHA extraction, and containing a few additional solvents with interesting properties. Then, six solvent selection criteria were formulated, and the initial database of 35 solvents was assessed according to these criteria. Subsequently, six solvents (1-butanol, 2-butanol, 2-ethyl hexanol, DMC, MIBK, and acetone) were selected for experimental assessment, comprising: 1) the determination of the precipitation strategy with cooling and antisolvent tests using extracted PHBV, 2) small-scale biomass extractions, where yield, purity and molecular weight were monitored as output. PHBV mass balances were constructed to validate the reliability of the obtained values of the biomass extractions. With the obtained data, we tried to increase the understanding about the factors affecting PHBV extraction. Lastly, the best solvent choice is discussed, including the role of case-specific factors, such as the properties of the input biomass and the intended application of the polymer. To our knowledge, this is the first time that such a systematic solvent screening was conducted for PHA extraction, and the first time that a diverse range of solvents was tested on waste-derived pilot plant PHA-rich biomass.

4.2. MATERIALS AND METHODS

4.2.1. PILOT PLANT PRODUCTION AND THERMAL DRYING OF BIOMASS

The PHBV-rich biomass used in the experiments was produced at a pilot plant (Orgaworld, Lelystad, the Netherlands) where OFMSW is used as a raw material for PHBV production. The upstream production process of this pilot plant consists

of a hydrolysis and acidification stage, a PHBV producing biomass enrichment stage, and a PHBV accumulation stage. The operating conditions of the enrichment reactor and the accumulation reactor are described by Mulders *et al.*, 2020. The first part of the downstream processing was conducted on-site and consisted of centrifugation and oven-drying (18 h at 120 °C) of the PHBV-rich biomass. For this research, two different biomass batches were used, one for the medium-scale extraction (Section 4.2.2) and one for the biomass extraction experiments (Section 4.2.7).

4.2.2. Medium-scale extraction for production of 'extracted' PHBV

Purified or so-called 'extracted' PHBV was produced to study the dissolution and precipitation without having interference of the biomass components (see Fig. 4.1). To this end, the dried PHBV-rich biomass was processed further under laboratory conditions. The PHBV was extracted using 1-hexanol as a solvent. An amount of 200 g PHBV-rich biomass was heated together with 1.5 L solvent to 140 °C. The material was incubated at this temperature for 30 min under continuous stirring (100 rpm). Subsequently, the mixture was filtered to remove non-dissolved biomass, using a 1.2 μm filter paper that was placed in a Büchner funnel. Before filtering, the Büchner funnel and the filter paper were preheated to 105 °C in an oven. After filtering, the filtrate was allowed to cool down to room temperature under continuous stirring (100 rpm). The PHBV precipitated during the cooling procedure. In a second filtration step, the PHBV was filtered from the solution, using a cotton cloth. The purified PHBV was subsequently oven dried at 60 °C for 48 h to remove traces of 1-hexanol.

4.2.3. Solvent selection procedure

A database was constructed of 35 solvents including all solvents described in literature in relation to PHA extraction, retrieved from a recent review by Pagliano *et al.*, 2021 and from another recent research article by Alfano *et al.*, 2021. Out of the 35 solvents, 9 solvents were added which are, to our knowledge, not yet described in academic literature in relation to PHA extraction (i.e. 2-propanol, 1-pentanol, 1-hexanol, 1-octanol, 2-ethylhexanol, DIBK, toluene, xylene, pyridine). Six solvent selection criteria were formulated which were deemed important for a PHBV downstream processing design (Table 4.1). An explanation of the six criteria can be found in the appendix A. Here, it was assumed that the downstream process consisted of the following elements: biomass dewatering, solvent extraction, solid/liquid separation 1, PHBV precipitation, solid/liquid separation 2, PHBV drying, and solvent-(antisolvent) recovery and regeneration. From the 35 solvents, 15 were instantly eliminated because of the suggested rejection boundary (i.e. DMF, pyridine, n-hexane, MTBE, chloroform, 1,2-dichloroethane because of the unfavorable ACS SHE recommendation; 1-octanol, 1,2-propylene carbonate, ethylene carbonate, DMSO, γ-butyrolactone because of the high boiling point; 1-hexanol, ethyl propionate, ethyl butyrate, phenetole because of the high solvent price).

The 20 remaining solvents were assessed according to the selection criteria and the corresponding parameters in Table 4.1. The results of this assessment and background information are available in the appendices (1 and Table C.1). Six solvents were chosen which were deemed promising based on the assessment in Table C.1, 1-butanol, 2-butanol, 2-ethyl hexanol (2-EH), dimethyl carbonate (DMC), methyl isobutyl ketone (MIBK), and acetone. 2-EH was mainly chosen because of the combination of its affordability and its low water solubility, and therefore high solvent regeneration potential, as explained in appendix C1

Table 4.1 Solvent selection criteria with corresponding parameters, and the suggested rejection boundaries. The solvents that were not eliminated by the suggested rejection boundary were assessed according to these criteria. An explanation of the criteria and the outcome of the assessment can be found in the appendices (C1 and Table C.1).

Solvent selection criteria	Corresponding parameters	Rejection boundary
1. Safety, health & environment	SHE score ACS^a, Recommendation ACS^a	ACS adjusted ranking = (Highly) Hazardous
2. PHBV solubilization potential	Molar volume solvent, Hansen $distance^b$, PHBV solubility at RT (exp.)^c	No boundary
3. Solvent recovery from biomass /product	Density, Boiling point (BP), Vapor pressure at 60 °C	BP >185 °C
4. Solvent regeneration	Solubility water in solvent, boiling point difference with water, azeotrope with water	No boundary
5. Precipitation strategy	PHBV solubility at RT (exp.)^c, Boiling point, Miscibility with water	No boundary
6. Costs solvent/antisolvents	euro/L^d	Price >2 euro/L

Note:
a Solvent selection tool on website of American Chemical Society (ACS)
b Distance between Hansen parameters of PHBV (31 wt% HV) and different solvents
c Data of experiments with extracted PHBV, see materials & methods for details
d Estimation of price, retrieved from zauba.com

Table 4.1.: Solvent selection criteria with corresponding parameters, and the suggested rejection boundaries. The solvents that were not eliminated by the suggested rejection boundary were assessed according to these criteria. An explanation of the criteria and the outcome of the assessment can be found in the appendices (C1 and Table C.1).

4.2.4. ANTISOLVENT SELECTION PROCEDURE

The PHBV solubility of PHBV-solvent mixture can be lowered by adding an antisolvent. Because the PHBV polymer is semi-polar, substances that are very polar or very non-polar can act as antisolvent to precipitate the PHBV. This is reflected in the solubility tests where water, alcohols and alkanes revealed a low PHBV

solubility (see Section 4.3.1). As water is only miscible with acetone, another antisolvent was required for DMC and MIBK. From the alcohols, 2-butanol was chosen as anti-solvent because of its affordability and low PHBV solubility (Fig. 4.2 and Table C.1). From the alkanes, n-pentane was chosen because it is less toxic than hexane. Heptane was not chosen because it has no boiling point difference with DMC, and forms an azeotrope with MIBK. For comparison, the combination of acetone with pentane was also included in the precipitation experiments.

4.2.5. PHBV SOLUBILITY TESTS

After the first selection, 20 solvents were subjected to a PHBV solubility test. In addition, the antisolvents water, pentane, and heptane were tested, and chloroform and acetonitrile were added as a reference solvent. Extracted PHBV as described in Section 4.2.2 was used for this test. First, 250 mg of extracted PHBV was added to a tube with 2.5 ml of solvent to reach a concentration of 100 g PHBV/L. The tube was vortexed and incubated at room temperature (RT) for 1 h. Then, the contents of the tube were filtered (0.4 mm glass fiber filter). The filtrate was captured in pre-weighed tubes, and subsequently oven dried until a constant weight was reached. The precipitate was weighed to calculate the PHBV solubility. The PHBV on the filter was also oven dried and weighed to construct a mass balance of every experiment (data not shown).

4.2.6. PHBV PRECIPITATION

COOLING TO RT

Temperature dependent dissolution and precipitation tests were conducted to measure the precipitation yield of the solvents. The same batch of extracted PHBV was used as in Section 4.2.5. First, 250 mg of extracted PHBV was added to a tube with 5 ml of solvent to reach a concentration 50 g PHBV/L. The same concentration was used as for the biomass extraction experiments (Section 4.2.7). The tubes were heated for 1 h at a temperature of 5% below the boiling point of the solvent. Acetone formed an exception, because 72 °C was required to dissolve all the PHBV. Then, the tubes were incubated for 1 h at RT, after which the precipitated PHBV was collected by centrifugation (5 min at 4000 g). The remaining solvent was decanted and the precipitated PHBV was oven dried until no weight loss was detected. The dried PHBV was weighed to calculate the precipitation yield. The experiment was conducted in duplicate.

ANTISOLVENT

DMC, MIBK, and acetone required an antisolvent to precipitate the PHBV. Two antisolvents were tested in different ratios for these solvents. 2-butanol was tested on DMC, and MIBK and water were tested on acetone, all with a ratio of 1/1, 3/1, and 5/1 (v/v). Pentane was tested on DMC, MIBK and acetone with a ratio of 1/1 and 3/1 (v/v). Extracted PHBV was dissolved as described in Section 4.2.6. Then, the different antisolvents in different ratios were added. The tubes

were vortexed and incubated at RT for 1 h, after which the precipitated PHBV was collected by centrifugation (5 min at 4000 g). The acetone tubes with water formed an exception and were centrifuged for 1 h. The remaining solvent was decanted and the precipitated PHBV was oven dried until no weight loss was detected. The dried PHBV was weighed to calculate the precipitation yield. This experiment was also conducted in duplicate.

4.2.7. BIOMASS EXTRACTION EXPERIMENTS

Small-scale biomass extractions were conducted to compare the six selected solvents. First, 1.2 g of biomass was dried for 2 h at 60 °C to remove traces of water. Then, the biomass was incubated for 5 minutes at 120 °C to reduce the crystallinity of the polymer supposedly. This was directly followed by the addition of the biomass to the extraction tubes with 10 ml solvent. The extractions were executed in a glycerol heating bath at two different temperature regimes, at 5% below boiling point and at 140 °C. For extractions below boiling point, the solvent was pre-heated. Extractions with 2-EH were only conducted at 140 °C, because the boiling point is above 140 °C. Extractions with acetone were only conducted at 125 °C, because the boiling point is too low (56 °C) for conducting an effective extraction below this value, and because 140 °C generated too much pressure for the used equipment. Three consecutive extraction cycles of 1h were performed, with every cycle a new batch of solvent (see Fig. 4.1). The tubes were manually shaken every 5 minutes.

After every extraction cycle, the PHBV-rich solvent was poured in a small Büchner funnel with a 1 μm filter while the biomass remained in the extraction tube. A tube was placed below the funnel to collect the PHBV-rich solution. The filter set-up was placed in an oven at a temperature of 5% below boiling point of the solvent to prevent premature PHBV precipitation. For the extractions above boiling point, the tubes were first cooled in a water bath at RT until atmospheric pressure was achieved.

Pentane was chosen as antisolvent for DMC, MIBK, and acetone (3/1 ratio). In addition, water was tested as antisolvent for acetone (1/1 ratio), and solvent evaporation was tested for acetone. First, the PHBV-rich solution was cooled for 3 minutes, then 3 volumes of pentane were added or 1 volume of water was added. Subsequently, the tubes were vortexed and incubated at RT for 1 h. For poor solvents, the PHBV-rich solution was taken out of the filtration set-up and incubated at RT for 2 h. After precipitation, all tubes were centrifuged (5 minutes at 4000 g), and the supernatant was decanted and collected. The PHBV was dried at 50 °C for 2 days in a convection oven. The PHBV extracted with 2-EH was dried for several weeks to achieve a constant weight. All experiments were conducted in triplicate. For the acetone evaporation experiment, the tubes with PHBV-rich solution were after filtration directly placed in the oven at 50 °C for 2 days. As a reference, an extraction with chloroform and acetonitrile at 140 °C, and methanol at 125 °C were added to the experiments. Because the main objective was to obtain the extraction yield (Section 4.2.11), the solvent was evaporated in a fume hood directly after filtration.

Special pressure resistant tubes (Sigma-Aldrich, USA) were used for extractions above boiling point. For DMC and acetone, the vacuum of the Büchner filter set-up resulted in premature PHBV precipitation due to low boiling point. To close the mass balances for these two solvents with a low boiling point, a syringe-filter combination was used instead.

4.2.8. Extraction of freeze-dried biomass

A small portion of wet biomass from the pilot was freeze-dried and compared to a portion which was oven dried. For both portions, the PHBV of 1 gram of dried biomass was extracted with 10 ml of chloroform at 60 °C for 4 h. The solution was filtered, precipitated with 3-volumes of n-hexane, incubated, centrifuged and dried as described in Section 4.2.7. At last, M_w was determined by GPC (Section 4.2.12).

4.2.9. Hansen solubility parameters and Teas diagram

The cohesive interactions between a solvent and a polymer largely determine the solubility. A polymer tends to dissolve better in a solvent with similar types of cohesive energies, also known as the 'like dissolves like' principle. An approach to predict polymer solubility is by quantifying this cohesive energy in the form of three Hansen solubility parameters (HSP), as in equation 4.1 (C. M. Hansen, 1967).

$$\delta^2 = \delta_D^2 + \delta_P^2 + \delta_H^2 \tag{4.1}$$

Here, δ_D is the energy density from dispersion bonds between molecules, δ_P is the energy from dipolar intermolecular force between molecules and are produced by permanent dipole–dipole interactions, and δ_H is the energy density from hydrogen bonding, expressed in $MPa^{1/2}$.

The disadvantage of the HSP is that a three-dimensional (3D) graphical representation is required, while for practical applications, a two-dimensional (2D) method is to be preferred. The Teas diagram is a plotting technique to display the three HSP in a 2D plot (Teas, 1968). The fractional solubility parameters were calculated with the equations in 4.2, and were subsequently plotted in a ternary graph.

$$f_D = \delta_D / (\delta_D + \delta_P + \delta_H)$$
$$f_P = \delta_P / (\delta_D + \delta_P + \delta_H)$$
$$f_H = \delta_H / (\delta_D + \delta_P + \delta_H) \tag{4.2}$$

4.2.10. Mass balance construction

PHBV mass balances were constructed for every biomass extraction to confirm the reliability of the obtained data. Moreover, the mass balances gave insight into the PHBV flows of the process. Here, one ingoing stream was identified (PHBV$_{X,in}$), and three outgoing PHBV streams were identified, including PHBV in the depleted

biomass ($PHBV_{X,out}$), PHBV as product ($PHBV_{Product}$), and PHBV remaining in the solvent (-antisolvent) ($PHBV_{SA}$).

$$PHBV_{X,\,in} = PHBV_{X,\,out} + PHBV_{Product} + PHBV_{SA} \qquad (4.3)$$

The terms in equation 4.3 can be further specified.

$$X_{in}(g)^* f_{PHBV,in} = X_{out}(g)^* f_{PHBV,out} + \sum_{i=1}^{3} (Product_i(g) * Purity_i) + \sum_{j=1}^{3} \left(Preciptate_j(g) * \frac{_{SA} total\,(g)}{_{SA} samples_j(g)} * Purity_j \right)$$
$$(4.4)$$

Here, X_{in} and X_{out} represent the weighed biomass before and after extraction respectively, and f_{PHBV} represent the corresponding weight fraction of PHBV determined by gas chromatography (GC) analysis.

The third part of the formula represents the sum of the obtained PHBV products from the three consecutive extractions. The dried product of each extraction (i = 1, 2, or 3) was weighed and multiplied by its corresponding purity determined by GC analysis.

The fourth part of the formula represents the sum of the PHBV remaining in the solvent (-antisolvent) liquid over the three consecutive extractions. An additional precipitation experiment was done to quantify this fraction. To this end, a sample (SA_{sample}) of the total solvent (-antisolvent) liquid (SA_{total}) was taken and 10 volumes of heptane were added to precipitate the remaining PHBV. After an incubation period of 1 week, the sample was centrifuged (5 min at 4000 g). The solvent-antisolvent liquid was decanted and the precipitated PHBV was oven dried until no weight loss was detected. A PHBV purity fraction of 0.8 was assumed. For the acetone experiment with water as antisolvent, heptane precipitation was not possible due to immiscibility with the solvent-antisolvent liquid. Therefore, a sample of the solution was evaporated, and the PHBV content of the precipitate was determined by GC analysis.

4.2.11. Output variable definition

For the precipitation tests (Section 4.3.2), the precipitation yield was defined as the fraction of PHBV precipitated from the total amount of extracted PHBV dissolved.

$$\text{Precipitation yield}(wt\%) = \left(\frac{PHBV_{Precipitated}}{PHBV_{in}} \right) * 100\% \qquad (4.5)$$

For the biomass extractions (Section 4.3.3), solvent comparison was performed by calculating and analyzing four output variables, including: purity, molecular weight (M_w), product yield, and extraction yield.

The purity and molecular weight (M_w) were calculated as a weighted average of the obtained PHBV in the individual extractions ($PHBV_{product,i}$).

$$\text{Purity}\,(wt\%) = \sum_{i=1}^{3} \left(Purity_i * \frac{PHBV_{product,i}}{PHBV_{product}} \right) \qquad (4.6)$$

$$M_w = \sum_{i=1}^{3} \left(M_{w,i} * \frac{PHBV_{\text{product},i}}{PHBV_{\text{product}}} \right) \tag{4.7}$$

Purity$i$ was determined by GC analysis, while M_{w},i was determined by gel permeation chromatography (GPC), both analytical techniques are described in the Section 4.2.12.

The product yield was defined as the fraction of PHBV ending up as product, and was determined by summing up the products of the three individual extraction. It was defined by using the terms in equation 4.3.

$$\text{Product yield } (wt\%) = \left(1 - \frac{PHBV_{\text{product}}}{PHBV_{X,in}} \right) * 100\% \tag{4.8}$$

The extraction yield was defined as the fraction of PHBV which was extracted from the biomass, and was only determined after three consecutive extractions. This variable focusses only on the extraction step, by measuring the PHBV that remained in the biomass (i.e. the non-extracted PHBV). It was defined by using the terms in equation 4.3.

$$\text{Extraction yield } (wt\%) = \left(1 - \frac{PHBV_{X,\text{ out}}}{PHBV_{X,in}} \right) * 100\% \tag{4.9}$$

4.2.12. ANALYTICAL METHODS

GC ANALYSIS FOR PHBV QUANTIFICATION

The PHBV after extraction was analyzed for purity and monomer content (hydroxybutyrate (HB) and hydroxyvalerate (HV)) using gas chromatography (GC). The method is described in detail by Johnson, 2009b. In brief, the PHBV was hydrolyzed and esterified in the presence of concentrated HCl, 1-propanol, and dichlorethane with a ratio of 1/4/5 (v/v/v) for 3 h at 100 °C. The formed esters, which accumulated in the organic phase, were analyzed by a gas chromatograph (model 6890 N, Agilent, USA). A mixture of methyl-3-hydroxybutyrate and methyl-3-hydroxyvalerate (Sigma Aldrich, USA) was used as standard due to a reduced purity of the commonly used standard (P(3HB-co- 3HV) with 12 mol% HV (Sigma Aldrich, USA), as shown by Burniol-Figols *et al.*, 2020.

GPC ANALYSIS FOR MOLECULAR WEIGHT ANALYSIS

A gel permeation chromatography (GPC) measurement was performed to measure the molecular weight distribution of the PHBV product using a Shimadzu Prominence GPC system equipped with a Shodex LF-804 column. For almost all PHBV samples, tetrahydrofuran (THF) was used as eluent, but for PHBV samples extracted with acetone dimethylformamide (DMF) was used as the eluent, both at a flow rate of 1 mL/min at 40 °C. A small comparison study was done to compare both eluents, and a correction factor (1.06) was implemented for the samples measured with DMF (See Fig. C.1 for more information).

Before injection, the PHBV sample was dissolved in chloroform and then mixed

with eluent at a ratio of 1/9 (v/v) and a final concentration of 3 mg PHBV/mL, and subsequently filtered. Data of the refractive index detector was quantified with a universal calibration of monodisperse polystyrene standards with the help of LabSolutions software.
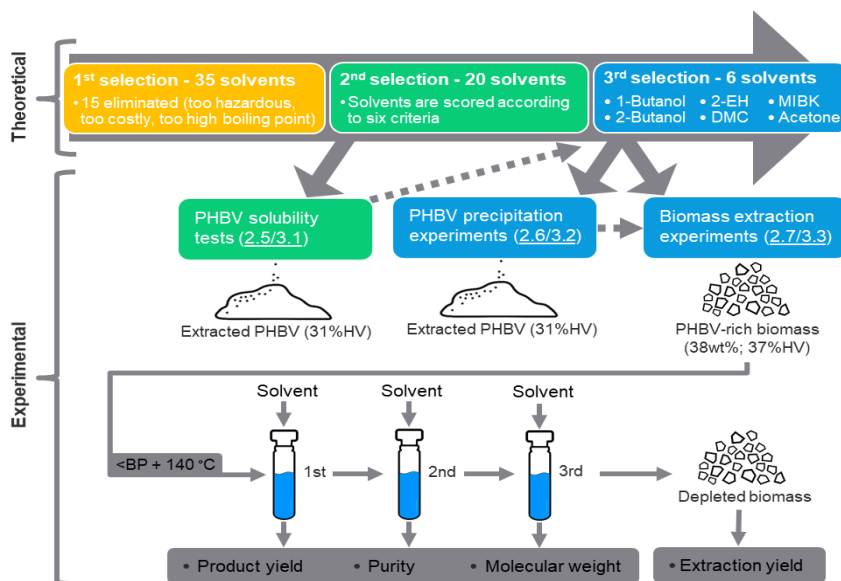
Figure 4.1.: Flow-chart of all actions in this study. The dashed line represents the influence of the result of one step on the strategy of another step. The underlined numbers refer to the sections where this step is described. The term '<BP' refers to an extraction temperature of 5% below the boiling point.

4.3. RESULTS AND DISCUSSION

4.3.1. PHBV SOLUBILITY TESTS

The theoretical and experimental actions performed in this study are shown in the flow-chart of Fig. 4.1. First, PHBV-rich biomass was produced at pilot-scale and processed at laboratorial scale to obtain extracted PHBV with a purity of 95 wt%, an HV content of 31 wt%, and an M_w of 30 kDa. This material was used to measure the PHBV solubility in the 20 selected solvents and three selected antisolvents at room temperature (RT). Fig. 4.2 shows the values obtained from the solubility tests, and at the same time shows the relation between measured PHBV solubility and the Hansen solubility parameters (HSP), displayed in a Teas diagram.

A clear inverse relation between the solubility of the (anti-)solvents at RT and the distance to PHBV-31% in the Teas diagram can be observed. The antisolvents have a very low PHBV solubility, and reveal the largest distance to PHBV-31% in

the Teas diagram. 2-butanol, which was used both as solvent and as antisolvent in this study, also showed a very low solubility at RT but the distance to PHBV-31% is much smaller. In general, all alcohols showed a very low PHBV solubility at RT, pointing out their high PHBV precipitation potential. Methanol showed the highest solubility, although its distance to PHBV-31% is the largest. This could be explained by the small molar volume of methanol compared to the other alcohols. According to C. M. Hansen, 1967 and according to Flory-Huggins theory of polymer solutions (Kennedy, 1954), smaller solvents can have improved solubilization rates and improved solubility, even though the solubility parameters are identical.
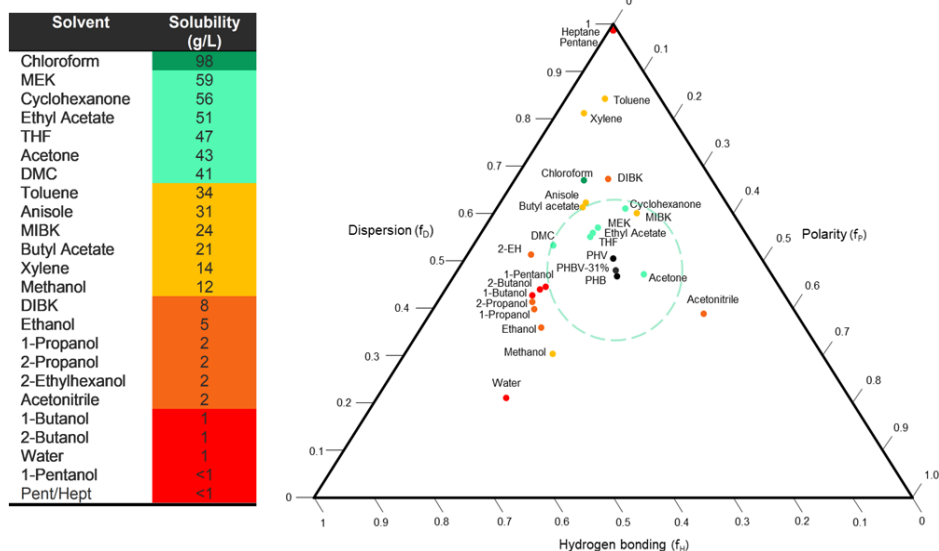
Figure 4.2.: The table on the left shows the outcome of the PHBV-31% solubility tests after 1 h at RT. The ternary graph on the right is a Teas diagram which displays all solvents plotted against their three fractional solubility parameters (f_D, f_P, f_H) (Graham *et al.*, 2000). The color scale in the table is linked to the colors of the markers in the Teas diagram. The location of PHB, PHV, and PHBV-31% (used for the solubility tests) in the Teas diagram is represented by a black marker (Terada *et al.*, 1999). The green dashed circle is drawn with PHBV-31% in the center. It represents the so-called solubility window where solvents can be found with a high PHBV solubility. MEK = methyl ethyl ketone, THF = tetrahydrofuran, and DIBK = diisobutyl ketone.

A green dashed circle was drawn with PHBV-31% in the center. All solvents with a high PHBV solubility (light green marker) are located within this so-called solubility window. Chloroform forms the only exception. It has a superior PHBV solubility at RT, while the solvent is not close to the solubility window and its molar volume is larger than acetone. According to Shephard *et al.*, 2015, chloroform's extreme

ability to dissolve a large range of substances at high concentrations can be explained by the phenomenon of polar stacking. MIBK shows a somewhat lower PHBV solubility, but is also the solvent with the highest molar volume within the solubility window.

Thus, predicting PHBV solubility of a given PHBV polymer in a solvent is more complicated than only measuring the distance in the Teas diagram. Moreover, the PHBV solubility at RT is not linearly related to the PHBV solubility at elevated temperature during extractions, as shall be discussed in Section 4.3.4. Nevertheless, the Teas diagram can be applied as a useful tool to evaluate which solvents require an anti-solvent and which antisolvents are suitable. Furthermore, the Teas diagram reveals that the HV content of the polymer has only a minor effect on the location of the solubility window in the Teas diagram, and has from this perspective presumably a minor influence on the choice of solvent.

The observed link between the solubility results and the HSP, which are based on thermodynamic considerations, suggest that the maximal PHBV solubility is approached in this experiment. However, it is not excluded that kinetic effects also play a role in the obtained solubility values. On the other hand, it is important to realize that the M_w of the PHBV used was low (30 kDa), which had a positive effect on polymer solubility due to a larger entropy change and had a positive effect on solubilization rates due to less entanglements (Jacquel, 2015; Miller-Chou *et al.*, 2003).

4.3.2. PHBV PRECIPITATION EXPERIMENTS

Six solvents were selected from Table C.1: 1-butanol, 2-butanol, 2-EH, DMC, MIBK, and acetone. Two different methods for precipitation were tested with extracted PHBV, cooling and antisolvent addition.

Cooling was tested for all solvents. The precipitation yield was determined and plotted in Fig. 4.3 a. It shows that the alcohols have a high precipitation yield, where the bulky molecules of 2-EH obtained the highest precipitation yield of 96 ± 2%.

The alcohols can be applied in a process without the addition of antisolvents, and are referred to as poor solvents. DMC, MIBK, and acetone have a much lower precipitation yield. They require the addition of an antisolvent or the evaporation of the solvent for an economically feasible process, and are referred to as good solvents. In general, the precipitation yields in Fig. 4.3 a reveal a clear inverse relation with the PHBV solubility in Fig. 4.2.

The antisolvent experiment was only conducted for the good solvents, where two different antisolvents in different ratios were tested for each good solvent. For DMC and MIBK, addition of 2-butanol resulted in precipitation, but ten volumes were required to precipitate only 54 ± 12% and 72 ± 6% of the dissolved PHBV respectively (Fig. 4.3 b-c). Pentane appeared to be a much more effective anti-sol% in DMC and 97 ± 1% in MIBK, thereby reaching a similar precipitation yield as the best performing poor solvent, 2-EH. Water appeared to be very effective in the precipitation of PHBV in acetone. One volume of water was already enough to precipitate 95 ± 1% (Fig. 4.3 d).
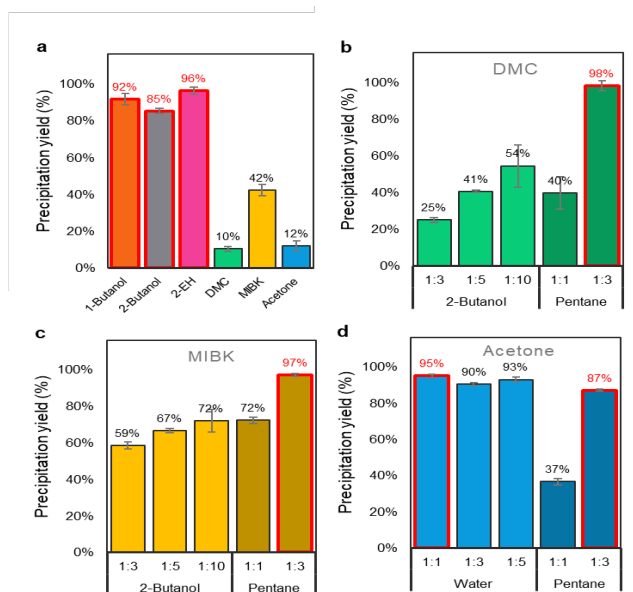
Figure 4.3.: Precipitation yields of cooling and antisolvents experiments performed with extracted PHBV. **a** shows the results of the cooling to RT experiment. **b-d** show the results of the antisolvents test which were conducted with the good solvents (DMC, MIBK, and acetone). The bars with a red outline represent the precipitation method chosen for each solvent during the biomass extractions in Section 4.3.3

For acetone, the combination with pentane was slightly less effective (precipitation yield of 87 ± 1%), but was selected for the subsequent biomass extractions experiments for comparative purposes. The bars with a red outline in Fig. 4.3 are the precipitation strategies that were chosen for the biomass extractions in Section 4.3.3. The molecular weight of the polymer also had an influence on the results. While a low molecular weight of a polymer in general facilitates the dissolution process, it impedes the precipitation process (Jacquel, 2015). This means that if higher molecular weight PHBV would have been used for this experiment, presumably higher precipitation yields would have been obtained or lower amounts of antisolvent would have been required.

4.3.3. BIOMASS EXTRACTION EXPERIMENTS

Extraction experiments with PHBV-rich biomass were conducted with the six selected solvents and the precipitation strategy determined in Section 4.3.2. The PHBV-rich biomass contained 38 ± 0.1% PHBV of the TSS with an HV content of 37 ± 0.1 wt%. The outcomes of the experiments by means of the different output variables are described one by one in the following subsections.

PURITY

Most experiments obtained PHBV with a high purity, above 95% (Fig. 4.4a). The experiments below boiling point resulted in the highest purities, implying that a lower extraction temperature results in the extraction and precipitation of less contaminants. The usage of water as antisolvent compared to pentane appeared to reduce the purity slightly although the difference was not significant. The acetone evaporation experiment is a clear exception. Here, all contaminants that were not removed in the filtration step remained in the solvent and therefore ended up in the final product, resulting in a significantly lower purity. Furthermore, no significant difference in purity was observed over the consecutive extraction cycles of all solvents (data not shown).

From literature, it is known that solvent extractions result on average in a high purity (above 90%), regardless of solvent type and cultivation strategy (pure culture or MMC) (Pagliano *et al.*, 2021). This is in line with the data obtained in this study and underlines the robustness of solvent extraction in terms of purity.

MOLECULAR WEIGHT

The molecular weight (M_w) of the PHBV product was measured for all experiments (Fig. 4.4 b). A clear difference was observed between the molecular weight values obtained for extractions conducted below boiling point and the extractions conducted at 140 °C for the individual solvents (blue bars versus orange bars). A higher temperature results in a higher random scission rate, and therefore a lower molecular weight (McChalicher *et al.*, 2010; McNeill *et al.*, 1985).

For experiments below boiling point, it is hard to discriminate between the effect of the solvent and the effect of temperature, because the temperature varies for every solvent. It was observed that the PHBV obtained from extraction with DMC and MIKB had the highest molecular weight. For experiments at 140 °C, solvents could be compared. Again, it appeared that DMC and MIBK had the highest values, indicating that these solvent had a relatively low reactivity towards PHBV. The alcohols appeared to have a higher reactivity, although the effect slightly decreased as the carbon chain lengthened (2-EH), or when the alcohol group was at a secondary position (2-butanol) (Zhang *et al.*, 2018).

The experiments with acetone revealed very little variation in molecular weight, showing that the precipitation strategy had a minor effect on this variable. Surprisingly, the molecular weight of acetone was lower than for MIBK, the other ketone, while the extraction temperature was lower. This implies that the ketone group also acted as a reactive group in the transesterification process, and that an increasing length of the carbon chain reduces the reactivity of ketones, similar as with the alcohols.

Interestingly, the molecular weight showed little variation over the different extraction cycles (data not shown). For 7 out of 12 experiments, there was a small decrease when comparing the first with the third extraction (17 ± 4%). Four experiments did not show a significant decrease or increase, and one experiment, 2-butanol below boiling point, showed an increase in molecular weight (16%). As discussed before, high molecular weight PHBV has a lower extraction rate than

low molecular weight PHBV. Therefore, it seems that the final molecular weight of each extraction cycle was the result of two seemingly opposing forces, random scission and selective extraction rates. For the same reason, it is very challenging to measure the molecular weight of the input material, because for short extraction times, only short molecular weight polymer is extracted, and for long extraction times, the polymer is significantly degraded.

For this research, it is assumed that the input molecular weight after oven drying was around 270 kDa. This is the value obtained for the extraction with DMC below boiling point.The molecular weight distribution was quantified in terms of the polydispersity index (PDI). The obtained values were high and showed substantial variation. The weighted average of the product fractions of all biomass extractions was 4.2 ± 1.1, while the maximum was 6.5 and the minimum was 2.3. In addition, it was noticed that in most experiments the molecular weight was lower than the typical values reported in literature (between 200 kDa and 3000 kDa) (Laycock *et al.*, 2013).

To understand the reason behind this, PHBV-rich biomass from the same pilot plant was freeze-dried and compared to oven dried biomass. Here, it appeared that the M_w was 1470 kDa and the PDI was 2.7, while for the oven dried counterpart the M_w was 258 and the PDI 3.7, thereby clarifying that the strong decrease in M_w is a result of the long oven-drying step.

According to Cox, 1995, the mechanical properties of the polymer start to degrade when the M_w is lower than 400 kDa. For this reason, optimizing the biomass drying step can be a valuable topic for future research. On the other hand, low molecular weight PHBV will probably facilitate the extraction process. Moreover, research showed that low molecular weight PHBV can be particularly interesting for certain applications (Boyandin *et al.*, 2017).

Product yield

The product yield represents the fraction of PHBV ending up as a purified product per amount of PHBV entering the extraction procedure, a variable with important economic consequences. The product yield, as a sum of three extractions, is shown in Fig. 4.4 c, while the individual fractions are displayed as a part of the mass balance in Fig. 4.5. Fig. 4.5 reveals that the third extraction has a minor contribution to the product yield (1 to 6 %), indicating that under the applied conditions the maximal PHBV yield is approached. A potential fourth extraction will yield an even smaller fraction, and will most likely not be economical.

For most solvents, a higher extraction temperature results in a higher product yield. Remarkably, the differences between extraction below boiling point and at 140 °C were small for 1-butanol and MIBK. For these solvents, it will likely not pay-off to increase the extraction temperature, considering the increase in cost of working under pressure and the extra loss in molecular weight. It should be noted that this might change for higher M_w polymers or polymers with a different HV content.

A higher product yield was obtained with the good solvents than with the poor solvents, with DMC (89-94%) and acetone (90-95%) having the highest values.

For DMC, an increase in extraction temperature leads to an increase in product yield (94 ± 1% compared to 89 ± 2%). For acetone, the type of antisolvent does not influence the product yield significantly (89 ± 2.9% for pentane and 91 ± 1% for water), whereas the solvent evaporation strategy does increase the product yield (95 ± 3%). These values are higher than the values obtained in other studies where MMC PHBV produced from synthetic substrates was extracted. For DMC, de Souza Reis *et al.*, 2020 obtained a maximal value of 81%, and Samorì *et al.*, 2015 obtained a maximal value of 82% after adding a hypochlorite pretreatment. For acetone, Chan *et al.*, 2017 was able to extract 51% of the PHBV at the same temperature.

The poor solvents suffer from a low precipitation yield compared to the good solvents. As can be seen in Fig. 4.5, the amount of PHBV remaining in the solvent is relatively high for the poor solvents for both temperature regimes. Therefore, the product yield of the poor solvents (77% at maximum for 1-butanol and 2-butanol) is lower than the values for the good solvents, and lower than values reported in literature. For 2-butanol, Werker *et al.*, 2014 obtained an product yield of 83% when extracting PHB from MMC. The higher product yield for the alcohols was probably related to the higher molecular weight PHBV used by these authors.

EXTRACTION YIELD

The extraction yield is the fraction of the PHBV extracted from the biomass per amount of PHBV entering the extraction procedure. This variable can contribute to a better understanding of the critical factors affecting PHBV extraction by zooming in on the extraction step while disregarding the precipitation step.

Fig. 4.4 d reveals that a higher extraction temperature resulted in a higher extraction yield for each individual solvent (blue bars versus orange bars). Here, the largest increase is observed for 2-butanol. A closer look at the extractions below boiling point reveal that DMC had among the highest extraction yields while it had the lowest extraction temperature. Therefore, solvent properties also played a role in establishing the extraction yield. From the PHBV solubility tests (Section 4.3.1), it was already known that DMC has a higher solvency for PHBV than MIBK and especially than the alcohols.

The extractions above boiling point (140 and 125 °C) showed a very homogenous outcome in six out of eight experiments, reaching an average extraction yield of 94.1 ± 0.2%. Only 2-EH and MIBK had a somewhat lower extraction yield. Acetone also reached an extraction yield of approximately 94% while its extraction temperature is only 125 °C. No clear relationship seems to exist between the obtained values and the HSP or the solubility tests in Section 4.3.1. This issue will be further discussed in Section 4.3.5. As expected, the three acetone extractions had a very similar extraction yield, because there were no differences in extraction conditions only in precipitation conditions, which emphasizes the reproducibility of the experiments. The extraction yield was measured by measuring the PHBV remaining in the biomass after three extractions. It must be realized that part of the remaining PHBV came from the solvent surrounding the biomass after decantation.
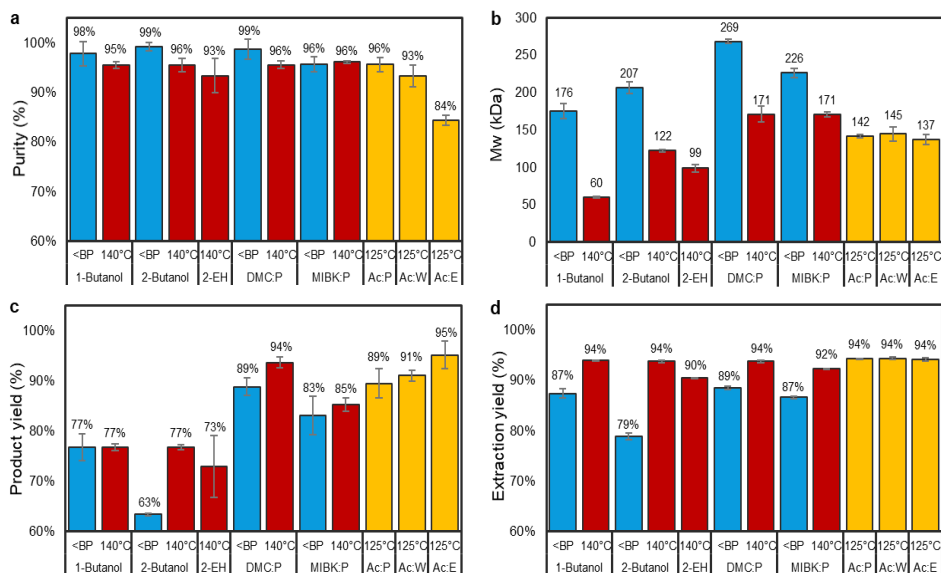
Figure 4.4.: Overview of the four output variables for the biomass extraction experiments including purity (a), molecular weight (b), product yield (c), and extraction yield (d). The term '<BP' refers to an extraction temperature of 5% below the boiling point (i.e. 112 °C for 1-butanol, 95 °C for 2-butanol, 86 °C for DMC, and 110 °C for MIBK). Ac = Acetone, P = Pentane, W = water, and E = evaporation.

This PHBV was dissolved into the solvent, but the solvent remained in the biomass matrix. Based on the PHBV and solvent mass balances, it was calculated that in all experiments on average 1.1±0.4% of the total amount of PHBV added could be traced back as this type of PHBV. This is a small value compared to the amount of PHBV remaining in the biomass (i.e. between 5.6% and 21%). Another point of attention is that it is not certain if the maximal extraction yield was reached in every experiment. Therefore, different extraction rates could also have influenced the measured extraction yield. On the other hand, the small fraction of product obtained in the third extraction cycle (Fig. 4.5) suggests that the maximal obtainable extraction yield under the applied conditions is roughly approached.

PHBV MASS BALANCES

PHBV mass balances were constructed to validate the obtained values. Fig. 4.5 reveals that nine out of twelve mass balances closed with a maximal deviation of 3%, the other three mass balances closed with a maximal deviation of 6%. On average, the mass balances closed for 99.9 ± 3% indicating that there are no large systematic errors in the measurements and calculations. It is believed that these values are acceptable considering the large number of process steps and analyses executed for the construction of each mass balance. However, the

mass balances also reveal that the product yields of some experiments could be a few percent higher or lower than described earlier.
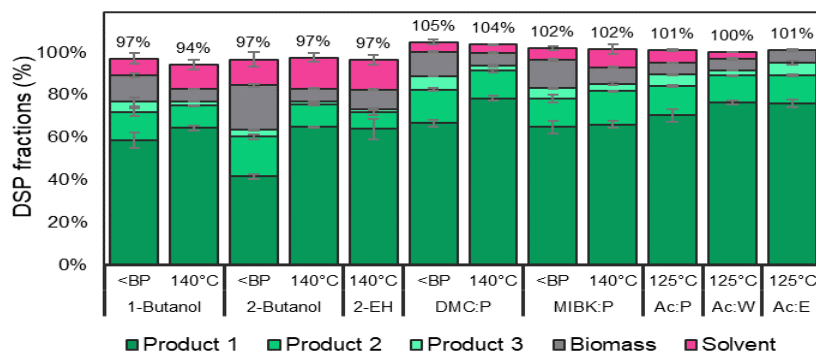
Figure 4.5.: PHBV mass balances constructed for all biomass extraction experiments. The three green fractions resemble the product fraction obtained in the consecutive extraction cycles, and together form the product yield. The term '<BP' refers to an extraction temperature of 5% below the boiling point (i.e. 112 °C for 1-butanol, 95 °C for 2-butanol, 86 °C for DMC, and 110 °C for MIBK). Ac = Acetone, P = Pentane, W = water, and E = evaporation.

4.3.4. CRITICAL FACTORS FOR PHBV EXTRACTION

TIME, TEMPERATURE, AND HV CONTENT

An apparent observation from Fig. 4.5 is that time is a noteworthy factor in PHBV extraction. A longer extraction time results in more PHBV extracted, where a maximum is approached after 3 or 4 extractions of 1 h. The number of extraction cycles required to maximize PHBV yield is defined by the extraction kinetics, which are a function of temperature. Fig. 4.5 reveals that for extractions below boiling point a larger fraction of the PHBV is extracted in the second and third cycle compared to extractions at 140 °C. Therefore, extractions at 140 °C will presumably need less cycles or shorter extraction durations than extraction below boiling point to maximize PHBV yield.

Temperature does not only have an effect on extraction kinetics but also on the total amount of extracted PHBV. A higher extraction temperature results in a higher extraction yield (Fig. 4.4c), assuming that the maximal extraction yield is approached under the applied conditions. An explanation for this phenomenon is that the polymer melting temperature (Tm) is a function of HV content, where a higher HV content results in a lower Tm (Bengsston *et al.*, 2017). Assuming that the HV monomers are not uniformly distributed over the polymer, there are regions with a high HV content (and low Tm) and regions with a low HV content (and high Tm). For this reason, a higher extraction temperature will result in the

melting and dissolution of more HV-poor regions of the polymer, thereby increasing the extraction yield.

Support for the theory described above was found in the data. In all biomass extractions, the PHBV in the biomass after extraction showed a significantly lower HV content than the PHBV in the biomass before extraction (27 ± 0.9 wt% compared to 37 ± 0.1 wt%), verifying that HV-rich regions are more effectively extracted.

Solvent properties

In Section 4.3.1, a relationship was observed between the distance in the Teas diagram and the solubility of PHBV at RT. Besides, it was noted that the molar volume of the solvent also had a modest effect on the solubility or solubilization rate at RT. The biomass extractions above boiling point (Section 4.3.3) revealed a very distinct outcome than the solubility test conducted at RT. The results suggest that the physicochemical solvent properties described by the HSP have an insignificant influence on the extraction yield at elevated temperatures, and the effect of the molar volume of the solvent on extraction yield is more pronounced. Despite the large distances between the solvents in the Teas diagram, the extraction yield showed a surprisingly constant outcome of $94.1 \pm 0.2\%$, apart from MIBK and 2-EH. Although the solubility of acetone and DMC at RT was among the highest, its extraction yield at elevated temperatures reached a virtually identical value as for 1-butanol and 2-butanol, while their solubility at RT was among lowest. Once the extraction yields are plotted against molar volume of the solvent, a relationship seems to appear (Fig. 4.6). This relationship offers an explanation why MIBK and 2-EH have a lower extraction yield, and why acetone, operated at lower temperature, still has a high extraction yield.

Additional extractions were conducted to strengthen the above-described relationship. One solvent with an extremely high solvency at RT was tested, chloroform, and two solvents with a smaller molar volume were tested, acetonitrile and methanol. As predicted, the chloroform extraction at 140 °C reached an almost identical value as the other solvents with similar molar volume ($94.1 \pm 0.1\%$). In addition, the acetonitrile and methanol extraction at 140 °C revealed that the extraction yield can be increased (95.2 ± 0.3 %and $98.0 \pm 0.1\%$ respectively) when a solvent with a lower molar volume is chosen (Fig. 4.6). Interestingly, for methanol and acetonitrile, the solvency at RT was among the lowest, and their distance in the Teas diagram among the highest. These additional results further underline that the physicochemical solvent properties as described by the HSP have a very limited influence on the extraction yield at elevated temperatures, while the molar volume has a significant influence. Moreover, for methanol, the HV content in the remaining biomass (22 ± 1.0 wt%) appeared to be significantly lower than the average of all experiments (27 ± 0.9 wt%), which points out the idea that the bottleneck to extract all PHBV are regions of the polymer with a high HB content.

In literature, molar volume of the solvent has been suggested as an important fourth parameter in polymer solubility (Hansen, 2007; Louwerse *et al.*, 2017),

where a small molar volume result in a high solubility or in high solubilization rates of the polymer. This idea is also supported by the Flory-Huggins solution theory, which comprises a thermodynamic expression for the Gibbs energy change (ΔG_m) accompanying the mixing of polymers in solvents. It states that ΔG_m decreases if the molar volume of the solvent decreases, in particular at elevated temperatures, as explained in detail in appendix C.2. A more negative ΔG_m presumably results in a higher extraction yield.
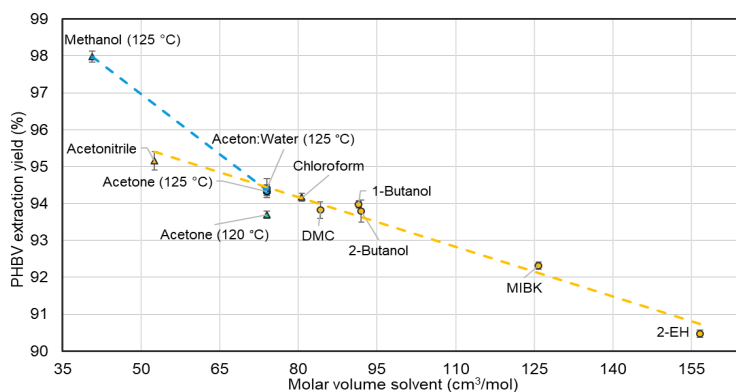
Figure 4.6.: PHBV extraction yield of biomass extractions versus the molar volume (Mv) of the solvent of all biomass extractions above boiling point (•), complemented with additional experiments (▲). A trendline was added to all data points obtained from extractions at 140 °C (yellow markers and line), and a trendline was added to data points obtained from extractions at 125 °C (blue markers and line). A test run with acetone at 120 °C in duplicate was added to the figure to underline the significance of the observed trends.

4.3.5. WHAT DETERMINES THE BEST SOLVENT CHOICE?

CONCLUSION BASED ON THIS STUDY

The experimental results showed a comparison between six solvents from multiple solvent families at two different temperature regimes, thereby revealing evident strengths and weaknesses of each solvent. The highest purities were obtained for 1-butanol, 2-butanol, and DMC, and the highest molecular weights were obtained for MIBK and DMC, both below boiling point. The highest yields were obtained at 140 °C or 125 °C for DMC and acetone respectively. The results indicated that solvents with a small molar volume, such as acetone, are more effective in PHBV extraction seemingly independent of their solubility parameters. Acetone has the advantage that water instead of pentane can be used as an effective anti-solvent. Alternatively, acetone can be evaporated directly without substantial polymer degradation, thereby merging the PHBV precipitation step, the solid/liquid (PHBV/solvent) separation step, and the solvent regeneration step. These advantages make a potential process simpler and more af-

fordable. If it is assumed that polymer quality requirements are for many applications not very stringent, then we argue that based on this study acetone is a very interesting option considering its high product yield and the avoidance of the usage of a costly, hazardous, and unsustainable anti-solvent.

OTHER CONSIDERATIONS

The question which solvent is the best choice for PHBV extraction does unfortunately not end in an unambiguous, universal answer. First, the specifications of the input biomass play a role. The PHBV-rich biomass of this pilot had a high HV content (31-37 wt% HV) compared to other pilot plants (Estévez-Alonso *et al.*, 2021) and a relatively low molecular weight due to a harsh thermal pre-treatment, which both make the polymer particularly suitable for solvent extraction. Therefore, the results presented in this study should be applied with care when working with other PHBV polymers (e.g. higher M_w or lower HV content).

Second, the intended application of the PHBV contributes to the solvent choice. In general, high-value applications require PHBV with higher specifications (high purity, high M_w), while other applications require lower specifications (low purity, low M_w). Extractions with 2-butanol or DMC below boiling point will result in higher specifications, while extraction with DMC at 140 °C or acetone at 125 °C will result in lower specifications but in a higher product yield.

In addition, it should be noted that the other process conditions such as PHBV loading rate, mixing regime, cooling rate, and precipitation time were not optimized in this study and might improve the obtained values. Furthermore, besides the four output variables defined in this study, other variables might be important, such as gel formation during precipitation or compactness of the final product. Then, scale-up efforts should identify potential bottlenecks for a full-scale. Finally, a detailed process design including an economic analysis needs to be created to give decisive answers about the solvent choice.

OUTLOOK

Although the discovery of a universal solvent for PHBV extraction is unrealistic, the development of a universal solvent selection procedure will not be. The number of solvents produced on industrial scale is limited, therefore the solvent choice for PHBV extraction is also limited. By applying a systematic approach and formulating the right selection criteria, the number of solvents to be tested experimentally can be limited even more. In this study, we aimed to provide a framework for guidance through the solvent selection process. The framework includes selection criteria that represented a wider process perspective. Although improvements can be implemented, for example, by adding solvents to the database, by optimizing the selection criteria, by testing additional types of PHBV-rich biomass, we believe that this framework can form a starting point for the solvent selection process of other PHBV extraction processes.

C

APPENDIX-CHAPTER 4

C.1. APPENDIX: SOLVENT SELECTION CRITERIA

Six solvent selection criteria were formulated which were deemed important for a PHBV downstream processing design (Table 4.1). All criteria could be linked to quantitative parameters. However, other minor criteria are conceivable, which are more complicated to quantify (i.e. PHBV scission potential, chemical and thermal stability of the solvent). For this reason, they are not taken into account in this study.

1. Safety health, environment

The SHE score is an important parameter when aiming at producing a more sustainable alternative to petrochemical plastics, for environmental concerns but also for marketing purposes. In addition, a solvent with a high SHE score will require extra safety, regulatory and environmental costs, and will, therefore, increase production costs (Curzons *et al.*, 1999). For this criterion, the solvent selection guide of the American Chemical Society (ACS) was used (ACS website). Solvents with an adjusted ACS ranking of hazardous or highly hazardous were rejected.

2. PHBV solubilization potential

The type of solvent will affect the amount of PHBV that will be extracted. Molar volume of the solvent and the distance between PHBV and solvent in the Hansen solubility space are theoretical parameters which are known to be related to the polymer solubilization potential (Hansen, 2007; Jacquel, 2015). However, these values merely give indications of the actual solubility, therefore, also experiments were conducted (Section 4.2.4 and 4.3.1).

3. Solvent recovery from biomass/product

After extraction and precipitation, a significant amount of solvent will remain in the depleted biomass and the product stream. For economic and sustainability reasons, this must be recovered as efficient as possible. To recover this by evaporation and condensation, the boiling point of the solvent should not be too high, otherwise costly vacuum drying equipment is required. In addition, when the biomass needs to be dried at high temperatures more contaminants will evaporate, and will end up in the recovered solvent (Smallwood, 2002). A rejection

boundary was set at 185 °C.

4. Solvent regeneration

Readily reuse of the bulk volume of solvent is also an important factor. Although a dewatering step will be implemented in a full-scale process, the biomass will most likely not be completely free from water. Therefore, the concentration of water can build-up in the solvent. At the same, other extracted compounds can contaminate the solvent. The result is that the PHBV solubilization potential of the solvent and the final PHBV purity can decrease. Therefore, the solvent needs to be regenerated occasionally. When the solvent has a very low water solubility, accumulated water can be removed by a simple decantation step. If this is not the case, water and contaminants can be removed by distillation, therefore a boiling point difference with water is required, and preferably no azeotrope formation (Smallwood, 2002).

5. Precipitation strategy

The precipitation strategy determines the process design and therefore the costs. PHBV solubility at RT determines if an antisolvent is required to recover the PHBV. In case of a good solvent, the choice of antisolvent brings the same SHE and cost considerations. If the solvent is miscible with water, water can be considered as antisolvent resulting in improved economics and sustainability. If the boiling point of the solvent is low enough, evaporation can be considered as an option for PHBV recovery without severe polymer degradation.

6. Solvent costs

As solvent losses cannot be banished completely, solvent expenditures will be part of the operational costs. Therefore, the price of the solvent will play an economic role. The prices showed in Table C.1 in the appendix are an approximation and will fluctuate over time. A rejection boundary was set at 2 €/

C

Solvent class	Solvents	1. Safety, health & environment		2. PHBV solubilization potential			3. Solvent recovery from biomass/product			4. Solvent regeneration			5. Precipitation strategy				6. Solvent costs
		Sum of SHE score ACS[a]	Recommended by ACS[a]	Molar volume (cm³/mol)[b]	Hansen distance to PHBV (37 wt% HV)[b,c]	PHBV solubility at RT (g/L)[d]	Density (kg/L)[e]	Boiling point (°C)	Vapor pressure at 60 °C (bar)	Solubility water in (anti-)solvent (g/100 mL)	Boiling point difference with water (°C)	Azeotrope with water?	PHBV solubility at RT (g/L)	Misc ibility with water[f]	Boiling point (°C)	Type of solvent g / evaporation[h] / water[f]	(Anti-)Solvent price (euro/L)[j]
Alcohols	Methanol	16	Recommended	40.7	14.5	12	0.79	64	0.85	Miscible	36	No	12	+	64	Good/E/W	0.15
	Ethanol	10	Recommended	58.5	11.1	5	0.79	78	0.47	Miscible	22	Yes	5	+	78	Poor/W	0.69
	1-Propanol	12	Problematic	75.2	9.3	2	0.80	97	0.20	Miscible	3	Yes	2	+	97	Poor/W	0.57
	2-Propanol	10	Recommended	76.8	8.4	2	0.79	83	0.39	Miscible	18	Yes	2	+	83	Poor/W	0.32
	1-Butanol	10	Recommended	91.5	8	1	0.81	118	0.08	24.7	18	Yes	1	+/-	118	Poor	0.39
	2-Butanol	8	Recommended	92	6.8	1	0.81	100	0.18	45	0	Yes	1	+/-	100	Poor	0.57
	1-Pentanol	8	Recommended	108.6	6.2	0	0.81	138	0.03	10.2	38	Yes	0	-	138	Poor	1.53
	2-EH	11	Problematic	156.6	6.4	2	0.83	185	0.00	0.02	NA	NA	2	-	185	Poor	0.53
Ketones	Acetone	13	Recommended	74	2.2	43	0.78	56	1.13	Miscible	44	No	43	+	56	Good/E/W	0.39
	MEK	11	Recommended	90.1	4.7	59	0.81	80	0.53	14.9	20	Yes	59	-	80	Good	0.51
	Cyclo hexanone	10	Problematic	104	5.9	56	0.95	156	0.11	8.7	56	Yes	56	-	156	Good	0.81
	MIBK	9	Recommended	125.8	5	24	0.80	117	0.15	2.4	17	Yes	24	-	117	Good	0.64
	DIBK	13	Problematic	177.1	6.6	8	0.81	168	0.02	0.26 k	NA	Yes	8	-	168	Poor	1.77
Carbonate esters	DMC	7	Recommended	84.2	4.9	41	1.07	90	0.35	2.9	10	No	41	-	90	Good	0.65
Esters	Ethyl Acetate	11	Recommended	98.5	3.5	51	0.90	77	0.56	3.3	23	Yes	51	-	77	Good	1.07 l
	Butyl Acetate	9	Recommended	132.5	5.3	21	0.88	126	0.09	1.9	26	Yes	21	-	126	Good	0.54
Cyclic ethers	THF	18	Problematic	81.7	3.8	47	0.89	66	0.84	Miscible	34	Yes	47	+	80	Good	1.22
Aromatic hydro carbons	Anisole	10	Recommended	119.1	6.4	31	1.00	154	0.04	1.60	54	Yes	31	-	154	Good	1.01
	Toluene	14	Problematic	106.8	10.7	34	0.87	111	0.19	0.04	NA	NA	34	-	111	Good	0.45
	Xylene	11	Problematic	123.3	10.1	14	0.87	139	0.07	0.04	NA	NA	14	-	139	Good	0.44
Anti-solvents	n-Pentane	18	Hazardous	116.2	12.9	0.1	0.63	36	2.16	0.01	64	NA	0.1	NA	36	Anti-solvent	0.32
	Water	3	Recommended	18	34.4	1	1.00	100	0.21	NA	NA	NA	1	NA	100	Anti-solvent	0.002 m

a) https://www.acs.org/content/acs/en/greenchemistry/research-innovation/tools-for-green-chemistry/solvent-selection-tool.html
b) (Hansen, 2007)
c) Solubility parameters solvents: (Hansen, 2007); Solubility parameters PHBV: (Terada et al., 1999); Calculated with equation in materials & methods.
d) Data of experiments with purified PHBV, see materials & methods for details
e) For centrifugal separation of PHBV from the solvent there must be a significant density difference with PHBV 1.20 g/cm³ (Koller et al., 2010
f) If miscible with water +, if solubility water in solvent is > 20g/L then +/-, otherwise -
g) If PHBV solubility at RT<10 g/L solvent is defined as 'poor', otherwise 'good'.

h) If boiling point is < 75 °C, evaporation ('E') is considered as an option.
i) If solvent is miscible with water, water ('W') can be used as anti-solvent.
j) Estimation of price, retrieved from zauba.com on April 2021, converted from INR/kg to Euro/L..
k) Solubility solvent in water (g/100mL), not water in solvent
l) echemi.com (January, 2022)
m) https://www.processindustryinformer.com/process-industry-water-cost (October, 2015)

Table C.1.: Assessment of 20 solvents according to the six selection criteria. Each separate column was given a color scale from green towards red, indicating potentially advantageous towards disadvantageous for the selection criteria. 2-EH = 2-ethyl hexanol, MEK = methyl ethyl ketone, MIBK = methyl isobutyl ketone, DIBK = Diisobutyl ketone, DMC = dimethyl carbonate, and THF = tetrahydrofuran.
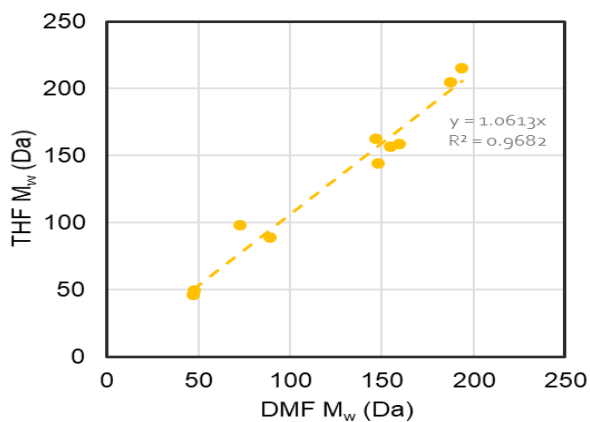
Figure C.1.: During this research, the eluent of the gel permeation chromatograph was changed, therefore the acetone extraction experiment samples were measured with DMF instead of THF. A small comparison study was conducted to show that the difference between the two eluents was small. The molecular weight of a number of samples from the 1-butanol, 2-butanol, 2-EH, and DMC extraction was measured again with DMF as eluent and plotted against the THF values. For comparative purposes, a correction factor of 1.06 was used to correct the M_w values of the acetone extraction.

C.2. APPENDIX: FLORY-HUGGINS SOLUTION THEORY

Molar volume of the solvent has been suggested as an important fourth parameter in polymer solubility (Hansen, 2007;Louwerse et al., 2017). Once the extraction yields are plotted against molar volume of the solvent, a relationship seems to appear (Fig. 4.6). This relationship offers an explanation why MIBK and 2-EH have a lower extraction yield, and why acetone, operated at lower temperature, still has a high extraction yield. These results suggest that the effect of the molar volume of the solvent on extraction yield is more pronounced at elevated temperatures. The above-described hypothesis is supported by the Flory-Huggins solution theory. It states that the thermodynamic expression for the Gibbs energy change (ΔG_m) accompanying the mixing of polymers and solvents is, as follows:

$$\Delta G_m = \Delta H_m + T\Delta_{S_m} \tag{C.1}$$

where ΔH_m is the enthalpy of mixing; ΔS_m is the entropy of mixing.
Smaller solvents give rise to a system where more states are possible thereby increasing the entropy term, resulting in a more negative Gibbs energy change, and presumably a higher extraction yield. As temperature increases, the T-dependent entropy term becomes even more dominant, thereby increasing the effect of solvent size, as observed in the data.
The enthalpy term can be expressed as a function of the Flory-Huggins interaction parameter X_{12}, (van Krevelen et al., 2009)as follows:

$$\Delta H_m = nRT\chi_{12}\varphi_1\varphi_2 \tag{C.2}$$

where n is the number of lattice moles; $\psi 1$ and $\psi 2$ are volume fractions of solvent and polymer respectively. The Flory-Huggins interaction parameter can be expressed as a function of the HSP (Hansen, 2007).

$$\chi_{12} = V_m \left[(\delta_{D2} - \delta_{D1})^2 + 0.25(\delta_{P2} - \delta_{P1})^2 + 0.25(\delta_{H2} - \delta_{H1})^2 \right] / RT \tag{C.3}$$

Equation A4.3 points out that the enthalpy term is affected by the molar volume of the solvent (V_m). Here, a smaller solvent results in a smaller enthalpy term, thereby relatively increasing the effect of the entropy term, resulting in a more negative Gibbs energy change and presumably a higher extraction yield. Combining equations C.2 and C.3 reveals that T can be omitted from the enthalpy term. Nevertheless, the Hansen parameters do have a temperature dependency. According to Hansen, 2007, the HSP for most solvents decrease with increased temperature, especially δ_H, while the HSP of most polymers remain reasonably constant. This development could bring about that at elevated temperature the distances in the Teas diagram become smaller for all solvents, thereby reducing the effect of the HSP on the extraction yield, as has been observed in the data.

5

FROM WASTE TO SELF-HEALING CONCRETE: A PROOF-OF-CONCEPT OF A NEW APPLICATION FOR POLYHYDROXYALKANOATE

Polyhydroxyalkanoate (PHA) production is a promising opportunity to recover organic carbon from waste streams. However, widespread application of waste-derived PHA as biodegradable plastic is restricted by expensive purification steps, high quality requirements, and a fierce competition with the conventional plastic market. To overcome these challenges, we propose a new application for waste-derived PHA, using it as bacterial substrate in self-healing concrete. Self-healing concrete is an established technology developed to overcome the inevitable problem of crack formation in concrete structures, by incorporating a so-called bacteria-based healing agent. Currently, this technology is hampered by the cost involved in the preparation of this healing agent. This study provides a proof-of-concept for the use of waste-derived PHA as bacterial substrate in healing agent. The results show that a PHA-based healing agent, produced from PHA unsuitable for thermoplastic applications, can induce crack healing in concrete specimens, thereby reducing the water permeability of the cracks significantly compared to specimens without a healing agent. For the first time these two emerging fields of engineering, waste-derived PHA and self-healing concrete, both driven by the need for environmental sustainability, are successfully linked. We foresee that this new application will facilitate the implementation of waste-derived PHA technology, while simultaneously supplying circular and potentially more affordable raw materials for self-healing concrete.

5.1. INTRODUCTION

Polyhydroxyalkanoate (PHA) has attracted widespread attention as an alternative to petrochemical-based plastics. PHA is biobased, completely biodegradable, and has thermoplastic properties (S. Y. Lee, 1996). An opportunity to produce PHA cost-effectively is by using mixed microbial communities and organic waste streams as feedstock. These technologies diminish the relatively large expenses for raw substrates and sterilization (Kleerebezem et al., 2007), and consequently, avoid part of the waste disposal costs (Fernández-Dacosta et al., 2015). To date, a multitude of organic waste streams have been assessed successfully for PHA production in laboratory experiments (Rodriguez-Perez et al., 2018). Moreover, pilot projects, using industrial waste water or activated waste water sludge as feedstock, reached promising PHA productivities for achieving an economically viable process (Jia et al., 2014; Jiang, 2012; J. Tamis et al., 2014).

While the biotechnological process to produce PHA from waste is reasonably well-established, challenges remain in its conversion into a marketable thermoplastic. First of all, the purification costs are responsible for a large fraction of the total production cost due to high energy and chemical demand (Gurieff et al., 2007). A second challenge is to achieve a high and consistent quality product as required for commercially interesting plastics. More research is required to predict the relationship between raw material input, process parameters, and final mechanical properties of the produced PHA accurately (Laycock et al., 2013). Finally, introducing waste-derived PHA into the conventional plastic market is a lasting and complicated procedure. This is mainly caused by a lack of distribution channels, a lack of experience in bioplastic processing, and by the small scale at which PHA is currently produced compared to petrochemical plastics (Bengsston et al., 2017; Iles et al., 2013).

In light of these challenges, we believe that a market entry of waste-derived PHA has a higher chance of success if the initial aim is not to produce bioplastics. Instead, the focus should be on new applications where minor fractions of impurities, and small variations in polymer characteristics are not regarded as problematic. Such a niche application can stimulate the introduction of waste-derived PHA into the market, while avoiding the obstacles and the complexity of the conventional plastic industry. Moreover, these applications can potentially exploit the unique properties of PHA (e.g., biodegradability) more effectively (Kleerebezem et al., 2015; Tamis, 2015).

For PHA, some innovative niche applications have been explored already, such as bio-based paper coating (Lauzier et al., 1993), bio-based glue (Pereira et al., 2019), and slow-release fertilizer/herbicide (Boyandin et al., 2017; Cao et al., 2019) . However, none of these applications are well-established yet. Therefore, we introduce and demonstrate a new application for waste-derived PHA, using it as bacterial substrate in self-healing concrete.

The technology of self-healing concrete was developed to overcome the almost inevitable problem of crack formation in aging concrete. Aggressive substances which enter through cracks can deteriorate the concrete, and decrease the service life of constructions considerably (Yang et al., 2004). In this way, the tech-

nology of self-healing concrete is capable of decreasing maintenance costs and increasing service life of constructions, and consequently, reducing part of the enormous amount of carbon dioxide emitted by the concrete industry (Quéré *et al.*, 2018). Field trials of self-healing concrete structures have now demonstrated this technology at larger scale (Wiktor *et al.*, 2016). However, for large-scale implementation there is still an urgent need for a more cost-effective production of healing agent (F. B. Silva *et al.*, 2015).

The self-healing properties of the concrete are established through inclusion of a granulated healing agent in the concrete before casting. This healing agent consists mainly of a bacterial substrate, supplemented with a small fraction of bacterial spores and other essential nutrients. Once incorporated in the concrete, the spores become active when water intrudes due to crack formation. Upon activation the bacteria are able to metabolize the bacterial substrate to carbon dioxide. Due to the alkaline (pH of 12-13) and calcium-rich environment of the concrete, the carbon dioxide reacts to calcium carbonate. In this way, bacterial growth induces the formation of mineral precipitates in the crack, which decrease the water permeability of the concrete (Jonkers, 2007; R. Mors *et al.*, 2017; Tziviloglou *et al.*, 2016). In previous research, other bacterial substrates have been investigated, namely urea (Wang *et al.*, 2015), peptone (Xu *et al.*, 2018), different organic calcium acids (calcium lactate, calcium acetate, calcium gluconate, calcium formate) (De Belie *et al.*, 2018), magnesium acetate (Palin *et al.*, 2017), and a lactate derivative (R. M. Mors *et al.*, 2015). Most substrates (e.g. lactate derivative) are obtained from valuable agro-industrial feedstock (i.e., sucrose or glucose), and potentially impose larger economic limitations to the product application than substrates derived from waste streams (Fernández-Dacosta *et al.*, 2015; van den Oever *et al.*, 2017).

By applying waste-derived PHA as bacterial substrate in self-healing concrete, we aim to maximize the added value of biodegradability by using waste-derived PHA as substrate for bacteria. Also, we envision that the purity and physicochemical properties of the PHA, such as monomer composition, molar mass distribution, and melting temperature, are of secondary importance in this application. Finally, using waste-derived PHA in concrete opens the possibility to use secondary resources in a bulk product, thereby contributing substantially to the principles of the circular economy. We propose that linking waste-derived PHA to self-healing concrete can boost the development of both technologies that aim for more effective use of resources. To our knowledge, this is the first time that waste-derived PHA technology is used in a civil engineering application, and the first time that a waste-derived material is used as main nutrient in self-healing concrete. The aim of this study was to introduce the concept of using waste-derived PHA as bacterial substrate in self-healing concrete, and to evaluate its feasibility.

To this end, PHA-rich biomass was received from a pilot plant that uses organic waste as raw material. The PHA was extracted and converted under laboratory conditions to a healing agent, and subsequently cast in concrete specimens. Three requirements were set to assess the performance of waste-derived PHA as bacterial substrate in self-healing concrete:

1. The ability of the self-healing bacteria to metabolize extracellular PHA, the ability of PHA-based healing agent to

2. Induce mineral precipitation on the crack surface of concrete specimens,

3. The ability of PHA-based healing agent to decrease the water permeability of cracks in concrete specimens.

These conditions need to be met for a first validation of the proposed application.

5.2. MATERIALS AND METHODS

5.2.1. SOURCE OF PHA-RICH BIOMASS

The PHA-rich biomass was received from a pilot plant (Orgaworld/Paques, Lelystad, the Netherlands) where the organic fraction of municipal solid waste (OFMSW) is used as a raw material. The upstream production process of this pilot plant consists of a hydrolysis and acidification stage, a PHA producing biomass enrichment stage, and a PHA accumulation stage. The operating conditions of the enrichment reactor and the accumulation reactor are described by Mulders *et al.*, 2020. The first part of the purification process was conducted on-site and consisted of centrifugation and oven-drying (20 hours at 105 °C) of the PHA-rich biomass.
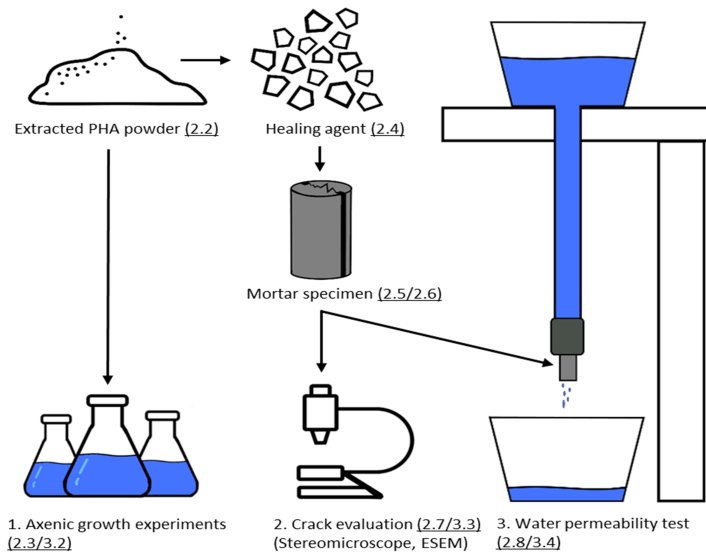

Figure 5.1.: Experimental flow chart of this study and a schematic representation of the experimental set-up of the water permeability test. The underlined numbers refer to the sections of the Materials and Methods and Results and Discussion where this step of the flow chart is described. The three experimental outputs of this study (1, 2, and 3) are shown at the lower part of the chart.

5.2.2. PHA EXTRACTION PROCESS

The dried PHA-rich biomass was processed further under laboratory conditions. The PHA was extracted using 1-hexanol as a solvent. An amount of 210 gram PHA-rich biomass was heated together with 1.6 L 1-hexanol to 140 °C. The material was incubated at this temperature for 30 minutes under continuous stirring (100 rpm). Subsequently, the 1-hexanol mixture was filtered to remove non-dissolved biomass, using a 1.2 µm filter paper (GE Healthcare Life Sciences, UK) that was placed in a Büchner funnel. Before filtering, the Büchner funnel and the filter paper were preheated to 105 °C in an oven. After filtering, the filtrate was allowed to cool down to room temperature under continuous stirring (100 rpm). The PHA precipitated during the cooling procedure. In a second filtration step, the PHA was filtered from the solution, using a cotton cloth. The purified PHA was subsequently vacuum dried at 50 °C for 24 h to remove traces of 1-hexanol.

5.2.3. AXENIC GROWTH EXPERIMENT

The purified PHA was used as substrate in an axenic growth experiment to verify the growth of the self-healing bacterial strain, a *Bacillus cohnii*-related strain. To this end, three shake flasks were filled with 20 mL of carbon-free minimal medium consisting of 3.75 mM KNO_3, 3.7 mM NH_4Cl, 0.15 mM KH_2PO_4, 1 mM $MgCl_2$, 50 mM $NaHCO_3$, 50 mM Na_2CO_3, 1 mL/L trace elements solution according to Vishniac *et al.*, 1957 and 1 mL/L vitamin solution according to Phillips *et al.*, 1993. In addition, 60 mg UV-sterilized PHA and 2 mL of an axenic B. cohnii-related culture (1.5*109 cells/mL) were added. As control experiments, flasks were prepared with the same medium, but supplemented with either PHA or the B. cohnii-related culture, again in triplicate.

Flasks were incubated at room temperature for 48 h while stirring at 200 rpm. Flasks with only PHA were incubated longer (11 days) to verify the axenic conditions of the experiment. Over time, the cell concentration was measured with a BD Accuri C6® flow cytometer (BD Accuri cytometers, Belgium). Before measuring, samples were stained with 10 µL/mL SYBR® Green I (1:100 dilution in demineralized water) (Invitrogen, USA), by incubating the sample and the stain for 10 min at 35 °C in the dark. Flow cytometric measurements and data analysis were performed as described by Pinel *et al.*, 2020.

5.2.4. HEALING AGENT FORMULATION

Purified PHA (5 g) was ground with a mortar and a pestle to a powder. Lyophilized spores (20 mg) of the Bacillus cohnii-related strain and additional nutrients in the form of yeast extract (102 mg) (Scharlau, Spain) were added to the PHA powder. The obtained mixture was melted for 30 seconds at 100 ± 10 °C and simultaneously flattened to a sheet with a thickness of 0.75 ± 0.25 mm. The sheet was kept for 2 days at room temperature to solidify, and after that ground to particles using a miniature grinding machine (Princess household supplies, Breda, the Netherlands) for 10 seconds. After grinding, the particles were sieved in order to obtain a fraction with a size between 0.5 and 1.0 mm. The larger

100
5. From Waste to Self-healing Concrete:
A Proof-of-concept of a New Application for Polyhydroxyalkanoate

faction (> 1.0 mm) was ground again, and the smaller fraction (< 0.5 mm) was first melted and solidified, and later ground again. Lastly, 4.3 g particles with a size between 0.5 and 1.0 mm were obtained, which was partly used as healing agent in the experiments below.

5.2.5. PREPARATION OF CONCRETE SPECIMENS

The concrete specimens were prepared using an adapted version of the method described by Palin *et al.*, 2016. In fact, mortar was chosen for this experiment as a substitute for concrete; however, we will refer to concrete in the rest of the publication. Three concrete specimen series were prepared, each consisting of 7 cylinder-shaped pieces (diameter 35 mm; height 60 mm). A series was prepared without healing agent (further referred to as negative control specimens); a series was prepared with a currently marketed healing agent (further referred to as positive control specimens) containing a lactate derivative (Basilisk, Delft, the Netherlands) (R. Mors *et al.*, 2017); and a series was prepared with healing agent containing PHA (further referred to as PHA specimens) (see Section 5.2.4).

Each specimen series was prepared by homogeneously mixing the following ingredients: 110.5 g Portland cement (CEM I 42,5 N), 55.3 g tap water, 109.4 g sand (grainsize of 1-2 mm), 112.7 g sand (grainsize of 0.5-1 mm), 69.6 g sand (grainsize of 0.25-0.5 mm), 39.8 g sand (grainsize of 0.125-0.25 mm), and 3.0 g healing agent with a size of 0.5-1.0 mm (not added to the negative control specimens). The resulting concrete mixtures were cast in a plastic cylinder-shaped mold, which was designed such that the obtained specimens contained two opposite grooves (2 mm wide and 3 mm deep) running along their sides. All specimens were cured inside the plastic mold at room temperature for 28 days.

5.2.6. CRACK FORMATION AND INCUBATION

After curing for 28 days, a crack was made in every specimen with a servohydraulic testing machine (Instron Corp., Canton, MA). A compressive load was applied until the specimens split from groove to groove. After splitting, the crack width was fixed at 0.4 mm using spacers (2.4 mm wide and 3 mm deep) that fitted in the grooves. Details of this procedure have been presented by Palin *et al.*, 2016. However, instead of using temporary Perspex spacers, specifically developed permanent spacers were used. The spacers were secured with a universal glue, which was allowed to dry for 24 hours at room temperature. Specimens were incubated under humid conditions (> 95% RH) at 20 ± 2 °C for 56 days.

5.2.7. CRACK EVALUATION

Before and after incubation, the cracks at the top and bottom of the specimens were imaged with a stereomicroscope (Leica MZ6, Nussloch, Germany). The photos before incubation were used to measure the crack width and to calculate the average crack width, making use of imaging analysis software (ImageJ).

Environmental scanning electron microscopy (ESEM) was conducted to analyze

the precipitates formed on the crack surface using a Philips XL30 Series under Back-scatter electron mode (BSE). As preparation, an incubated specimen was broken into its two halves directly before analysis, such that the crack surface was completely exposed and precipitates could be examined.The stereomicroscopic and ESEM photos acquired were used to link the visual observations to the functional properties of the specimens (i.e., water permeability experiment in Section 5.2.8).

5.2.8. WATER PERMEABILITY EXPERIMENT

Three specimens from each series (negative control, positive control, and PHA) were assessed on their water permeability without being subjected to an incubation period. The average of these specimens represent the initial water permeability for all specimens belonging to this series. Four other specimens from each series were assessed on their water permeability after incubation under humid conditions; these specimens provide the final water permeability. In addition, the incubated specimens were dried at 36 °C for 7 days before the final water permeability was tested.

The permeability of the specimens was measured using a method developed by Palin *et al.*, 2016. A schematic representation of the experimental set-up is shown in Fig. 5.1. Accordingly, specimens were placed in a permeability cell and then attached to the bottom of a 1m column. At the top of the column a water reservoir was placed. Water, which flowed from the reservoir through the column and finally through the crack of the specimens, was collected in buckets and weighted at 5, 10, and 15 minutes. The water level in the reservoir was manually kept constant during the measurements. In doing so, the crack experienced an almost constant water pressure of 0.1 bar.

The data retrieved from this experiment was used to calculate the reduction of the water flow (RWF) as follows:

$$\text{RWF} = \left(\frac{W_{i,\text{ average}} - W_{f,\text{ n}}}{W_{i, average}} \right) * 100\% \tag{5.1}$$

where $W_{i,\text{ average}}$ is the average (out of three specimens) amount of water that flowed through the cracks of non-incubated specimens (every specimen is measured in triplicate); $W_{f,\text{ n}}$ is the amount of water that flowed through the crack of an incubated specimen (every specimen is measured in triplicate).

5.2.9. PHA CHARACTERIZATION

The PHA after extraction was analyzed for purity and monomer content (hydroxybutyrate (HB) and hydroxyvalerate (HV)) using gas chromatography. The method is described in detail by Johnson, 2009b. In brief, the PHA was hydrolyzed and esterified in the presence of concentrated HCl, propanol, and dichlorethane with a ratio of 1/4/5 (v/v/v) for 2h at 100 °C. The formed esters, which accumulated in the organic phase, were analyzed by a gas chromatograph (model 6890N,

Agilent, USA). However, a mixture of methyl-3-hydroxybutyrate and methyl-3-hydroxyvalerate (Sigma Aldrich, USA) was used as standard due to a reduced purity of the commonly used standard (P(3HB-co- 3HV) with 12 mol% 3-HV (Sigma Aldrich, USA), as shown by Burniol-Figols *et al.*, 2020. A differential scanning calorimeter (DSC) measurement was performed to measure the glass transition (Tg) and melting (Tm) temperature using a Perkin Elmer DSC-7. The PHA sample was heated from 25 to 140 °C at a rate of 10 °C/min. After 1 min at 140 °C, the sample was cooled to -20 °C at the same rate. In a second run, the sample was heated again to 140 °C at the same rate. All steps were performed under a nitrogen atmosphere.

A thermogravimetric analysis (TGA) was performed to measure the decomposition temperature (Td) using a Perkin Elmer TGA 8000. The PHA sample was heated from 30 °C to 350 °C at 10 °C/min under a nitrogen atmosphere. A gel permeation chromatography (GPC) measurement was performed to measure the molecular weight distribution of PHA using a Shimadzu Prominence GPC system equipped with a Shodex LF−804 column. Tetrahydrofuran (THF) was used as the eluent at a flow rate of 1 mL/min at 40 °C. Before injection, the PHA sample was dissolved in chloroform at a concentration of 3 mg/mL, and subsequently filtered. Data of the refractive index detector was quantified with a universal calibration of monodisperse polystyrene standards with the help of LabSolutions software.

5.3. Results and Discussion

5.3.1. Characterization of the PHA polymer

The results of the characterization of the PHA polymer are shown in Fig. 5.1

Purity and physicochemical characteristics of PHA	
Purity (wt%)	97.4
HV (wt%)	36
$T_g(°C)$	-4
$T_m(°C)$	89
$T_d(°C)$	269
$M_w(kDa)$	47
$M_n(kDa)$	18
PDI (M_w/M_n)	2.6

Table 5.1.: Purity and physicochemical characteristics of the PHA polymer used for experiments in this study

The purity of the extracted PHA used for the experiments was high. The fraction of HV monomers (36% wt%) resulted in a relatively low melting temperature (T_m) (175-180 °C for pure PHB). The value of the molecular weight (M_w) appeared to be very low, probably caused by prolonged drying of the PHA-rich biomass and extracting at relatively high temperatures (typically between 200 and 3,000 kDa) (Laycock *et al.*, 2013). According to Kanesawa *et al.*, 1990, the tensile strength

starts to decrease at a M_n of 70 kDa, and approaches zero around a M_n of 17 kDa. Furthermore, the high polydispersity index (PDI) revealed a heterogeneous polymer in terms of molecular weight (typically between 1.5 and 2.0). This suggests that the quality of the PHA polymer in this study is unsuitable for plastic applications. It should be noted that the purification method adopted in this study was not optimized for any of the polymer characteristics.

5.3.2. AXENIC GROWTH EXPERIMENT

An axenic growth experiment was conducted to verify the PHA-consuming ability of the *B. cohnii*-related strain (Section 5.2.3 of Materials and Methods). The shake flasks which contained PHA and the *B. cohnii*-related strain showed a 100-fold increase in cell concentration after 48 hours (blue series; Fig. 5.2). In addition, microscopic analysis of the suspension revealed that the PHA particles were covered by mobile bacterial cells (Fig. 5.3). No growth was observed in absence of PHA (red series; Fig. 5.2). This implies that the growth in the shake flasks incubated with the B. cohnii-related strain and PHA was directly related to PHA consumption. Also, no growth was observed in absence of the *B. cohnii*-related strain as inoculum (grey series; Fig. 5.2), not even after 11 days (data not shown). This implies that the growth in the shake flasks incubated with the *B. cohnii*-related strain and PHA cannot be caused by contaminating species. Together, these results supply evidence that this *B. cohnii*-related strain is capable of utilizing extracellular PHA as substrate.
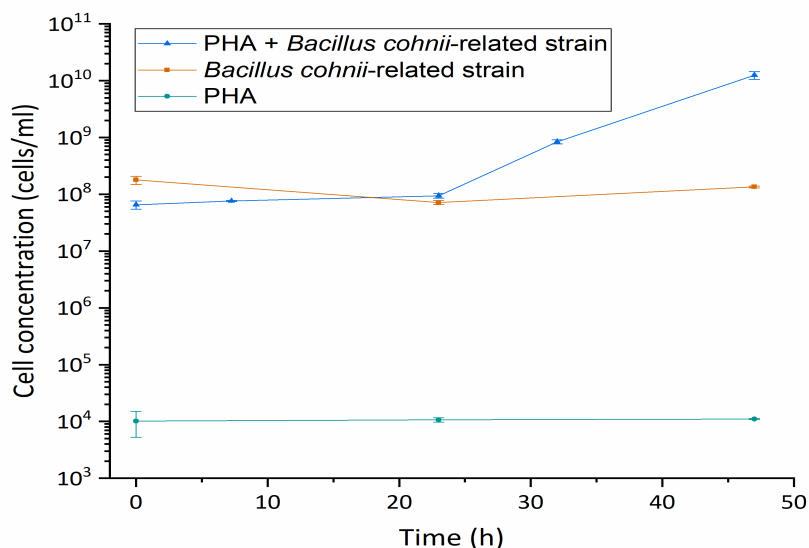

Figure 5.2.: Flow cytometric cell counts of axenic growth experiments in shake flasks. All three shake flask series were carried out in triplicate.

To support these findings, the genomic sequence data of *B. cohnii* was explored. The key enzyme required for extracellular PHA consumption is an extracellular PHA depolymerase, because a PHA molecule cannot be transported across the cell membrane as a polymer (Mukai *et al.*, 1993). According to the GenBank database, *B. cohnii* is in the possession of an extracellular PHA depolymerase, like many Bacillus species. (Accession no. AST93050.1 - NCBI) (Knoll *et al.*, 2009). Hence, it was presumed that the *B. cohnii*-related strain used in this study also must possess an extracellular PHA depolymerase enzyme.
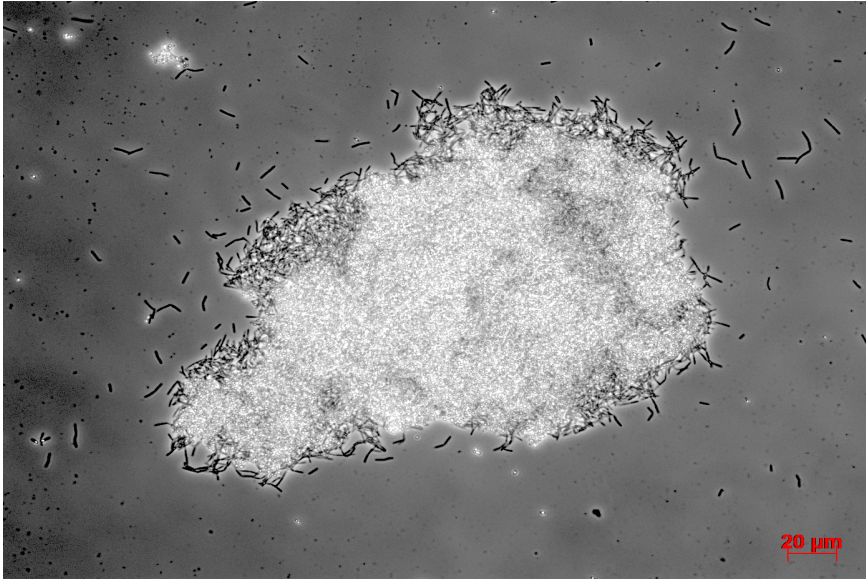

Figure 5.3.: A microscopic photo of a PHA particle surrounded by cells of a *Bacillus cohnii*-related strain. Phase contrast image at 400x magnification.

5.3.3. CRACK EVALUATION

Different series of mortar specimens were prepared and incubated (see Section 5.2.4, 5.2.5, and 5.2.6 of Materials and Methods). Before incubation, the crack widths of the specimens were analyzed with a stereomicroscope. The average crack widths (out of 7 specimens) were as follows: 0.46 ± 0.05 mm for all negative control specimens (no healing agent included), 0.48 ± 0.05 mm for all positive control specimens (lactate derivative based healing agent included), and 0.46 ± 0.04 mm for all PHA specimens. Although this was slightly higher than the intended 0.4 mm, the differences of the average crack width between the different treatments were very small.

Stereomicroscopic photos were taken of the same crack before and after incubation (see Fig. 5.4, left and middle column). The crack of the negative control specimen (Fig. 5.4, row A) shows some degree of healing, although the crack opening

is still clearly visible. This can be explained by so-called autogenous healing, a process which occurs in conventional, mainly young concrete structures primarily due to continuous hydration of cement (Van Tittelboom *et al.*, 2013). This process allows for the healing of the smallest cracks (widths of $0.1-0.2$ mm) (Rooij *et al.*, 2013). In the crack of the positive control specimen (Fig. 5.4, row B) and the PHA specimen (Fig. 5.4, row C) substantially more precipitation is visible. Here, the cracks are completely covered with precipitate, indicating the efficacy of the self-healing concrete technology.

The ESEM photos of the crack surface of incubated specimens (see Fig. 5.4, right column) reveal that the surface was indeed covered with a mineral precipitate consisting of cubic and rhombohedral shaped crystals, probably formations of calcium carbonate. The crystals formed in the positive control and the PHA specimens (Fig. 5.4, row B and C) were considerably larger than the crystals formed in the negative control specimen (Fig. 5.4, row A), again indicating the efficacy of the self-healing concrete technology. A remarkable observation were the presence of many rod-shaped cavities (± 1 μm by ± 4 μm) on the crack surface of the PHA specimen (Fig. 5.4, row C), indicated by the red arrows. These cavities resemble the bacterial imprints observed in other studies which examined microbially induced precipitation (Cacchio *et al.*, 2003; Tziviloglou *et al.*, 2016).

While choosing the photos, a representative selection has been made. However, the obtained photos cover only a minor fraction of the total amount of crack length incubated, and could therefore be slightly biased. Therefore, the photos should be regarded as an indication of the effectiveness of crack healing and not as definite proof. The water permeability test, on the other hand, quantifies the effectiveness of crack healing of the whole crack of multiple specimens (see Section 5.3.3). More3over, the most important functionality of self-healing concrete is assessed by measuring water permeability.

5.3.4. WATER PERMEABILITY EXPERIMENT

The water flow through the crack was measured before and after incubation of the specimens (see Section 5.2.8 of Materials and Methods). The water flow before incubation (Wi,average) was as follows: 7.6 ± 0.9 mL/s for the negative control specimens, 6.7 ± 0.9 mL/s for the positive control specimens, and 6.7 ± 0.8 mL/s for the PHA specimens. These values demonstrate, in accordance with the average crack width, an acceptable degree of homogeneity between and within the specimen series. The strategy of using different sets of specimens for measuring the initial and final water permeability is based on the assumption of homogeneity between the samples.

However, this assumption is only valid to a certain extent. In an ideal experiment, the self-healing capacity of an individual specimen should be measured. Nevertheless, the current strategy was chosen to exclude the risk of flushing out healing agent or other reactive components from the crack before incubation. The initial and final water flow values were used to calculate the reduction of water flow (RWF) (shown in Fig. 5.5).

The PHA specimens have a significantly higher mean RWF than the negative con-
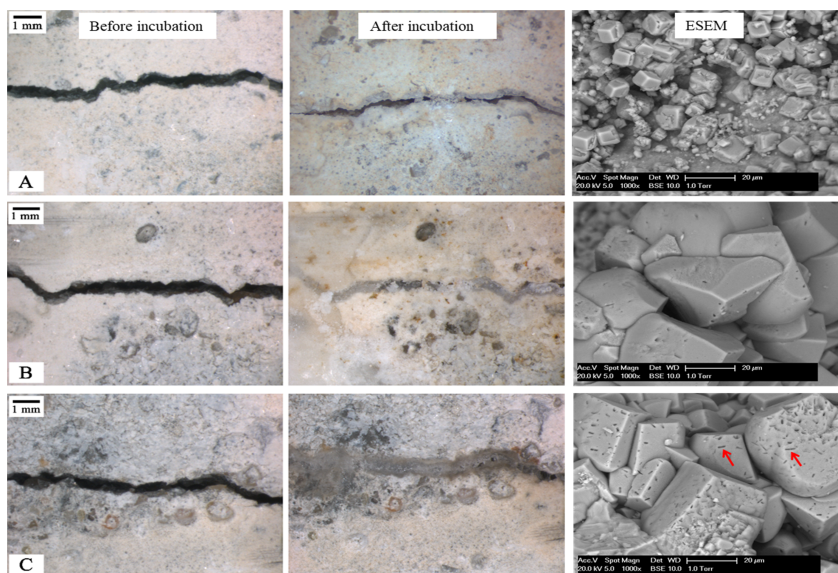
Figure 5.4.: Stereomicroscopic and ESEM analysis of the cracks. Row A) Negative control specimen, without healing agent; Row B) Positive control specimen, with healing agent composed of a lactate derivative; Row C) PHA specimen, with healing agent composed of waste-derived PHA. The stereomicroscopic photos in the left column depict the cracks before incubation, the stereomicroscopic photos in the middle column depict the crack after incubation, and the ESEM photos in the right column depict precipitates on the surface of an incubated, freshly broken specimen.
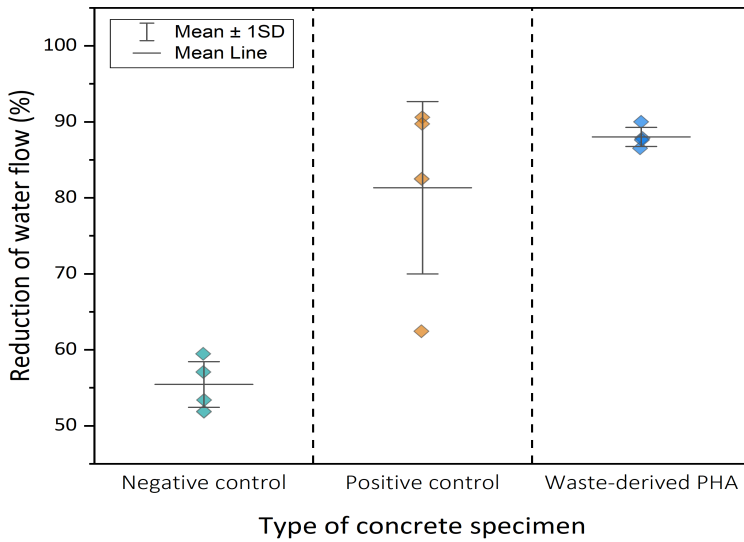
Figure 5.5.: Reduction of water flow (RWF) of concrete specimens after 56 days of incubation under humid conditions. Negative control specimens do not contain healing agent; positive control specimens contain healing agent composed of a lactate derivative; PHA specimens contain healing agent composed of PHA derived from organic waste. The whiskers represent ±1 standard deviation.

trol specimens (88 ± 1.3% compared to 55 ± 3.0%) and a slightly higher mean RWF than the positive control (88 ± 1.3% compared to 81 ± 11.3%). This shows that the PHA specimens possess a healing capacity which is significantly higher than the autogenous healing process in the negative control specimens. Moreover, the healing capacity is comparable to the currently marketed lactate derivative based technology represented by the positive control specimens. These findings are in line with the microscopic analysis of the crack mouths in Section 5.3.3. Fig. 5.5 also displays that none of the samples reached complete water tightness (RWF = 100%) after 56 days of incubation. Although the microscopic photos reveal complete healing of some of the cracks, the formed precipitates are not able to completely withstand the water pressure in the experimental set-up. This observation is in accordance with other publications with similar experimental set-ups. For example, Tziviloglou *et al.*, 2015 show that the RWF of specimens with a significantly smaller average crack width (0.35 mm) no complete water tightness is achieved after 56 days (RWF = 98%). Larger crack widths (0.6 mm) were established by Palin *et al.*, 2017. They describe that a RWF of 93% was reached after 56 days of submersion in artificial seawater, where it should be noted that seawater can enhance the autogenous healing capacity (Palin *et al.*, 2016).

As in Section 5.3.3, it appears that autogenous healing is a significant factor in the healing capacity of the cracks. This widely studied phenomenon has also been observed and quantified by other authors (Edvardsen, 1999; Reinhardt *et al.*, 2003 and Aldea *et al.*, 1999), recorded a water permeability reduction of 56% in normal strength concrete in samples without any healing agent, comparable to the results in this study (55 ± 3.0%). Autogenous healing is mainly caused by the continuation of the cement hydration reaction in the period after casting (i.e., 28 days). Aging concrete structures, which are usually facing the problem of cracking, will possess this type of autogenous healing capacity to a smaller extent. Therefore, we can expect that the relative difference in healing capacity between PHA-based healing agent and negative control specimens will increase even further, as the concrete ages.

Another noticeable observation in Fig. 5.5 is the relatively large scatter of the values of the positive control specimens. The crack width of the specimen which forms the outlier (RWF = 62.5%) is slightly above the average for this series (0.51 mm). Another specimen in this series has a crack width of 0.56 mm and reaches a RWF of 89.7%. Therefore, it is unlikely that this deviation is merely caused by increased crack width. Another explanation is the intrinsic, stochastic factor linked to a healing agent consisting of particles. This means that a formed crack has a certain probability that it will hit an embedded particle, which affects the degree of healing.

5.3.5. SUMMARY OF RESULTS: WASTE-DERIVED PHA CAN BE APPLIED AS HEALING AGENT IN CONCRETE

The presented data suggest that self-healing concrete is a promising new application for waste-derived PHA. The self-healing bacterial strain (*B. cohnii*-related) has the metabolic machinery present to consume extracellular PHA. Moreover, healing agent composed of waste-derived PHA induces crack healing in concrete structures, while simultaneously reducing the water permeability of the cracks. The obtained results are comparable to the performance of the currently marketed lactate derivative based technology.

5.3.6. FUNCTIONAL PROPERTIES OF CONCRETE

When additives are mixed with concrete, the influence on the functional properties of the concrete must be within the acceptable range. It is known that the compressive strength and/or the cement hydration reaction of concrete can be critically affected by the components of healing agent (i.e., PHA, spores, yeast extract, and unknown impurities in the PHA) (Basaran Bundur *et al.*, 2015 and Luo *et al.*, 2016). However, R. Mors *et al.*, 2017 demonstrate that the compressive strength of concrete containing a comparable healing agent (i.e., a lactate derivative based healing agent; the positive control in this study) is not compromised after 28 or 56 days of curing. Nevertheless, future research should confirm the compatibility of concrete with healing agent composed of waste-derived PHA.

5.3.7. SPECIFICATIONS OF THE PHA POLYMER

In this study, PHA with a high purity (97.4%) was cast in the concrete. However, a high purity generally requires an extensive and costly purification process. On the other hand, a large fraction of impurities might have an adverse effect on the functional properties of the concrete. However, it is possible that that the melting step during the particle formulation will neutralize the effect of the impurities by encapsulating them. Altogether, it would be interesting to study which fraction of impurities still allows for a healing agent which is concrete compatible. Implementing this idea can reduce the costs for PHA purification.

As described in Section 5.3.1, the PHA used in this study has a low molecular weight with a broad mass distribution. From the perspective of bioplastic manufacturing, this polymer would have a low quality. Nevertheless, this study demonstrates that the specification are sufficient for an application in self-healing concrete. This finding opens possibilities for PHA batches unsuitable for plastic applications in future production facilities. However, it should be pointed out that the polymer needs to meet some specifications, such as the ability to be processed into particles which can withstand the frictional forces of concrete mixing, and the ability of the particles to be consumed by the self-healing bacteria. Future trials with different batches of PHA comprising a range of physicochemical characteristics (HV content, molar mass distribution, melting temperature) must determine the impact of polymer properties on both the particle formulation process and the self-healing capacity.

5.3.8. GENERAL CONSIDERATIONS FOR VALUE CHAIN DEVELOPMENT OF WASTE-DERIVED MATERIALS

The necessity for a more circular approach for wastewater treatment has been underlined by the scientific community for many years now. In this view, wastewater is regarded as resource, and the wastewater treatment plant is regarded as a resource recovery facility, where water, energy, nutrients, and products are collected in a centralized manner (Guest *et al.*, 2009; Van Loosdrecht *et al.*, 2014). As a consequence, waste water treatment moves from a process with a single objective to a more complicated and multidisciplinary operation, involving novel aspects, such as product and value chain development (Bozkurt *et al.*, 2017). A closer examination of other potential technologies to recover waste-derived materials, such as extracellular polymeric substances (EPS), medium chain fatty acids (MCFA), cellulose, and struvite, reveals that their level of implementation in the wastewater sector is still limited, as it is for PHA. Moreover, it appears that the challenges underlying this limited success show similarities between the different waste-derived materials (Kehrein *et al.*, 2020).

A challenge, which is applicable to almost all waste-derived materials, is the small amount of resources available in waste streams. Because organic waste streams are a side-product of an agro-industrial process, the quantity is not available in a scalable amount, in contrast to conventional agricultural or fossil resources. This means that the quantity of product that can be generated from a waste stream will be much smaller than in conventional production processes. Therefore, the advantage of optimization by scaling, which is crucial for the production of commodities, is limited for waste-derived materials (Kleerebezem *et al.*, 2015). This emphasizes that the production of waste-derived PHA applied as bioplastic is such an ambitious undertaking.

Another limitation associated with waste-based production processes is the quality of the feedstock compared to sugar- or fossil-based processes. All waste streams have compositional fluctuations to a certain degree which can result in a variable amount and type of impurities in the final product. Moreover, for EPS, PHA, and MCFA variations in waste water composition result in variations in the chemical composition of the product itself, which brings along uncertainty about the market value. However, important to realize is that quality is defined by the final application (Valentino *et al.*, 2017). Not all applications need the highest specifications, as it is envisioned for the usage of EPS as brick additive (van der Roest *et al.*, 2015), the usage of cellulose as aggregate for asphalt (Visser *et al.*, 2016), or, as proposed in this study, the usage of PHA in self-healing concrete.

A critical obstacle for widespread implementation of waste-derived materials are the final production costs. Most resource recovery processes are not cost-effective because of high operational and/or investment cost compared to conventional industrial production. When PHA is applied as high-quality bioplastic, high purity and mechanical requirements result in a complex and expensive process. Another example is phosphate recovery as struvite, which can be applied as fertilizer. Here, a high chemical and energy demand for the production of struvite results in a high price compared to conventional phosphate fertilizer production (Le

Corre *et al.*, 2009). EPS production has a clear advantage at this point, because no additional investments in the upstream process are required when an aerobic granular sludge reactor is in place (Lin *et al.*, 2015). On the other hand, product yields and product purities in the upstream process are significantly lower compared to other resource recovery processes described here.

Due to the factors described above, waste-derived materials experience a strong competition with the conventionally produced materials. The exploration of new application routes can form a solution to these problems. Waste-derived materials used in niche applications will encounter less competition when their unique selling points are utilized. Fortunately, the number of examples of these new applications in literature increases. Waste-derived cellulose has proven useful as soil conditioner (Ruiken *et al.*, 2013) and insulation material (Eijlander *et al.*, 2019). And, although understanding of the chemical structure of EPS is still minimal, different applications have been proposed and tested, such as flame retardant (Kim *et al.*, 2020), paper coating (Lin *et al.*, 2015), and cement coating (Zlopasa *et al.*, 2014).

For PHA, a number of innovative applications have been explored, as described in the Introduction section. With this study, we would like to add the use of PHA as healing agent in self-healing concrete to the list of innovative applications for waste-derived PHA. In our opinion, more creativity in establishing connections between developments that aim for resource recovery, and developments that use recovered resources is one of the main challenges we are facing in the transition to a more circular economy.

5.4. Conclusions

This study demonstrates the potential of a new application for waste-derived PHA, as bacterial substrate in self-healing concrete. The experimental data shows that a PHA-based healing agent produced from PHA unsuitable for thermoplastic applications, induces crack healing in concrete specimens, and consequently, reduces the water permeability of the cracks. Although questions for future work remain, this study provides a proof-of-concept which successfully connects two separate fields of sustainable engineering. We foresee that this new application may counteract some of the key challenges for the large-scale implementation of waste-derived PHA, while simultaneously supplying circular and potentially more affordable raw materials for the production of self-healing agent.

6

GENERAL DISCUSSION AND OUTLOOK

You can do what you want.
The opportunity's on.
And if you find a new way
Then you can do it today.

Cat Stevens

6.1. INTRODUCTION

The aim of this thesis was to optimize and balance waste-derived PHA biosynthesis with recovery, and to target for an application of PHA in self-healing concrete. To this end, research was conducted on all parts of the value chain from waste to self-healing concrete: PHA biosynthesis, PHA recovery and the application of PHA. In this section, topics were selected for an overarching or general discussion. Finally, an outlook will be given for each part of the value chain.

6.2. PHA BIOSYNTHESIS

6.2.1. COMPARISON OF ALL FATTY ACIDS STUDIED AT EBT

In the past years, the PHA work at the Environmental Biotechnology group (EBT) at TU Delft gave rise to a collection of studies that tested fatty acids under virtually identical conditions. In Chapter 2 and 3 of this thesis, isobutyrate and octanoate were studied as substrate for PHA production. Hexanoate was also studied as substrate during the project that resulted in this thesis (unpublished work). In this section, a comparison is made between the fatty acids in all studies, including acetate, propionate, lactate, butyrate, isobutyrate, hexanoate, and octanoate Fig. .

The variables of all graphs in Fig. 6.1 seem to be correlated. A possible explanation is that with a high biomass specific PHA production rate (Fig. 6.1 b), a relatively small fraction of the substrate is channeled towards growth, resulting in a high PHA yield and a high PHA content at the end of the cycle (Fig. 6.1 a and c). If this is a valid explanation, the question follows, what causes a high biomass specific PHA production rate?

The substrates that are converted completely into PHB have the highest biomass specific PHA production rates. Moreover, these substrate are able to maximize their PHA yield by channeling almost all substrate towards PHA, while minimizing growth. Acetate and lactate have a lower theoretical PHA yield, which makes butyrate the preferred substrate in every aspects. Lastly, these enrichments were dominated by Plasticicumulans acidvorans (acetate, butyrate), or a close relative (lactate). The community of the propionate enrichment was also dominated by P. acidivorans. In this case, this superior PHA producer revealed among the lowest biomass specific PHA production rates of all fatty acids. These results could be explained by the length of the metabolic route from substrate towards PHA, which is shorter for butyrate then for acetate, lactate, and propionate.

The enrichment with isobutyrate, hexanoate, and octanoate also resulted in uncommon PHA polymers (PHiB, PHHx, and PHO) which closely resembled the substrate, and therefore, required short metabolic synthesis routes. Still, the community also produced other PHA types, especially for hexanoate in the form of PHB. Despite the presence of a short metabolic route towards PHA, the biomass specific PHA production rates were significantly lower than for butyrate. Therefore, other factors than the length of the metabolic pathway will presumably play a role in determining the biomass specific PHA production rates, such as enzyme kinetics, enzyme expression levels, redox balancing and cell morphology.
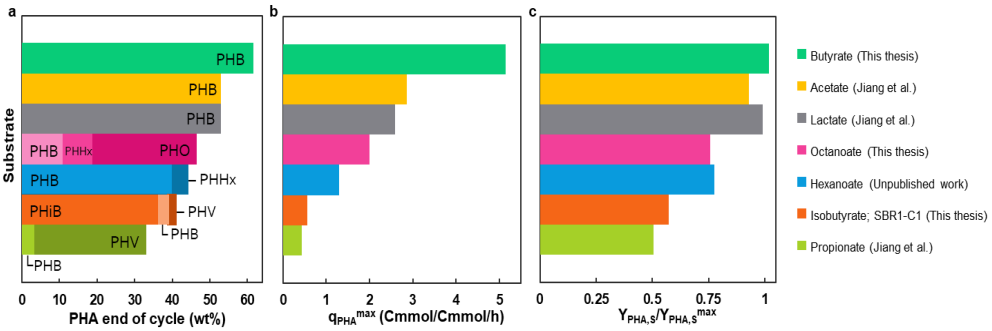
Figure 6.1.: Comparison of seven fatty acids studied under virtually identical experimental conditions. a: PHA content at the end of the cycle as a percentage of the dry weight. b: Biomass specific PHA production rate in the feast phase of the SBR. c: The PHA yield as a fraction of the maximal theoretical yield as derived from the metabolic pathways.

6.2.2. Outlook medium-chain-length PHA production from waste

Octanoate is a promising substrate to produce mcl-PHA. However, octanoate is an expensive substance and its concentration in waste valorization routes is until now low (Kucek, 2016). Therefore, it is not likely that the work in Chapter 3 has a large economic potential on the short term unless high-value applications can be reached. However, the theoretical concepts developed in Chapter 3 are universal, and could be tested on more accessible substrates, such as hexanoate.

As can be seen in Fig. 6.1, the unpublished study on hexanoate resulted mainly in PHB. This polymer can be produced much more effectively via acetate, butyrate or lactate. As a solution, oxygen limitation could be applied to increase the fraction of PHHx in the polymer similar to Chapter 3. An additional asset of oxygen limitation is that a high oxygen transfer rate comes at a high cost. Therefore, oxygen transfer has already been identified as principal limiting factor for the productivity of a PHA production process (Tamis, 2015). By applying oxygen limitation to increase mcl-PHA production, the oxygen transfer capacity is utilized optimally which makes the process more cost-effective.

6.3. PHA recovery

6.3.1. Mechanism of PHBV extraction from biomass

The work conducted in this thesis provided many thoughts on the mechanism of PHBV extraction from biomass. Although extraction of PHBV is often regarded as a black box, in this section, I want to combine the ideas collected during my research to propose a basis for a simple mechanistic model that comprises the main factors affecting the different steps in the extraction process.

In the model, the PHBV is represented by a semi-crystalline particle embedded

within a biomass granule Fig. 6.2. This biomass granule is a cluster of bacteria with a diameter of ±1 mm depending on the drying and shredding process. The granule contains pores, and is penetrable by solvent molecules. During extraction the following steps can be identified:

1. Solvent enters biomass matrix (pink arrows)

2. Solubilization of PHBV when solvents reaches PHBV particle (blue arrows)

3. Diffusion of solubilized PHBV chains through biomass matrix towards bulk solutions (green arrows)
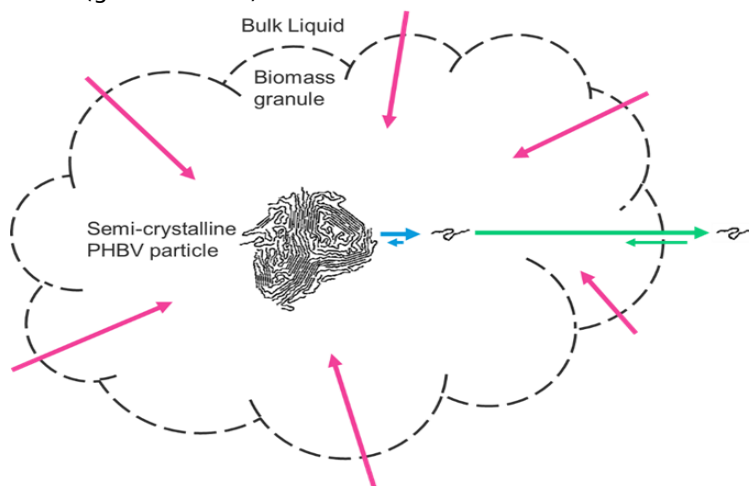

Figure 6.2.: Schematic representation of a mechanistic model for PHBV extraction (not to scale). Pink arrows represent solvent entering the biomass granule (±1 mm). Blue arrows represent solubilization of PHBV. Green arrows represent diffusion of solubilized PHBV.

Step 2 and step 3 are the most crucial steps in PHBV extraction. The extent of these steps combined is defined as the extraction yield in this thesis.
In step 2, the properties of the PHBV such as HV content and molecular weight play an important role. The amorphous PHBV strains containing a higher HV content are more accessible and will dissolve faster and more effectively than the crystalline PHBV strains containing a lower HV content. Second, the process conditions have a large influence on step 2. The rate and extent of PHBV solubilization is largely determined by temperature and solvent type. Here, a higher temperate and a solvent with a smaller molar volume will have a higher rate and extent of polymer solubilization. In this thesis, step 2 turned out to be the largest bottleneck in obtaining an extraction yield of 100%, because very high temperatures result in undesirable high pressures and M_w scission rates.
Step 3 is the second important step in PHBV extraction. Solubilzed PHBV will keep diffusing towards the bulk liquid until an equilibrium is reached between the concentration of PHBV in the biomass matrix and the concentration in the

bulk liquid. The rate of this step is determined by the size and structure of the biomass granules, the molecular weight of the polymer, and the flow velocity of the liquid as a result of agitation and convection. The equilibrium situation of this reaction step is mainly determined by the biomass to solvent ratio. For example, in Chapter 4, ±20% of the total amount of solvent added in the experiment was retained by the biomass matrix after separation of the bulk liquid. Therefore, ±20% of the solubilized PHBV also remained in the biomass matrix. This problem was largely solved by applying a series of extractions, where new equilibria were formed in every new extraction. In this case, the concentration of PHBV in the biomass matrix is diluted every extraction by a factor of approximately 5. In large-scale installations, this issue can be approached by implementing a counter-current extraction process thereby keeping the concentration difference of PHBV in the biomass matrix and in the bulk solution high during the whole extraction. A biomass washing step can be another approach to recover most of the solubilized PHBV.

6.3.2. POLYMER QUALITY VERSUS POLYMER YIELD TRADE-OFF

In most chemical and biochemical purification processes, a higher product purity comes at the cost of a lower product yield. To obtain a higher purity, additional purification steps need to be added to the process which give rise to additional yield losses. A similar outcome was found in the data obtained for the research described in Chapter 4. Because this outcome implies an important trade-off for future plant design, the issue will be discussed in this section in more detail.

To this end, the most promising extraction experiments from Chapter 4 were ranked from high purity to low purity Fig. 6.3. It appears that the PHBV product yield shows an inverse trend from low yield to high yield. On the left, the extraction with 2-butanol below boiling point resulted in a purity of 99.2 ± 0.9%, while the product yield was only 63.4 ± 0.2%. On the right, the acetone evaporation extraction resulted in a much higher yield (95.1 ± 2.7%), while the obtained product purity was much lower (84.4 ± 1.0%). The general trend is that the highest purities and the lowest yields were obtained with extractions at lower temperature. Extraction temperature also has a major influence on molecular weight of the PHBV product. Fig. 6.3 shows that besides purity also molecular weight reveals a slight inverse trend with product yield.

In addition, unpurified PHBV-rich biomass (38 wt% PHBV) was added to the graph (PHBV-X). Research has shown that PHBV-rich biomass can be utilized directly via thermal processing without a costly and wasteful purification process (Coats *et al.*, 2008). The result is that no PHBV is lost (100% product yield) after biomass drying, but that the purity is very low (38 wt%). Therefore, this utilization route also fits the proposed trend in Fig. 6.3.

An advantage of aiming for a PHBV application with a low demand concerning product purity is that the quantity of product per quantity of input biomass increases significantly. First, the product yield is higher. Second, a large amount of other substances end up as product. Moreover, these substances do not have to be treated as waste. Comparing the 2-butanol extraction at boiling point with the
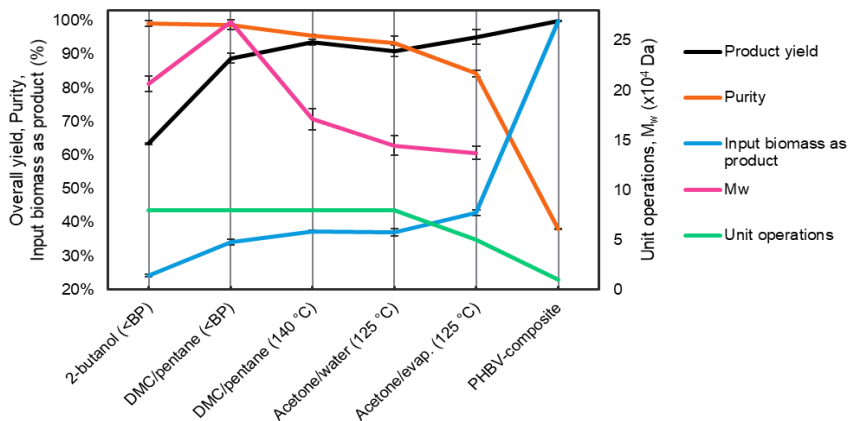
Figure 6.3.: Comparison of most promising extraction configurations in terms of product yield, purity, molecular weight (M_w), percentage of input biomass that ends up as product, and number of unit operations in the process. <BP indicates extraction at 5% below boiling point.

acetone evaporation extraction, it appears that the quantity of product increased with 76%. Another advantage of aiming for a PHBV application with a low demand concerning product purity is presumably a more affordable purification process. A smaller number of unit operations is required to reach a low purity Fig. 6.3.

In conclusion, by choosing solvent type and process conditions a trade-off can be made between high product quality (both molecular weight and purity) on the one hand, and high product yield and, presumably, a more cost-effective process on the other hand. The final decision is largely determined by the intended application.

6.3.3. OUTLOOK PHA RECOVERY

The experiments performed in this thesis revealed that the extractions with methanol resulted in the highest product yield. Meth-anol also has a lower PHBV solubility than acetone, and therefore less water will be required to precipitate all the PHBV in the antisolvent step, which will reduce water evaporation costs. Also, due to the absence of an azeotrope no pervaporation step will be required to separate the water from the solvent unlike acetone.For these reasons, it would be interesting to study methanol in more detail.

However, methanol has the highest polymer scission rate of all the alcohols, so molecular weight of the PHBV product can become low. A recommendation for a future experiment would be to investigate methanol as extraction solvent at lower extraction temperature. Lower extraction temperatures will increase the molecular weight of the PHA obtained, while it will lower the energy requirements for heating. Another idea is to increase the extraction temperature from the first

to the third extraction series (e.g. 85 °C; 105 °C; 125 °C). In this way, on average a relatively high molecular weight and a relatively high product yield can be obtained. The fractions of PHBV obtained from the different extraction series will have a different molecular weight, but can be applied in different types of applications.

The biomass used for the solvent extractions contained PHBV with a low molecular weight due to a destructive thermal drying step. Future methods for biomass drying will need to aim for minimization of the molecular weight decrease. Therefore, it is recommended to repeat the extraction experiments with biomass that has been dried in different ways to assess the impact on purity, extraction yield, and product yield. It is expected that a higher molecular weight will impede the extraction yield. At the same time, it will facilitate the precipitation, especially for the poor solvents where the PHBV solubility is relatively high compared to the solvent-antisolvent mixtures. The net effect of changes in extraction and precipitation yield, as described by the final product yield, need to be determined experimentally. Furthermore, it is expected that high molecular weight polymers result in more severe gel formation upon precipitation, which can complicate the process.

The experimental result in Chapter 4 suggest that optimization of PHBV extraction is dependent on the objectives of the downstream processing. A higher extraction temperature or longer extraction time improve the PHBV yield, but decrease PHBV purity and molecular weight. Furthermore, contaminants will accumulate in the solvent, and timely regeneration of the solvent is essential to retain the performance of the extraction process. To find the optimum extraction conditions, it is required to implement or develop techniques to monitor the extraction process (e.g. optical or viscosity-based measurements to determine PHBV or contaminant concentrations). In this case, pilot- or full-scale equipment can be utilized more efficiently. Moreover, these monitoring techniques will allow for a better anticipation towards the variabilities in the biomass.

6.4. Application of PHA

6.4.1. Outlook

In Chapter 5, a proof-of-concept is established for the application of PHBV in self-healing concrete. This study formed the beginning of a development trajectory to bring PHBV to the market. The next step of this trajectory is described in Rossi *et al.*, 2021 where the effect of the PHBV-based healing agent on the concrete properties is studied. It shows that the PHBV-based healing agent performs as good as or better than the current PLA-based technology in the isothermal calorimetry test and the compression strength test. The Vicat test showed a slightly higher (8%) setting time for the PHBV-based healing agent compared to the PLA-based healing agent. In brief, the effect of the PHBV-based healing agent on the concrete properties is minimal and do not obstruct the development trajectory.

Another innovation regarding the application in self-healing concrete is the usage of a PHBV-composite. The idea is that the costly PHBV recovery step is circum-

vented, and PHBV-rich biomass is thermally processed to form healing agent. The challenge for this strategy is to avoid leaching of water-soluble biomass components into the concrete matrix because they can have a detrimental effect on the concrete properties. This innovation is currently being tested, and could potentially shorten the development trajectory to bring waste-derived PHBV to the market.

The PHBV as healing agent in self-healing concrete is an example of an application where biodegradability is required, while material properties are not critical. Other examples in this category are paper coatings and adhesives or fertilizer coatings/additives. These markets are most likely willing to pay the extra costs of a biodegradable alternative, such as PHBV. Once these markets are established, the increase in production capacity will allow for a decrease in cost price, and an increase in experience on PHBV processing (Molenveld et al., 2022).

The next phase should focus on applications where biodegradability is required while material properties are also important. Examples in this category are mulch films, plant plugs, agricultural netting, and temporary marine structures. A third phase can focus on applications that could benefit from biodegradation, while material properties are also important, including tableware, plastic bags or clothing. Lastly, a phase can be reached where applications are explored where biodegradation is not required, but that benefit from a low CO2 footprint, which are basically all remaining plastics. Every new phase allows for an increase in market size, and, consequently, a decrease in cost price and an increase in know-how on PHA processing. The latest prognosis is that PHA production capacity will experience a 10-fold increase in the coming 5 years (Molenveld et al., 2022).

Bibliography

Levi, P. G., & Cullen, J. M. (2018). Mapping global flows of chemicals: From fossil fuel feedstocks to chemical products. *Environmental science & technology*, *52*(4), 1725–1734.

Millican, J. M., & Agarwal, S. (2021). Plastic Pollution: A Material Problem? *Macromolecules*, *54*(10), 4455–4469. https://doi.org/10.1021/ACS.MACROMOL.0C02814/ASSET/IMAGES/LARGE/MA0C02814_0013.JPEG

Ziajahromi, S., Drapper, D., Hornbuckle, A., Rintoul, L., & Leusch, F. D. (2020). Microplastic pollution in a stormwater floating treatment wetland: Detection of tyre particles in sediment. *Science of The Total Environment*, *713*, 136356. https://doi.org/10.1016/J.SCITOTENV.2019.136356

Meereboer, K. W., Misra, M., & Mohanty, A. K. (2020). Review of recent advances in the biodegradability of polyhydroxyalkanoate (PHA) bioplastics and their composites. *Green Chemistry*, *22*(17), 5519–5558. https://doi.org/10.1039/D0GC01647K

Skoczinski, P., Carus, M., de Guzman, D., Käb, H., Chinthapalli, R., Ravenstijn, J., Baltus, W., & Raschka, A. (2021). Bio-based Building Blocks and Polymers – Global Capacities, Production and Trends 2020 – 2025. (January). www.renewable-carbon.eu/graphics%20https://renewable-carbon.eu/publications/product/bio-based-building-blocks-and-polymers-global-capacities-production-and-trends-2020-2025-short-version/

Plastics Europe. (2015). An analysis of European plastics production, demand and waste data. *https://plasticseurope.org/wp-content/uploads/2021/10/2015-Plastics-the-facts.pdf*, 1–34. https://plasticseurope.org/wp-content/uploads/2021/10/2015-Plastics-the-facts.pdf

Bentsen, N. S., Felby, C., & Thorsen, B. J. (2014). Agricultural residue production and potentials for energy and materials services. *Progress in Energy and Combustion Science*, *40*(1), 59–73. https://doi.org/10.1016/J.PECS.2013.09.003

Schanes, K., Dobernig, K., & Gözet, B. (2018). Food waste matters - A systematic review of household food waste practices and their policy implications. *Journal of Cleaner Production*, *182*, 978–991. https://doi.org/10.1016/J.JCLEPRO.2018.02.030

Marang. (2019). *Scale-Up Aspects of PHA Production by Microbial Enrichment Cultures* (Doctoral dissertation). PhD thesis, Delft University of Technology. https://doi.org/10.4233/uuid:1f3b0744-cc0a-44cb-95b1-d19354a0b157

Emadian, S. M., Onay, T. T., & Demirel, B. (2017). Biodegradation of bioplastics in natural environments. *Waste Management*, *59*, 526–536. https://doi.org/10.1016/J.WASMAN.2016.10.006

van den Oever, M., Molenveld, K., van der Zee, M., & Bos, H. (2017). *Bio-based and biodegradable plastics : facts and figures : focus on food packaging in the Netherlands*. https://doi.org/10.18174/408350

Rodriguez-Perez, S., Serrano, A., Pantión, A. A., & Alonso-Fariñas, B. (2018). Challenges of scaling-up PHA production from waste streams. A review. *Journal of Environmental Management*, *205*, 215–230. https://doi.org/10.1016/j.jenvman.2017.09.083

Steinbüchel, A. (1991). Polyhydroxyalkanoic acids. In *Biomaterials* (pp. 123–213). Palgrave Macmillan UK. https://doi.org/10.1007/978-1-349-11167-1_3

Steinbüchel, A., & Valentin, H. E. (1995). Diversity of bacterial polyhydroxyalkanoic acids. *FEMS Microbiology Letters*, *128*(3), 219–228. https://doi.org/10.1111/j.1574-6968.1995.tb07528.x

Zheng, Y., Chen, J. C., Ma, Y. M., & Chen, G. Q. (2020). Engineering biosynthesis of polyhydroxyalkanoates (PHA) for diversity and cost reduction. *Metabolic Engineering*, *58*, 82–93. https://doi.org/10.1016/j.ymben.2019.07.004

Laycock, B., Halley, P., Pratt, S., Werker, A., & Lant, P. (2013). The chemomechanical properties of microbial polyhydroxyalkanoates. *Progress in Polymer Science*, *38*(3-4), 536–583. https://doi.org/10.1016/j.progpolymsci.2012.06.003

Molenveld, K., Post, W., Ferreira, S. F., de Sévaux, G., & Hartstra, M. (2022). Paving the way for biobased materials, 72. https://research.wur.nl/en/publications/paving-the-way-for-biobased-materials-a-roadmap-for-the-market-in

Fernández-Dacosta, C., Posada, J. A., Kleerebezem, R., Cuellar, M. C., & Ramirez, A. (2015). Microbial community-based polyhydroxyalkanoates (PHAs) production from wastewater: Techno-economic analysis and ex-ante environmental assessment. *Bioresource Technology*, *185*, 368–377. https://doi.org/10.1016/j.biortech.2015.03.025

Kleerebezem, R., & van Loosdrecht, M. C. (2007). Mixed culture biotechnology for bioenergy production. *Current Opinion in Biotechnology*, *18*(3), 207–212. https://doi.org/10.1016/J.COPBIO.2007.05.001

Estévez-Alonso, Á., Pei, R., van Loosdrecht, M. C., Kleerebezem, R., & Werker, A. (2021). Scaling-up microbial community-based polyhydroxyalkanoate production: Status and challenges. *Bioresource Technology*, *327*, 124790.

Silva, F., Matos, M., Pereira, B., Ralo, C., Pequito, D., Marques, N., Carvalho, G., & Reis, M. A. (2022). An integrated process for mixed culture production of 3-hydroxyhexanoate-rich polyhydroxyalkanoates from fruit waste. *Chemical Engineering Journal*, *427*(June 2021), 131908. https://doi.org/10.1016/j.cej.2021.131908

Van Loosdrecht, M. C., Pot, M. A., & Heijnen, J. J. (1997). Importance of bacterial storage polymers in bioprocesses. *Water Science and Technology*, *35*(1), 41–47. https://doi.org/10.1016/S0273-1223(96)00877-3

Anterrieu, S., Quadri, L., Geurkink, B., Dinkla, I., Bengtsson, S., Arcos-Hernandez, M., Alexandersson, T., Morgan-Sagastume, F., Karlsson, A., Hjort, M., Karabegovic, L., Magnusson, P., Johansson, P., Christensson, M., & Werker, A. (2014).

6

Integration of biopolymer production with process water treatment at a sugar factory. *New Biotechnology*, *31*(4), 308–323. https://doi.org/10.1016/J.NBT.2013.11.008

Mulders, M., Tamis, J., Stouten, G. R., & Kleerebezem, R. (2020). Simultaneous growth and poly(3-hydroxybutyrate) (PHB) accumulation in a Plasticicumulans acidivorans dominated enrichment culture. *Journal of Biotechnology: X*, *8*. https://doi.org/10.1016/j.btecx.2020.100027

Johnson. (2009a). Enrichment of a mixed bacterial culture with a high polyhydroxyalkanoate storage capacity. *Biomacromolecules*, *10*(4), 670–676.

Mannina, G., Presti, D., Montiel-Jarillo, G., Carrera, J., & Suárez-Ojeda, M. E. (2020). Recovery of polyhydroxyalkanoates (PHAs) from wastewater: A review. *Bioresource Technology*, *297*, 122478. https://doi.org/10.1016/J.BIORTECH.2019.122478

Alfano, S., Lorini, L., Majone, M., Sciubba, F., Valentino, F., & Martinelli, A. (2021). Ethylic Esters as Green Solvents for the Extraction of Intracellular Polyhydroxyalkanoates Produced by Mixed Microbial Culture. *Polymers 2021, Vol. 13, Page 2789*, *13*(16), 2789. https://doi.org/10.3390/POLYM13162789

Pagliano, G., Galletti, P., Samorì, C., Zaghini, A., & Torri, C. (2021). Recovery of Polyhydroxyalkanoates From Single and Mixed Microbial Cultures: A Review. *Frontiers in Bioengineering and Biotechnology*, *9*, 624021. https://doi.org/10.3389/fbioe.2021.624021

Samorì, C., Abbondanzi, F., Galletti, P., Giorgini, L., Mazzocchetti, L., Torri, C., & Tagliavini, E. (2015). Extraction of polyhydroxyalkanoates from mixed microbial cultures: Impact on polymer quality and recovery. *Bioresource Technology*, *189*, 195–202. https://doi.org/10.1016/J.BIORTECH.2015.03.062

Koller, M., & Niebelschütz, H. (2013). Strategies for recovery and purification of poly [(R) -3-hydroxyalkanoates] (PHA) biopolyesters from surrounding biomass. *1*, 549–562. https://doi.org/10.1002/elsc.201300021

Kunasundari, B., & Sudesh, K. (2011). Isolation and recovery of microbial polyhydroxyalkanoates. *Express Polymer Letters*, *5*(7), 620–634. https://doi.org/10.3144/expresspolymlett.2011.60

Madkour, M. H., Heinrich, D., Alghamdi, M. A., Shabbaj, I. I., & Steinbüchel, A. (2013). PHA recovery from biomass. *Biomacromolecules*, *14*(9), 2963–2972. https://doi.org/10.1021/BM4010244/ASSET/IMAGES/MEDIUM/BM-2013-010244_0005.GIF

Aramvash, A., Moazzeni Zavareh, F., & Gholami Banadkuki, N. (2018). Comparison of different solvents for extraction of polyhydroxybutyrate from Cupriavidus necator. *Engineering in Life Sciences*, *18*(1), 20–28. https://doi.org/10.1002/elsc.201700102

Jiang, G., Johnston, B., Townrow, D., Radecka, I., Koller, M., Chaber, P., Adamus, G., & Kowalczuk, M. (2018). Biomass Extraction Using Non-Chlorinated Solvents for Biocompatibility Improvement of Polyhydroxyalkanoates. *Polymers*, *10*(7), 731. https://doi.org/10.3390/polym10070731

6

Koller, M. (2020). Established and advanced approaches for recovery of microbial polyhydroxyalkanoate (PHA) biopolyesters from surrounding microbial biomass. *The EuroBiotech Journal*, *4*, 113–126. https://doi.org/10.2478/ebtj-2020-0013

Patel, M., Gapes, D. J., Newman, R. H., & Dare, P. H. (2009). Physico-chemical properties of polyhydroxyalkanoate produced by mixed-culture nitrogen-fixing bacteria. *Applied Microbiology and Biotechnology*, *82*(3), 545–555. https://doi.org/10.1007/s00253-008-1836-0

Saavedra del Oso, M., Mauricio-Iglesias, M., & Hospido, A. (2021). Evaluation and optimization of the environmental performance of PHA downstream processing. *Chemical Engineering Journal*, *412*, 127687. https://doi.org/10.1016/J.CEJ.2020.127687

Tamis. (2015). *Resource recovery from organic waste streams by microbial enrichment cultures* (PhD thesis). PhD thesis, Delft University of Technology.

Valentino, F., Moretto, G., Lorini, L., Bolzonella, D., Pavan, P., & Majone, M. (2019). Pilot-Scale Polyhydroxyalkanoate Production from Combined Treatment of Organic Fraction of Municipal Solid Waste and Sewage Sludge. *Industrial Engineering Chemistry Research*, *58*(27), 12149–12158. https://doi.org/10.1021/acs.iecr.9b01831

Gurieff, N., & Lant, P. (2007). Comparative life cycle assessment and financial analysis of mixed culture polyhydroxyalkanoate production. *Bioresource Technology*, *98*(17), 3393–3403. https://doi.org/10.1016/j.biortech.2006.10.046

Bengsston, S., Werker, A., Visser, C., & Korving, L. (2017). *PHARIO - stepping stone to a sustainable value chain for PHA bioplastic using municipal activated sludge*. STOWA.

Iles, A., & Martin, A. N. (2013). Expanding bioplastics production: sustainable business innovation in the chemical industry. *Journal of Cleaner Production*, *45*, 38–49. https://doi.org/10.1016/J.JCLEPRO.2012.05.008

Kleerebezem, R., Joosse, B., Rozendal, R., & Van Loosdrecht, M. C. (2015). Anaerobic digestion without biogas? *Reviews in Environmental Science and Biotechnology*, *14*(4), 787–801. https://doi.org/10.1007/s11157-015-9374-6

Lauzier, C., Monasterios, C., Saracovan, I., Marchessault, R., & Ramsay, B. (1993). Film formation and paper coating with poly(β-hydroxyalkanoate), a biodegradable latex. *Tappi journal*, *76*(5), 71–77. https://www.osti.gov/biblio/6428520

Pereira, J. R., Araújo, D., Marques, A. C., Neves, L. A., Grandfils, C., Sevrin, C., Alves, V. D., Fortunato, E., Reis, M. A., & Freitas, F. (2019). Demonstration of the adhesive properties of the medium-chain-length polyhydroxyalkanoate produced by Pseudomonas chlororaphis subsp. aurantiaca from glycerol. *International Journal of Biological Macromolecules*, *122*, 1144–1151. https://doi.org/10.1016/j.ijbiomac.2018.09.064

Boyandin, A. N., Kazantseva, E. A., Varygina, D. E., & Volova, T. G. (2017). Constructing Slow-Release Formulations of Ammonium Nitrate Fertilizer Based

6

on Degradable Poly(3-hydroxybutyrate). *Journal of Agricultural and Food Chemistry*, *65*(32), 6745–6752. https://doi.org/10.1021/acs.jafc.7b01217

Cao, L., Liu, Y., Xu, C., Zhou, Z., Zhao, P., Niu, S., & Huang, Q. (2019). Biodegradable poly(3-hydroxybutyrate-co-4-hydroxybutyrate) microcapsules for controlled release of trifluralin with improved photostability and herbicidal activity. *Materials Science and Engineering C*, *102*, 134–141. https://doi.org/10.1016/j.msec.2019.04.050

Yang, Z., Weiss, W., & Olek, J. (2004). Interaction between Micro-Cracking, Cracking, and Reduced Durability of Concrete: Developing Methods for Considering Cumulative Damage in Life-Cycle Modeling. *JTRP Technical Reports*, (August 2005). http://docs.lib.purdue.edu/jtrp/132

Quéré, C. L., Andrew, R., Friedlingstein, P., & Sitch, S. (2018). Global Carbon Budget 2017, Earth Syst. Sci. Data, 10, 405–448. https://scholar.google.nl/scholar?hl=en&as_sdt=0%5C%2C5&q=Le+Qu%7B%5C'%7Be%7D%7Dr%7B%5C'%7Be%7D%7D+2018&btnG=

Wiktor, V., & Jonkers, H. M. (2016). Bacteria-based concrete: from concept to market. *Smart Materials and Structures*, *25*(8), 084006. https://doi.org/10.1088/0964-1726/25/8/084006

Jonkers, H. M. (2007). Self Healing Concrete: A Biological Approach. In *Springer series in materials science* (pp. 195–204). Springer, Dordrecht. https://doi.org/10.1007/978-1-4020-6250-6_9

Wang, J., Mignon, A., Snoeck, D., Wiktor, V., Van Vliergerghe, S., Boon, N., & De Belie, N. (2015). Application of modified-alginate encapsulated carbonate producing bacteria in concrete: a promising strategy for crack self-healing. *Frontiers in Microbiology*, *6*(10), 1088. https://doi.org/10.3389/fmicb.2015.01088

De Belie, N., Gruyaert, E., Al-Tabbaa, A., Antonaci, P., Baera, C., Bajare, D., Darquennes, A., Davies, R., Ferrara, L., Jefferson, T., Litina, C., Miljevic, B., Otlewska, A., Ranogajec, J., Roig-Flores, M., Paine, K., Lukowski, P., Serna, P., Tulliani, J.-M., . . . Jonkers, H. M. (2018). A Review of Self-Healing Concrete for Damage Management of Structures. *Advanced Materials Interfaces*, *5*(17), 1800074. https://doi.org/10.1002/admi.201800074

Palin, D., Wiktor, V., & Jonkers, H. M. (2017). A Bacteria-Based Self-Healing Cementitious Composite for Application in Low-Temperature Marine Environments. *Biomimetics*, *2*(4), 13. https://doi.org/10.3390/biomimetics2030013

Mors, R. M., & Jonkers, H. M. (2015). Reduction of water permeation through cracks in mortar by addition of bacteria based healing agent. *International Conference on Self-Healing Materials (ICSHM2015)*. http://icshm2015.pratt.duke.edu/sites/icshm2015.pratt.duke.edu/files/webform/extendedabstracts/20150415-RMors%20-ExtAbstr-Red%20water%20perm%20through%20cracks%20in%20mortar%20of%20ba-based%20HA.pdf

Lee, S. Y. (1996). Plastic bacteria? Progress and prospects for polyhydroxyalkanoate production in bacteria. *Trends in Biotechnology*, *14*(11), 431–438. https://doi.org/10.1016/0167-7799(96)10061-5

6

Kumar, P., & Kim, B. S. (2018). Valorization of polyhydroxyalkanoates production process by co-synthesis of value-added products. https://doi.org/10.1016/j.biortech.2018.08.120

Serafim, L. S., Lemos, P. C., Albuquerque, M. G., & Reis, M. A. (2008). Strategies for PHA production by mixed cultures and renewable waste materials. https://doi.org/10.1007/s00253-008-1757-y

Kourmentza, C., Plácido, J., Venetsaneas, N., Burniol-Figols, A., Varrone, C., Gavala, H. N., & Reis, M. A. M. (2017). Recent Advances and Challenges towards Sustainable Polyhydroxyalkanoate (PHA) Production. *Bioengineering*, *4*(4), 55. https://doi.org/10.3390/bioengineering4020055

Reis, M. A., Serafim, L. S., Lemos, P. C., Ramos, A. M., Aguiar, F. R., & Van Loosdrecht, M. C. (2003). Production of polyhydroxyalkanoates by mixed microbial cultures. *Bioprocess and Biosystems Engineering*, *25*(6), 377–385. https://doi.org/10.1007/s00449-003-0322-4

Jiang. (2011a). Metabolic modeling of mixed substrate uptake for polyhydroxyalkanoate (PHA) production. *Water Research*, *45*(3), 1309–1321. https://doi.org/10.1016/j.watres.2010.10.009

Lemos, P. C., Serafim, L. S., & Reis, M. A. (2006). Synthesis of polyhydroxyalkanoates from different short-chain fatty acids by mixed cultures submitted to aerobic dynamic feeding. *Journal of Biotechnology*, *122*(2), 226–238. https://doi.org/10.1016/j.jbiotec.2005.09.006

Marang. (2013). Butyrate as preferred substrate for polyhydroxybutyrate production. *Bioresource Technology*, *142*, 232–239. https://doi.org/10.1016/J.BIORTECH.2013.05.031

Dias, J. M., Serafim, L. S., Lemos, P. C., Reis, M. A., & Oliveira, R. (2005). Mathematical modelling of a mixed culture cultivation process for the production of polyhydroxybutyrate. *Biotechnology and Bioengineering*, *92*(2), 209–222. https://doi.org/10.1002/bit.20598

Johnson. (2009b). Model-based data evaluation of polyhydroxybutyrate producing mixed microbial cultures in aerobic sequencing batch and fed-batch reactors. *Biotechnology and bioengineering*, *104*(1), 50–67.

Van Aalst-Van Leeuwen, M. A., Pot, M. A., Van Loosdrecht, M. C., & Heijnen, J. J. (1997). Kinetic modeling of poly(β-hydroxybutyrate) production and consumption by Paracoccus pantotrophus under dynamic substrate supply. *Biotechnology and Bioengineering*, *55*(5), 773–782. https://doi.org/10.1002/(SICI)1097-0290(19970905)55:5<773::AID-BIT7>3.0.CO;2-8

Dionisi, D., Carucci, G., Petrangeli Papini, M., Riccardi, C., Majone, M., & Carrasco, F. (2005). Olive oil mill effluents as a feedstock for production of biodegradable polymers. *Water Research*, *39*(10), 2076–2084. https://doi.org/10.1016/j.watres.2005.03.011

Mechichi, T., & Sayadi, S. (2005). Evaluating process imbalance of anaerobic digestion of olive mill wastewaters. *Process Biochemistry*, *40*(1), 139–145. https://doi.org/10.1016/j.procbio.2003.11.050

6

Tholozan, J. L., Samain, E., & Grivet, J. P. (1988). Isomerization between n-butyrate and isobutyrate in enrichment cultures. *FEMS Microbiology Letters*, *53*(3-4), 187–191. https://doi.org/10.1016/0378-1097(88)90441-7

Angelidaki, I., & Ahring, B. K. (1995). Isomerization of n- and i-butyrate in anaerobic methanogenic systems. *Antonie van Leeuwenhoek*, *68*(4), 285–291. https://doi.org/10.1007/BF00874138

Lovley, D. R., & Klug, M. J. (1982). Intermediary metabolism of organic matter in the sediments of a eutrophic lake. *Applied and Environmental Microbiology*, *43*(3), 552–560. https://doi.org/10.1128/aem.43.3.552-560.1982

Chen, W. S., Strik, D. P., Buisman, C. J., & Kroeze, C. (2017a). Production of Caproic Acid from Mixed Organic Waste: An Environmental Life Cycle Perspective. *Environmental Science and Technology*, *51*(12), 7159–7168. https://doi.org/10.1021/acs.est.6b06220

De Leeuw, K. D., De Smit, S. M., Van Oossanen, S., Moerland, M. J., Buisman, C. J., & Strik, D. P. (2020). Methanol-Based Chain Elongation with Acetate to n-Butyrate and Isobutyrate at Varying Selectivities Dependent on pH. *ACS Sustainable Chemistry and Engineering*, *8*(22), 8184–8194. https://doi.org/10.1021/acssuschemeng.0c00907

Menon, A., & Lyng, J. G. (2020). Circular bioeconomy solutions: driving anaerobic digestion of waste streams towards production of high value medium chain fatty acids. https://doi.org/10.1007/s11157-020-09559-5

Shi, H., Shiraishi, M., & Shimizu, K. (1997). Metabolic flux analysis for biosynthesis of poly(β-Hydroxybutyric Acid) in alcaligenes eutrophus from various carbon sources. *Journal of Fermentation and Bioengineering*, *84*(6), 579–587. https://doi.org/10.1016/S0922-338X(97)81915-0

Vishniac, W., & Santer, M. (1957). The thiobacilli. *Bacteriological reviews*, *21*(3), 195–213. http://www.ncbi.nlm.nih.gov/pubmed/13471458%20http://www.pubmedcentral.nih.gov/articlerender.fcgi?artid=PMC180898

Beun, J. J., Dircks, K., Van Loosdrecht, M. C., & Heijnen, J. J. (2002). Poly-β-hydroxybutyrate metabolism in dynamically fed mixed microbial cultures. *Water Research*, *36*(5), 1167–1180. https://doi.org/10.1016/S0043-1354(01)00317-7

Velasco Alvarez, M., ten Pierick, A., van Dam, P., Maleki Seifar, R., van Loosdrecht, M., & Wahl, S. (2017). Microscale Quantitative Analysis of Polyhydroxybutyrate in Prokaryotes Using IDMS. *Metabolites*, *7*(2), 19. https://doi.org/10.3390/metabo7020019

Massey, L. K., Sokatch, J. R., & Conrad, R. S. (1976). Branched chain amino acid catabolism in bacteria. https://doi.org/10.1128/mmbr.40.1.42-54.1976

Tamis, J. (2014). Modeling PHA-producing microbial enrichment cultures—towards a generalized model with predictive power. *New Biotechnology*, *31*(4), 324–334. https://doi.org/10.1016/J.NBT.2013.11.007

Stouten, G. R., Hogendoorn, C., Douwenga, S., Kilias, E. S., Muyzer, G., & Kleerebezem, R. (2019). Temperature as competitive strategy determining factor in pulse-fed aerobic bioreactors. *ISME Journal*, *13*(12), 3112–3125. https://doi.org/10.1038/s41396-019-0495-8

6

Fang, F., Xu, R. Z., Huang, Y. Q., Wang, S. N., Zhang, L. L., Dong, J. Y., Xie, W. M., Chen, X., & Cao, J. S. (2019). Production of polyhydroxyalkanoates and enrichment of associated microbes in bioreactors fed with rice winery wastewater at various organic loading rates. *Bioresource Technology*, *292*, 121978. https://doi.org/10.1016/j.biortech.2019.121978

Reis, M., Albuquerque, M., Villano, M., & Majone, M. (2011). Mixed Culture Processes for Polyhydroxyalkanoate Production from Agro-Industrial Surplus/Wastes as Feedstocks. In *Comprehensive biotechnology, second edition* (pp. 669–683). Elsevier. https://doi.org/10.1016/B978-0-08-088504-9.00464-5

Tamang, P., Arndt, C., Bruns-Hellberg, J., & Nogueira, R. (2021). Polyhydroxyalkanoates production from industrial wastewaters using a mixed culture enriched with Thauera sp.: Inhibitory effect of the wastewater matrix. *Environmental Technology and Innovation*, *21*, 101328. https://doi.org/10.1016/j.eti.2020.101328

Marx, A., Poetter, M., & Fuchs, G. (2015). *Microbiological production of 3-hydroxyisobutyric acid* (tech. rep.).

Kricheldorf, H. R., Lomadze, N., & Schwarz, G. (2008). Poly(hydroxyisobutyrate) by ring-opening polymerizations of 5,5-dimethyl-1,3,2-dioxithiolan-4-one-2-oxide. *Journal of Polymer Science, Part A: Polymer Chemistry*, *46*(18), 6229–6237. https://doi.org/10.1002/pola.22933

Pittman, C. U. J., Iqbal, M., Chen, C. Y., & Helbert, J. N. (1978). Radiation degradation of poly(a-hydroxyisobutyric acid) and poly(glycollic ester). *Journal of Polymer Science: Polymer Chemistry Edition*, *16*(10), 2721–2724. https://doi.org/10.1002/pol.1978.170161032

Odham, G., Tunlid, A., Westerdahl, G., & Marden, P. (1986). Combined determination of poly-β-hydroxyalkanoic and cellular fatty acids in starved marine bacteria and sewage sludge by gas chromatography with flame ionization or mass spectrometry detection. *Applied and Environmental Microbiology*, *52*(4), 905–910. https://doi.org/10.1128/aem.52.4.905-910.1986

Wallen, L. L., & Rohwedder, W. K. (1974). *Poly-ß-hydroxyalkanoate from Activated Sludge* (tech. rep.). UTC. https://doi.org/10.1021/es60091a007

Findlay, R. H., & White, D. C. (1983). Polymeric beta-hydroxyalkanoates from environmental samples and Bacillus megaterium. *Applied and Environmental Microbiology*, *45*(1), 71–78. https://doi.org/10.1128/AEM.45.1.71-78.1983

Lee, W. H., Azizan, M. N., & Sudesh, K. (2004). Effects of culture conditions on the composition of poly(3-hydroxybutyrate-co-4-hydroxybutyrate) synthesized by Comamonas acidovorans. *Polymer Degradation and Stability*, *84*(1), 129–134. https://doi.org/10.1016/J.POLYMDEGRADSTAB.2003.10.003

Saito, Y., & Doi, Y. (1994). Microbial synthesis and properties of poly(3-hydroxybutyrate-co-4-hydroxybutyrate) in Comamonas acidovorans. *International Journal of Biological Macromolecules*, *16*(2), 99–104. https://doi.org/10.1016/0141-8130(94)90022-1

6

Sudesh, K., Fukui, T., & Doi, Y. (1998). Genetic analysis of Comamonas acidovorans polyhydroxyalkanoate synthase and factors affecting the incorporation of 4-hydroxybutyrate monomer. *Applied and Environmental Microbiology*, *64*(9), 3437–3443. https://doi.org/10.1128/aem.64.9.3437-3443.1998

Oeding, V., & Schlegel, H. G. (1973). β Ketothiolase from Hydrogenomonas eutropha H16 and its significance in the regulation of poly β hydroxybutyrate metabolism. *Biochemical Journal*, *134*(1), 239–248. https://doi.org/10.1042/bj1340239

Senior, P. J., & Dawes, E. A. (1973). The regulation of poly β hydroxybutyrate metabolism in Azotobacter beijerinckii. *Biochemical Journal*, *134*(1), 225–238. https://doi.org/10.1042/bj1340225

Hibbing, M. E., Fuqua, C., Parsek, M. R., & Peterson, S. B. (2010). Bacterial competition: surviving and thriving in the microbial jungle. *Nature reviews. Microbiology*, *8*(1), 15. https://doi.org/10.1038/NRMICRO2259

Conthe Calvo, M. (2018). Life on N2O: On the ecophysiology on nitrous oxide reduction; its potential as a greenhouse gas sink in wastewater treatment. https://doi.org/10.4233/UUID:6CDF5170-69F6-48C5-B953-A790BC611AC8

Jiang. (2011b). Effect of temperature and cycle length on microbial competition in PHB-producing sequencing batch reactor. *The ISME Journal*, *5*(5), 896–907. https://doi.org/10.1038/ismej.2010.174

Beun, J. J., Paletta, F., Van Loosdrecht, M. C., & Heijnen, J. J. (2000). Stoichiometry and kinetics of poly-β-hydroxybutyrate metabolism in aerobic, slow growing, activated sludge cultures. *Biotechnology and Bioengineering*, *67*(4), 379–389. https://doi.org/10.1002/(SICI)1097-0290(20000220)67:4<379::AID-BIT1>3.0.CO;2-2

Jain, R., & Tiwari, A. (2015). Biosynthesis of planet friendly bioplastics using renewable carbon source. *Journal of Environmental Health Science and Engineering*, *13*(1). https://doi.org/10.1186/s40201-015-0165-3

Anjum, A., Zuber, M., Zia, K. M., Noreen, A., Anjum, M. N., & Tabasum, S. (2016). Microbial production of polyhydroxyalkanoates (PHAs) and its copolymers: A review of recent advancements. https://doi.org/10.1016/j.ijbiomac.2016.04.069

Rai, R., Keshavarz, T., Roether, J. A., Boccaccini, A. R., & Roy, I. (2011). Medium chain length polyhydroxyalkanoates, promising new biomedical materials for the future. https://doi.org/10.1016/j.mser.2010.11.002

Elbahloul, Y., & Steinbüchel, A. (2009). Large-scale production of poly(3-hydroxyoctanoic acid) by Pseudomonas putida GPo1 and a simplified downstream process. *Applied and Environmental Microbiology*, *75*(3), 643–651. https://doi.org/10.1128/AEM.01869-08

Tortajada, M., da Silva, L. F., & Prieto, M. A. (2013). Second-generation functionalized medium-chain-length polyhydroxyalkanoates: The gateway to high-value bioplastic applications. https://doi.org/10.2436/20.1501.01.175

6

Quillaguamán, J., Guzmán, H., Van-Thuoc, D., & Hatti-Kaul, R. (2010). Synthesis and production of polyhydroxyalkanoates by halophiles: Current potential and future prospects. *Applied Microbiology and Biotechnology*, *85*(6), 1687–1696. https://doi.org/10.1007/S00253-009-2397-6/FIGURES/5

Sudesh, K., Abe, H., & Doi, Y. (2000). Synthesis, structure and properties of polyhydroxyalkanoates: Biological polyesters. *Progress in Polymer Science (Oxford)*, *25*(10), 1503–1555. https://doi.org/10.1016/S0079-6700(00)00035-6

Alaux, E., Couvreur, M., Marie, B., Bounouba, M., & Hernandez-Raquet, G. (2022). Biosynthesis of Medium Chain Length Polyhydroxyalkanoates (Mcl-Pha) by Activated Sludge: Impact of Phosphorus Limitation on Pha Production and Microbial Diversity. *SSRN Electronic Journal*. https://doi.org/10.2139/ssrn.4028808

Chen, Z., Zhang, C., Shen, L., Li, H., Peng, Y., Wang, H., He, N., Li, Q., & Wang, Y. (2018). Synthesis of Short-Chain-Length and Medium-Chain-Length Polyhydroxyalkanoate Blends from Activated Sludge by Manipulating Octanoic Acid and Nonanoic Acid as Carbon Sources. *Journal of Agricultural and Food Chemistry*, *66*(42), 11043–11054. https://doi.org/10.1021/acs.jafc.8b04001

Lee, S. H., Kim, J. H., Mishra, D., Ni, Y. Y., & Rhee, Y. H. (2011). Production of medium-chain-length polyhydroxyalkanoates by activated sludge enriched under periodic feeding with nonanoic acid. *Bioresource Technology*, *102*(10), 6159–6166. https://doi.org/10.1016/j.biortech.2011.03.025

Shen, L., Hu, H., Ji, H., Zhang, C., He, N., Li, Q., & Wang, Y. (2015). Production of poly(3-hydroxybutyrate-co-3-hydroxyhexanoate) from excess activated sludge as a promising substitute of pure culture. *Bioresource Technology*, *189*, 236–242. https://doi.org/10.1016/j.biortech.2015.04.007

Angenent, L. T., Richter, H., Buckel, W., Spirito, C. M., Steinbusch, K. J., Plugge, C. M., Strik, D. P., Grootscholten, T. I., Buisman, C. J., & Hamelers, H. V. (2016). Chain Elongation with Reactor Microbiomes: Open-Culture Biotechnology to Produce Biochemicals. https://doi.org/10.1021/acs.est.5b04847

Kucek. (2016). Waste Conversion into n-Caprylate and n-Caproate: Resource Recovery from Wine Lees Using Anaerobic Reactor Microbiomes and In-line Extraction. *Frontiers in Microbiology*, *7*(NOV), 1892. https://doi.org/10.3389/fmicb.2016.01892

Li, D., Ma, X., Yin, F., Qiu, Y., & Yan, X. (2021). Creating biotransformation of volatile fatty acids and octanoate as co-substrate to high yield medium-chain-length polyhydroxyalkanoate. *Bioresource Technology*, *331*, 125031. https://doi.org/10.1016/j.biortech.2021.125031

Sun, Z., Ramsay, J. A., Guay, M., & Ramsay, B. A. (2007). Carbon-limited fed-batch production of medium-chain-length polyhydroxyalkanoates from nonanoic acid by Pseudomonas putida KT2440. *Applied Microbiology and Biotechnology*, *74*(1), 69–77. https://doi.org/10.1007/s00253-006-0655-4

Garcia-Ochoa, F., & Gomez, E. (2009). Bioreactor scale-up and oxygen transfer rate in microbial processes: An overview. *Biotechnology Advances*, *27*(2), 153–176. https://doi.org/10.1016/J.BIOTECHADV.2008.10.006

van 't Riet, K. (1979). Review of Measuring Methods and Results in Nonviscous Gas-Liquid Mass Transfer in Stirred Vessels. *Industrial and Engineering Chemistry Process Design and Development*, *18*(3), 357–364. https://doi.org/10.1021/I260071A001

Chen, W. S., Strik, D. P., Buisman, C. J., & Kroeze, C. (2017b). Production of Caproic Acid from Mixed Organic Waste: An Environmental Life Cycle Perspective. *Environmental Science and Technology*, *51*(12), 7159–7168. https://doi.org/10.1021/ACS.EST.6B06220/ASSET/IMAGES/LARGE/ES-2016-06220E_0003.JPEG

Pabst, M., Grouzdev, D. S., Lawson, C. E., Kleikamp, H. B., de Ram, C., Louwen, R., Lin, Y. M., Lücker, S., van Loosdrecht, M. C., & Laureni, M. (2021). A general approach to explore prokaryotic protein glycosylation reveals the unique surface layer modulation of an anammox bacterium. *The ISME Journal 2021 16:2*, *16*(2), 346–357. https://doi.org/10.1038/s41396-021-01073-y

Altschul, S. F., Gish, W., Miller, W., Myers, E. W., & Lipman, D. J. (1990). Basic local alignment search tool. *Journal of molecular biology*, *215*(3), 403–410. https://doi.org/10.1016/S0022-2836(05)80360-2

Marang. (2016). Combining the enrichment and accumulation step in non-axenic PHA production: Cultivation of Plasticicumulans acidivorans at high volume exchange ratios. *Journal of Biotechnology*, *231*, 260–267. https://doi.org/10.1016/J.JBIOTEC.2016.06.016

Vermeer, C. M., Bons, L. J., & Kleerebezem, R. (2022). Production of a newly discovered PHA family member with an isobutyrate-fed enrichment culture. *Applied Microbiology and Biotechnology 2022 106:2*, *106*(2), 605–618. https://doi.org/10.1007/S00253-021-11742-9

McCool, G. J., & Cannon, M. C. (2001). PhaC and PhaR are required for polyhydroxyalkanoic acid synthase activity in Bacillus megaterium. *Journal of Bacteriology*, *183*(14), 4235–4243. https://doi.org/10.1128/JB.183.14.4235-4243.2001/ASSET/3045738B-C58E-44A7-BCAE-73F4E3A09C19/ASSETS/GRAPHIC/JB1410037006.JPEG

Ollis, D., Cheah, E., Cygler, M., Dijkstra, B., Frolow, F., Franken, S., Harel, M., Remington, S., Silman, I., & Schrag, J. (1992). The alpha/beta hydrolase fold. *Protein engineering*, *5*(3), 197–211. https://doi.org/10.1093/protein/5.3.197

Whitman, W. B., Woyke, T., Klenk, H. P., Zhou, Y., Lilburn, T. G., Beck, B. J., De Vos, P., Vandamme, P., Eisen, J. A., Garrity, G., Hugenholtz, P., & Kyrpides, N. C. (2015). Genomic Encyclopedia of Bacterial and Archaeal Type Strains, Phase III: the genomes of soil and plant-associated and newly described type strains. *Standards in Genomic Sciences*, *10*(MAY2015), 26. https://doi.org/10.1186/S40793-015-0017-X

6

Jiang. (2011c). Polyhydroxybutyrate production from lactate using a mixed microbial culture. *Biotechnology and Bioengineering*, *108*(9), 2022–2035. https://doi.org/10.1002/bit.23148

Blunt, W., Dartiailh, C., Sparling, R., Gapes, D., Levin, D. B., & Cicek, N. (2017). Microaerophilic environments improve the productivity of medium chain length polyhydroxyalkanoate biosynthesis from fatty acids in Pseudomonas putida LS46. *Process Biochemistry*, *59*(September 2016), 18–25. https://doi.org/10.1016/j.procbio.2017.04.028

Fernández, D., Rodríguez, E., Bassas, M., Viñas, M., Solanas, A. M., Llorens, J., Marqués, A. M., & Manresa, A. (2005). Agro-industrial oily wastes as substrates for PHA production by the new strain Pseudomonas aeruginosa NCIB 40045: Effect of culture conditions. *Biochemical Engineering Journal*, *26*(2-3), 159–167. https://doi.org/10.1016/j.bej.2005.04.022

Pratt, S., Werker, A., Morgan-Sagastume, F., & Lant, P. (2012). Microaerophilic conditions support elevated mixed culture polyhydroxyalkanoate (PHA) yields, but result in decreased PHA production rates. *Water Science and Technology*, *65*(2), 243–246. https://doi.org/10.2166/wst.2012.086

Third, K. A., Newland, M., & Cord-Ruwisch, R. (n.d.). The effect of dissolved oxygen on PHB accumulation in activated sludge cultures. *Biotechnology and Bioengineering*, (2), 238–250. https://doi.org/10.1002/bit.10564

Takeda, N., Jonkers, H., & Mors, R. (2017). The effect on crack repair by bacteria-based healing under active water flow. *Unpublished results*, (1), 1–7.

Pellegrin, V., Juretschko, S., Wagner, M., & Cottenceau, G. (1999). Morphological and biochemical properties of a Sphaerotilus sp. isolated from paper mill slimes. *Applied and Environmental Microbiology*, *65*(1), 156–162. https://doi.org/10.1128/aem.65.1.156-162.1999

Grabovich, M. Y., Smolyakov, D. D., Beletsky, A. V., Mardanov, A. V., Gureeva, M. V., Markov, N. D., Rudenko, T. S., & Ravin, N. V. (2021). Reclassification of Sphaerotilus natans subsp. sulfidivorans Gridneva et al. 2011 as Sphaerotilus sulfidivorans sp. nov. and comparative genome analysis of the genus Sphaerotilus. *Archives of microbiology*, *203*(4), 1595–1599. https://doi.org/10.1007/S00203-020-02158-6

Cai, H., & Qiu, Z. (2009). Effect of comonomer content on the crystallization kinetics and morphology of biodegradable poly(3-hydroxybutyrate-co-3-hydroxyhexanoate). *Physical Chemistry Chemical Physics*, *11*(41), 9569–9577. https://doi.org/10.1039/B907677H

Ruiz, C., Kenny, S. T., Narancic, T., Babu, R., & Connor, K. O. (2019). Conversion of waste cooking oil into medium chain polyhydroxyalkanoates in a high cell density fermentation. *Journal of Biotechnology*, *306*(August), 9–15. https://doi.org/10.1016/j.jbiotec.2019.08.020

Alvarez-Santullano, N., Villegas, P., Mardones, M. S., Durán, R. E., Donoso, R., Gonzá-lez, A., Sanhueza, C., Navia, R., Acevedo, F., Pérez-Pantoja, D., & Seeger, M. (2021). Genome-Wide Metabolic Reconstruction of the Synthesis of Polyhydroxyalkanoates from Sugars and Fatty Acids by Burkholde-

6

ria Sensu Lato Species. *Microorganisms 2021, Vol. 9, Page 1290*, *9*(6), 1290. https://doi.org/10.3390/MICROORGANISMS9061-290

Holtzapple, M. T., Wu, H., Weimer, P. J., Dalke, R., Granda, C. B., Mai, J., & Urgun-Demirtas, M. (2022). Microbial communities for valorizing biomass using the carboxylate platform to produce volatile fatty acids: A review. *Bioresource Technology*, *344*, 126253. https://doi.org/10.1016/J.BIORTECH.2021.126253

Chen, W. S., Huang, S., Strik, D. P., & Buisman, C. J. (2017). Isobutyrate biosynthesis via methanol chain elongation: converting organic wastes to platform chemicals. *Journal of Chemical Technology and Biotechnology*, *92*(6), 1370–1379. https://doi.org/10.1002/jctb.5132

De Donno Novelli, L., Moreno Sayavedra, S., & Rene, E. R. (2021). Polyhydroxyalkanoate (PHA) production via resource recovery from industrial waste streams: A review of techniques and perspectives. *Bioresource Technology*, *331*, 124985. https://doi.org/10.1016/J.BIORTECH.2021.124985

de Souza Reis, G. A., Michels, M. H. A., Fajardo, G. L., Lamot, I., & de Best, J. H. (2020). Optimization of Green Extraction and Purification of PHA Produced by Mixed Microbial Cultures from Sludge. *Water*, *12*(4), 1185. https://doi.org/10.3390/w12041185

Hansen, C. M. (1967). The Three Dimensional Solubility Parameter and Solvent Diffusion Coefficient. Their Importance in Surface Coating Formulation. *J. Paint Technology*, 104. https://ci.nii.ac.jp/naid/10005102018/

Teas, J. P. (1968). Graphic analysis of resin solubilities. *Journal of Paint Technology*, *40*(516), 19–25. https://www.bcin.ca/bcin/detail.app?id=52094&wbdisable=true

Burniol-Figols, A., Skiadas, I. V., Daugaard, A. E., & Gavala, H. N. (2020). Polyhydroxyalkanoate (PHA) purification through dilute aqueous ammonia digestion at elevated temperatures. *Journal of Chemical Technology and Biotechnology*, jctb.6345. https://doi.org/10.1002/jctb.6345

Graham, D. J., & Midgley, N. G. (2000). Graphical representation of particle shape using triangular diagrams: An excel spreadsheet method. *Earth Surface Processes and Landforms*, *25*(13), 1473–1477. https://doi.org/10.1002/1096-9837(200012)25:13<1473::AID-ESP158>3.0.CO;2-C

Terada, M., & Marchessault, R. H. (1999). Determination of solubility parameters for poly(3-hydroxyalkanoates). *International Journal of Biological Macromolecules*, *25*(1-3), 207–215. https://doi.org/10.1016/S0141-8130(99)00036-7

Shephard, J. J., Soper, A. K., Callear, S. K., Imberti, S., Evans, J. S., & Salzmann, C. G. (2015). Polar stacking of molecules in liquid chloroform. *Chemical Communications*, *51*(23), 4770–4773. https://doi.org/10.1039/C4CC09235J

Jacquel, N. (2015). Solubility of Polyhydroxyalkanoates by Experiment and Thermodynamic Correlations. *56*(4), 1495–1502. https://doi.org/10.1002/aic

6

Miller-Chou, B. A., & Koenig, J. L. (2003). A review of polymer dissolution. *Progress in Polymer Science*, *28*(8), 1223–1270. https://doi.org/10.1016/S0079-6700(03)00045-5

McChalicher, C. W., Srienc, F., & Rouse, D. P. (2010). Solubility and degradation of polyhydroxyalkanoate biopolymers in propylene carbonate. *AIChE Journal*, *56*(6), 1616–1625. https://doi.org/10.1002/aic.12087

McNeill, I. C., & Leiper, H. A. (1985). Degradation studies of some polyesters and polycarbonates—1. Polylactide: General features of the degradation under programmed heating conditions. *Polymer Degradation and Stability*, *11*(3), 267–285. https://doi.org/10.1016/0141-3910(85)90050-3

Zhang, J., Cai, Q., Zhao, J., & Zang, S. (2018). Nano metal oxides as efficient catalysts for selective synthesis of 1-methoxy-2-propanol from methanol and propylene oxide. *RSC Advances*, *8*(8), 4478–4482. https://doi.org/10.1039/C7RA13119D

Cox, M. K. (1995). Recycling BIOPOL–Composting and Material Recycling. *Journal of Macromolecular Science, Part A*, *32*(4), 607–612. https://doi.org/10.1080/10601329508010274

Chan, C. M., Johansson, P., Magnusson, P., Vandi, L. J., Arcos-Hernandez, M., Halley, P., Laycock, B., Pratt, S., & Werker, A. (2017). Mixed culture polyhydroxyalkanoate-rich biomass assessment and quality control using thermogravimetric measurement methods. *Polymer Degradation and Stability*, *144*, 110–120. https://doi.org/10.1016/j.polymdegradstab.2017.07.029

Werker, A. G., Johansson, P. S. T., & Magnusson, P. O. G. (2014). Process for the extraction of polyhydroxyalkanoates from biomass. https://patents.google.com/patent/US20150368393A1/en%20http://www.google.com/patents/US7118897%20https://patents.google.com/patent/US20150368393A1/en%5C%0Ahttp://www.google.com/patents/US7118897

Hansen. (2007). *Hansen solubility parameter user's handbook* (2nd, Vol. 53). CRC Press. https://doi.org/10.1017/CBO9781107415324.004

Louwerse, M. J., Maldonado, A., Rousseau, S., Moreau-Masselon, C., Roux, B., & Rothenberg, G. (2017). Revisiting Hansen Solubility Parameters by Including Thermodynamics. *ChemPhysChem*, *18*(21), 2999–3006. https://doi.org/10.1002/CPHC.201700408

Curzons, A., Constable, D., & Cunningham, V. (1999). Solvent selection guide: a guide to the integration of environmental, health and safety criteria into the selection of solvents. *Clean Technologies and Environmental Policy*, *1*(2), 82–90. https://doi.org/10.1007/s100980050014

Smallwood, I. M. (2002). *Solvent Recovery Handbook, Second edition* (2nd). Blackwell Science.

Koller, M., Salerno, A., Dias, M., Reiterer, A., & Braunegg, G. (2010). Modern biotechnological polymer synthesis: a review. *core.ac.uk*, *48*(3), 255–269. https://core.ac.uk/download/pdf/14427669.pdf

van Krevelen, D., & te Nijenhuis, K. (2009). *Properties of polymers: their correlation with chemical structure; their numerical estimation and prediction from additive group contributions* (4th). Elsevier Science. https://books.

6

google.nl/books?hl=nl&lr=&id=bzRKwjZeQ2kC&oi=fnd&pg=PP1&ots=
w_Q3X1fAVk&sig=VhdhySixw_HvsoPt3K8ENKmvg-Y

Jia, Q., Xiong, H., Wang, H., Shi, H., Sheng, X., Sun, R., & Chen, G. (2014). Pro-
duction of polyhydroxyalkanoates (PHA) by bacterial consortium from
excess sludge fermentation liquid at laboratory and pilot scales. *Biore-
source Technology*, *171*, 159–167. https://doi.org/10.1016/J.BIORTECH.
2014.08.059

Jiang. (2012). Waste to resource: Converting paper mill wastewater to bioplastic.
Water Research, *46*(17), 5517–5530. https://doi.org/10.1016/J.WATRES.
2012.07.028

Tamis, J., Lužkov, K., Jiang, Y., Loosdrecht, M. C., & Kleerebezem, R. (2014). En-
richment of Plasticicumulans acidivorans at pilot-scale for PHA production
on industrial wastewater. *Journal of Biotechnology*, *192*(Part A), 161–169.
https://doi.org/10.1016/j.jbiotec.2014.10.022

Silva, F. B., Boon, N., De Belie, N., & Verstraete, W. (2015). Industrial application
of biological self-healing concrete: Challenges and economical feasibility.
Journal of Commercial Biotechnology, *21*(1), 31–38. https://doi.org/10.
5912/jcb662

Mors, R., & Jonkers, H. (2017). Feasibility of lactate derivative based agent as
additive for concrete for regain of crack water tightness by bacterial
metabolism. *Industrial Crops and Products*, *106*, 97–104. https://doi.org/
10.1016/J.INDCROP.2016.10.037

Tziviloglou, E., Van Tittelboom, K., Palin, D., Wang, J., Sierra-Beltrán, M. G., Erşan,
Y. Ç., Mors, R., Wiktor, V., Jonkers, H. M., Schlangen, E., & De Belie, N.
(2016). Bio-Based Self-Healing Concrete: From Research to Field Applica-
tion. Springer, Cham. https://doi.org/10.1007/12_2015_332

Xu, J., Wang, X., & Wang, B. (2018). Biochemical process of ureolysis-based mi-
crobial CaCO3 precipitation and its application in self-healing concrete.
Applied Microbiology and Biotechnology, *102*(7), 3121–3132. https://doi.
org/10.1007/s00253-018-8779-x

Phillips, J. R., Klasson, K. T., Clausen, E. C., & Gaddy, J. L. (1993). Biological pro-
duction of ethanol from coal synthesis gas. *Applied Biochemistry and
Biotechnology*, *39-40*(1), 559–571. https://doi.org/10.1007/BF02919018

Pinel, I., D.H., M., Vrouwenvelder, J., & Van Loosdrecht, M. (2020). Bacterial com-
munity dynamics and disinfection impact in cooling water systems. *Water
Research*, 115505. https://doi.org/10.1016/j.watres.2020.115505

Palin, D., Jonkers, H. M., & Wiktor, V. (2016). Autogenous healing of sea-water
exposed mortar: Quantification through a simple and rapid permeability
test. *Cement and Concrete Research*, *84*, 1–7. https://doi.org/10.1016/j.
cemconres.2016.02.011

Kanesawa, Y., & Doi, Y. (1990). Hydrolytic degradation of microbial poly(3-hydroxybutyrate-
co-3-hydroxyvalerate) fibers. *Die Makromolekulare Chemie, Rapid Com-
munications*, *11*(12), 679–682. https://doi.org/10.1002/marc.1990.
030111215

6

Mukai, K., Yamada, K., & Doi, Y. (1993). Kinetics and mechanism of heterogeneous hydrolysis of poly[(R)-3-hydroxybutyrate] film by PHA depolymerases. *International Journal of Biological Macromolecules*, *15*(6), 361–366. https://doi.org/10.1016/0141-8130(93)90054-P

Knoll, M., Hamm, T. M., Wagner, F., Martinez, V., & Pleiss, J. (2009). The PHA Depolymerase Engineering Database: A systematic analysis tool for the diverse family of polyhydroxyalkanoate (PHA) depolymerases. *BMC Bioinformatics*, *10*, 89. https://doi.org/10.1186/1471-2105-10-89

Van Tittelboom, K., & De Belie, N. (2013). Self-healing in cementitious materials-a review. *Materials*, *6*(6), 2182–2217. https://doi.org/10.3390/ma6062182

Rooij, M. D., Tittelboom, K. V., & Belie, N. D. (2013). Self-healing phenomena in cement-Based materials: state-of-the-art report of RILEM technical committee 221-SHC: self-Healing phenomena in cement. https://link.springer.com/content/pdf/10.1007/978-94-007-6624-2.pdf

Cacchio, P., Ercole, C., Cappuccio, G., & Lepidi, A. (2003). Calcium carbonate precipitation by bacterial strains isolated from a limestone cave and from a loamy soil. *Geomicrobiology Journal*, *20*(2), 85–98. https://doi.org/10.1080/01490450303883

Tziviloglou, E., Wiktor, V., Jonkers, H., & Schlangen, E. (2015). Performance requirements to ensure the crack sealing performance of bacteria-based self-healing concrete. *Proceedings of the 9th International Conference on Fracture Mechanics of Concrete and Concrete Structures*. https://doi.org/10.21012/FC9.148

Edvardsen, C. (1999). Water permeability and autogenous healing of cracks in concrete. *ACI Materials Journal*, *96*(4), 448–454. https://doi.org/10.14359/645

Reinhardt, H. W., & Jooss, M. (2003). Permeability and self-healing of cracked concrete as a function of temperature and crack width. *Cement and Concrete Research*, *33*(7), 981–985. https://doi.org/10.1016/S0008-8846(02)01099-2

Aldea, C. M., Shah, S. P., & Karr, A. (1999). Permeability of cracked concrete. *Materials and Structures/Materiaux et Constructions*, *32*(5), 370–376. https://doi.org/10.1007/bf02479629

Basaran Bundur, Z., Kirisits, M. J., & Ferron, R. D. (2015). Biomineralized cement-based materials: Impact of inoculating vegetative bacterial cells on hydration and strength. *Cement and Concrete Research*, *67*, 237–245. https://doi.org/10.1016/J.CEMCONRES.2014.10.002

Luo, M., & Qian, C. (2016). Influences of bacteria-based self-healing agents on cementitious materials hydration kinetics and compressive strength. *Construction and Building Materials*, *121*, 659–663. https://doi.org/10.1016/j.conbuildmat.2016.06.075

Guest, J. S., Skerlos, S. J., Barnard, J. L., Beck, M. B., Daigger, G. T., Hilger, H., Jackson, S. J., Karvazy, K., Kelly, L., Macpherson, L., Mihelcic, J. R., Pramanik, A., Raskin, L., Van Loosdrecht, M. C., Yeh, D., & Love, N. G. (2009). A new

6

planning and design paradigm to achieve sustainable resource recovery from wastewater. https://doi.org/10.1021/es9010515

Van Loosdrecht, M. C., & Brdjanovic, D. (2014). Anticipating the next century of wastewater treatment. https://doi.org/10.1126/science.1255183

Bozkurt, H., Gernaey, K. V., & Sin, G. (2017). Superstructure-based optimization tool for plant design and retrofitting. In J. M. Lema & S. S. Martinez (Eds.), *Innovative wastewater treatment and resource recovery technologies: Impacts on energy, economy and environment* (pp. 581–598). IWA Publishing. https://doi.org/10.2166/9781780407876_0581

Kehrein, P., van Loosdrecht, M., Osseweijer, P., Garfí, M., Dewulf, J., & Posada, J. (2020). A critical review of resource recovery from municipal wastewater treatment plants – market supply potentials, technologies and bottlenecks. *Environmental Science: Water Research and Technology*. https://doi.org/10.1039/C9EW00905A

Valentino, F., Morgan-Sagastume, F., Campanari, S., & Werker, A. (2017). Carbon recovery from wastewater through bioconversion into biodegradable polymers. *New Biotechnology*, *37*, 9–23. https://doi.org/10.1016/J.NBT.2016.05.007

van der Roest, H. F., van Loosdrecht, M. C. M., Langkamp, E. J., & Uijterlinde, C. (2015). Recovery and reuse of alginate from granular Nereda sludge. *Water*, *21*(17(2)), 48.

Visser, C., Odegard, I., Naber, N., Bergsma, G. C., van Nieuwenhuijzen, A. F., & Sanders, M. H. A. (2016). *Levenscyclusanalyse van grondstoffen uit rioolwater* (tech. rep.). STOWA. https://www.google.com/search?q=C.+Visser%5C%2C+I.+Odegard%5C%2C+N.+Naber%5C%2C+G.+C.+Bergsma%5C%2C+A.+F.+van+Nieuwenhuijzen+and+M.+H.+A.+Sanders%5C%2C+Levenscyclusanalyse+van+grondstoffen+uit+rioolwater%5C%2C+2016.&rlz=1C1GCEB_enNL856NL856&oq=C.+Visser%5C%2C+I.+Odegard%5C%2C+N.

Le Corre, K. S., Valsami-Jones, E., Hobbs, P., & Parsons, S. A. (2009). Phosphorus Recovery from Wastewater by Struvite Crystallization: A Review. *Critical Reviews in Environmental Science and Technology*, *39*(6), 433–477. https://doi.org/10.1080/10643380701640573

Lin, Y. M., Nierop, K. G., Girbal-Neuhauser, E., Adriaanse, M., & van Loosdrecht, M. C. (2015). Sustainable polysaccharide-based biomaterial recovered from waste aerobic granular sludge as a surface coating material. *Sustainable Materials and Technologies*, *4*, 24–29. https://doi.org/10.1016/j.susmat.2015.06.002

Ruiken, C. J., Breuer, G., Klaversma, E., Santiago, T., & van Loosdrecht, M. C. (2013). Sieving wastewater - Cellulose recovery, economic and energy evaluation. *Water Research*, *47*(1), 43–48. https://doi.org/10.1016/j.watres.2012.08.023

Eijlander, S., & Mulder, K. F. (2019). Sanitary systems: Challenges for innovation. *Journal of Sustainable Development of Energy, Water and Environment Systems*, *7*(2), 193–212. https://doi.org/10.13044/j.sdewes.d6.0231

6

Kim, N. K., Mao, N., Lin, R., Bhattacharyya, D., van Loosdrecht, M. C., & Lin, Y. (2020). Flame retardant property of flax fabrics coated by extracellular polymeric substances recovered from both activated sludge and aerobic granular sludge. *Water Research*, *170*. https://doi.org/10.1016/j.watres.2019.115344

Zlopasa, J., Koenders, E. A. B., & Picken, S. J. (2014). Using bio-based polymers for curing cement- based materials. *AMS 14 Proceedings of the Int. Conference on Ageing of Materials and Structures*, *1*(May), 220–226. https://doi.org/10.13140/2.1.2522.8800

Coats, E. R., Loge, F. J., Wolcott, M. P., Englund, K., & McDonald, A. G. (2008). Production of natural fiber reinforced thermoplastic composites through the use of polyhydroxybutyrate-rich biomass. *Bioresource Technology*, *99*(7), 2680–2686. https://doi.org/10.1016/j.biortech.2007.03.065

Rossi, E., Vermeer, C. M., Mors, R., Kleerebezem, R., Copuroglu, O., & Jonkers, H. M. (2021). On the Applicability of a Precursor Derived from Organic Waste Streams for Bacteria-Based Self-Healing Concrete. *Frontiers in Built Environment*, *7*, 2. https://doi.org/10.3389/FBUIL.2021.632921/BIBTEX

BIOGRAPHY

Chris Vermeer was born on the 19th of September in 1989 in Delft, the Netherlands, and grew up in 's-Gravenzande, the Netherlands. Passionate about the natural world, he started a BSc degree in Life Science & Technology in 2007 at the University of Leiden and the TU Delft. He finalized the BSc degree with a thesis at the Environmental Biotechnology group at the TU Delft. In 2011, he started a MSc degree in Life Science & Technology at the TU Delft specializing with the track Cell Factory. His MSc thesis was also completed at the Environmental Biotechnology group by working on the cultivation of microalgae for the production of lipids under supervision of Robbert Kleerebezem. Afterwards, during an industrial internship, he contributed to scale up the algae cultivation project at the company, Aqualia, Spain.

After graduation, he worked for a some months as researcher at a horticultural company in Kenya. Then, he started working as biotechnological researcher at Groen Agro Control, Delft. At this company, he conducted contract research on wide variety of topics ranging from biological crop protection to algae cultivation, and beer/cider brewing.

From 2018 to present, he returned to the Environmental Biotechnology group at the TU Delft to pursue a PhD under supervision of Robbert Kleerebezem. The name of the project name is 'From waste to self-healing concrete: the missing PHA-link', and is in collaboration with a group at the faculty of Civil Engineering and Geosciences. The project aims at optimizing and balancing waste-derived PHA biosynthesis with recovery, and targeting for an niche application of PHA in self-healing concrete. A part of the results are described in this thesis.

List of Publications

This Thesis

Vermeer, C.M.*, Rossi, E.*, Tamis, J., Jonkers, H.M., Kleerebezem, R. (2021). From waste to self-healing concrete: A proof-of-concept of a new application for poly-hydroxyalkanoate. *Resource, Conservation & Recycling* 164:105206. https://doi.org/10.1016/j.resconrec.2020.105206

Vermeer, C.M., Bons, L.J., Kleerebezem, R. (2022). Production of a newly discovered PHA family member with an isobutyrate-fed enrichment culture. *Applied Microbiology & Biotechnology* 2022 1062 106:605–618. https://doi.org/10.1007/S00253-021-11742-9

Vermeer, C.M., Nielsen, M., Eckhardt, V., Hortensius, M., Tamis, J., Picken, S. J., Kleerebezem, R. (2022). Systematic solvent screening and selection for polyhydroxyalkanoates (PHBV) recovery from biomass. *Environmental Chemical Engineering* 2022 10 6:108573. https://doi.org/10.1016/J.JECE.2022.108573

Other

Rossi E.*, Vermeer C.M.*, Mors R., Kleerebezem R., Copuroglu O., Jonkers H.M. (2021). On the Applicability of a Precursor Derived from Organic Waste Streams for Bacteria-Based Self-Healing Concrete. *Frontiers Built Environment* 7:2. https://doi.org/10.3389/FBUIL.2021.632921/BIBTEX

Rossi E., Vermeer C.M., Tamis J., Copuroglu O., Jonkers H. (2022). Gas chromatography to detect bacteria-based self-healing agents in concrete. *MATEC Web Conference* 361:07004. https://doi.org/10.1051/MATECCONF/202236107004

* These authors contributed equally to this work.

Conference contributions

Oral presentations

IWA Resource Recovery, Venice, Italy (2019). From Waste to Self-healing Concrete: a Proof-of-concept for a New Value Chain for PHA.

IWA Resource Recovery, Istanbul, Turkey (2021). The production of a newly discovered PHA family member, Poly(3-hydroxyisobutyrate), and Poly(3-hydroxybutyrate), from isobutyrate using a microbial enrichment.

Emerging Microbial Technologies, Delft, the Netherlands (2022). Production of a newly discovered PHA family member with an isobutyrate-fed enrichment culture

Workshops

Mixed microbial community PHA workshop, Venice, Italy (2019). From Waste to Self-healing Concrete: a Proof-of-concept for a New Value Chain for PHA.

Mixed microbial community PHA workshop, Valencia, Spain (2021). Characterization and optimization of medium chain length PHA-producing enrichments with octanoate as carbon source

ACKNOWLEDGEMENTS

Life did not take over the world by combat, but by networking.

Lynn Margulis

First of all, Robbert, I really appreciate that you gave me the opportunity to return to EBT and start this adventure to explore the wondrous world of science. I greatly enjoyed our meetings, and was always surprised by your calm and wise approach towards scientific or organisational complicated issues. Your role as advisor rather than supervisor of my project gave me freedom in my work which I greatly enjoyed. I'm very glad, that you stimulated me to run a bunch of bioreactors amidst of all polymer and concrete madness. Our shared conferences/workshops/excursions were a real pleasure every time ('Jullie willen toch niet morgen allemaal weer om 09:00 fris en fruitig over PHA ouwehoeren!?'). And, I will definitely miss your unique and enormous sense of humour.

Jelmer, without our accidental meeting by bike five years ago, I probably would not write this thesis right now. This occurrence characterizes your ability to see opportunities and your drive to make the PHA project successful. As captain of the White Pony's, you brought a lot of energy in the project. It is hard to think of person who has more knowledge of PHA than you. Besides your scientific knowledge, you also have a very interesting perspective on life in general. This opened my eyes for thinking beyond the scientific principles. You have the ability to create depth in a conversation within minutes.

Henk, your support was always very welcome. You were a binding factor in the project team. It was very valuable to have a fresh perspective or second opinion from an experienced and knowledgeable person. Thank you for all your encouraging advice.

Paranymphs (Emiel and Philipp), thank you so much for agreeing to being saddled up with this task. It means a lot to me to have you by my side during the defence and the rest of the day. Furthermore, I am very grateful to the PhD committee members for the time invested in reading and discussing my thesis.

Emanuele, thank you for being my PhD buddy. Although our expertise's lay miles apart, we were able to cooperate effectively. It was much better to prepare all the user committee meetings together than by myself. I was impressed by the pace of your research. Although we didn't start the project together, we at least finish it (almost) together.

My dear students, Larissa, Vincent, Lena, Emily, Tom, Maaike, Liangshin, Jeffrey, thank you very much for your contribution to this thesis. Of course, for all the valuable results and conclusions you obtained, but mostly for bringing the project to life. It is great to see how you all found your way in your career.

Jure, I'm impressed by the creative ideas that are generated by your mind (e.g. the idea for my project). And thank you for introducing me to the polymer world.

Gabrie and Stephen, without your expertise, I would be completely lost in the world of process technology and polymer science. Thank you for all the students you supervised, for all the white pony meeting's you attended, and for helping me out with the publication.

The Wetsus boys: Alan, thank you for our Schiphol meetings, for being a wonderful travel companion during conferences/workshops, and for being a critical reviewer of my work. Angel and Ruizhe, it was great to have some PHA buddy's within the country. It was a lot of fun to attend conferences and to organize PHA activities with you.

Team Paques Biomaterials (René, João, Henk), an inspiring group to work with. Very interesting to peek behind the scenes of a biotechnological start-up. I was happy with your faith in our project. Keep up the good work.

Mark, thanks for creating and facilitating this pleasant, academic environment, called EBT. It is remarkable to see how the current atmosphere in the group shows similarities with the atmosphere at the start of my BSc thesis in 2011 while the cast is almost completely replaced. Gerben, thanks a lot for providing the experimental infrastructure in the G-lab, and for helping out with laboratorial errors and scientific challenges.

Ben and Zita, many thanks for proving all the essential infrastructure within EBT. Although I sometimes took your guidelines a bit lightly (my apologies), I do realize EBT would be helpless without you. Apilena, Astrid, Jannie, thanks for the good vibes in the lab.

Of course, my dear office mates, I was lucky to have you in close proximity the last years. The little chats, coffees, and shared dinners were great. Thank you Diana (for your colourful opinions and outfits), Shengle (for your hospitality and your amazing hotpot), Francesc (for your genuine interest during conversations), Zejia (for your eternal optimism and the sharing of peculiar types of food), Philipp (for the table tennis nights and the great chats), Luz (for the lovely smell of your coconut hand crème), Lionel (for keeping the PHA-spirit high in the office and the lab).

Big thanks to all EBT'ers for contributing to the energetic, creative, and almost family-like atmosphere in the group. You made the whole pandemic surprisingly bearable. Ali (for being the real BBQ master), Hugo (for your original perspective on music, science, beer, and basically everything), Maxim (for always wanting to play BB), David (for being in the same PhD boat from day one), Sergio (for his inexhaustible party skills), Timmy (for the competitive tennis matches), Stefan (for your faith in the Chinese knitting lesson), Ingrid (for organizing the EBT retreat with me two times, in vain), Danny (for the nice musical adventures we had), Jules (for the interesting chats at the coffee machine and in the lab), Nina (for your fascination for our Guinea pigs), Sam (for your beer tasting skills), Lemin (for your great Sinterklaas poem), Rodoula, (for the Karaoke duet), Samarpita, Stef, Marta, Jitske, Simon, Patricia, Dirk, Dita, Dmitry, Alba, Goncalo, Sirous, Viktor, Marta, Michel, Felipe, Yuemei, David W., Michele, Martin, Rebeca, and many more. . .

Lieve familie en vrienden, ik heb het geweldig getroffen met jullie. Dank voor jullie liefde, steun en gezelligheid in de afgelopen jaren. Pa en Ma, jullie hebben me altijd mijn eigen pad laten kiezen in het leven, waarbij altijd alles goed was. Jullie liefde is oneindig, dank daarvoor. Lieve broers, jullie kennen me als geen ander. Ik ben blij met onze hechte band.

Liefste Anne, het was heel bijzonder om de afgelopen jaren het intense, en veelal mooie PhD avontuur met jou te delen. Het heeft ons nog dichter bij elkaar gebracht. Vaak grapte ik dat ik zonder jou de PhD nooit afgerond zou hebben, maar je hebt echt heel veel voor me betekend. Je gaf altijd het juiste advies, wanneer ik weer met een dilemma zat. Bedankt voor al je onmisbare praktische (proof-reading, matlab debugging, figuren verbeteren, hulp met TU procedures, latex crash course, proefdruk controleren) en vooral emotionele steun. Ik heb ontzettend veel zin onze toekomst samen.